PHENOTYPIC INTEGRATION CONTRIBUTES TO SKELETAL FUNCTIONALITY AND FRAGILITY

by

STEVEN M. TOMMASINI

A dissertation submitted to the Graduate Faculty in Biomedical Engineering in partial fulfillment of the requirements for the degree of Doctor of Philosophy,
The City University of New York

2008

INFORMATION TO USERS

The quality of this reproduction is dependent upon the quality of the copy submitted. Broken or indistinct print, colored or poor quality illustrations and photographs, print bleed-through, substandard margins, and improper alignment can adversely affect reproduction.

In the unlikely event that the author did not send a complete manuscript and there are missing pages, these will be noted. Also, if unauthorized copyright material had to be removed, a note will indicate the deletion.

ProQuest LLC
789 East Eisenhower Parkway
P.O. Box 1346
Ann Arbor, MI 48106-1346

This manuscript has been read and accepted for the
Graduate Faculty in Engineering in satisfaction of the
dissertation requirement for the degree of Doctor of Philosophy.

Dr. Karl J. Jepsen

Date — Chair of Examining Committee

Dr. Mumtaz Kassir

Date — Executive Officer

Dr. Susannah P. Fritton

Dr. Stephen C. Cowin

Dr. Luis Cardoso

Dr. Carl J. Terranova
Supervision Committee

THE CITY UNIVERSITY OF NEW YORK

ABSTRACT

PHENOTYPIC INTEGRATION CONTRIBUTES TO SKELETAL FUNCTIONALITY AND FRAGILITY

by

Steven M. Tommasini

Adviser: Dr. Karl J. Jepsen

Increased risk of bone fracture is generally attributed to the reduced load-bearing capacity associated with small cross-sectional size or mass. Previous studies in inbred mice demonstrated that phenotypic integration among bone traits is critical for establishing long bone functionality by compensating for genetic variants that compromise skeletal size, mass, and strength. However, phenotypic integration also contributes to fracture susceptibility by giving rise to trait sets that were more damageable and brittle. We set out to better understand how phenotypic integration creates sets of bone traits that are functional for daily activities, but contribute to skeletal fragility. An examination of young adult human tibiae revealed that the biological concepts observed in the mouse femur translate to the human skeleton. Slender tibiae compensated for small size by increasing cortical thickness and mineralization. This phenotypic integration produced functional structures, but increases in mineralization resulted in a more brittle and damageable material that would be expected to perform poorly under extreme load conditions (e.g., military training or falling). By combining a systems based approach with a newly developed network theory analysis, we found that phenotypic integration is not limited to long bones, but also affects corticocancellous skeletal sites like the vertebral body. Phenotypic integration among cortical and

trabecular traits compensated for genetic variants affecting skeletal size and mass in a manner that created functional load transfer networks in mouse vertebrae. Smaller vertebrae relative to body size would have been unable to support daily loads (i.e., not functional) without increasing tissue mineral density and the relative amounts of cortical and trabecular bone. However, increases in mineral content may increase fracture risk under extreme loading. Together, these results have great clinical significance because they provide two new areas of focus in studying skeletal fragility: 1) sets of traits arising from phenotypic integration that may be susceptible to fracture under challenging physiological conditions and 2) genetic or environmental variants that disrupt the biological processes involved in phenotypic integration and thus affect functionality. By understanding genetic variation in the interaction among sets of traits, our understanding of the genetic basis of skeletal functionality and fragility can be improved.

ACKNOWLEDGMENTS

I would like to take this moment to thank everyone who made the past seven-plus years the best experience anyone could imagine.

First and foremost, to my advisor Karl Jepsen who has been a constant source of encouragement and ideas. I am luck to have had the best mentor.

To my doctoral committee Susannah Fritton, Carl Terranova, Luis Cardoso, and Steve Cowin who provided immeasurable support and guidance. It was an honor to learn from you.

To everyone in the Orthopaedic Research Laboratory at Mount Sinai School of Medicine for their expertise, knowledge, and companionship. Special thanks to Mitch Schaffler and Evan Flatow for allowing me to be a part of the lab. To Bob Majeska for all the interesting discussions. No topic was ever off limits. To Phil Nasser for his technical skill, unlimited knowledge, entertaining discussions, and friendship. To Damien Laudier whose histological skills were probably under used.

Very big thanks to Chris Price, Hayden Courtland, Kelly Emerton, Danielle Casagrande, Joel Williams, Bin Hu, Matt Cordova, Justin Bird, Henock Wolde-Semait, Nimesh Pandey, Adrian Woo, Jean Shine, Desiree Aird, Whitney Booker, David Fung, Yilin Wang, and Chris Fritton. I cannot fit all of the good times we had in print. Thanks for being my second family and for making me look forward to going to the lab every day. I hate to leave and will miss you all.

To everyone else who contributed to the work presented in this dissertation including Susan Wearne, Patrick Hof, Joe Nadeau, Marjolein van der Meulen, Tim Morgan, Haviva Goldman, Richard Ghillani, Roger Levy, Kristine Wiren, Kurt Hankenson, Herb Sun, Valerie Williams, Musyoka Munyoki, Ozan Akkus, Brad Herman, Chaoyang Li, Vincent Wang, Liyun Wang, Laoise McNamara, and Chris Hernandez.

Last, but certainly not least, I would like to thank my family to whom I owe everything. Mom, Dad, Chris, Lauren, and Grandma Precious, I love you!

For Grandpa Pal.

TABLE OF CONTENTS

LIST OF TABLES

LIST OF FIGURES

CHAPTER 1

INTRODUCTION

Bone is a complex system whose main function is to support mechanical loads associated with everyday activities. Understanding how genetics and environment compromise functionality is important to improving prevention, diagnosis, and treatment of fracture. The objective of this chapter is to provide the reader with answers to three basic questions of skeletal functionality and fragility: 1) How are functional bones built? 2) Why is this important? and 3) What are the tools needed to improve our understanding of this complex system? As part of "Building a Functional Bone" (How), the essential components of bone will be defined. Then, the focus shifts to the interdependence of these components. In "Prevention, Diagnosis, and Treatment of Fractures" (Why), the prevalence of osteoporosis and fragility fractures is outlined along with current techniques for assessing and treating fracture risk The last sections (What) introduce the many approaches to improving our understanding of the biological basis of skeletal fragility including genetics (Genetics of Skeletal Fragility), animal models (Inbred Mice as a Model to Study Genetic Basis of Skeletal Functionality and Fragility), systems biology (Systems Biology Approach to Understanding Complex Systems), and network theory (Network Analysis Relates Form to Function). These tools are critical to reducing the morbidity and mortality associated with fragility fractures.

Building a Functional Bone

Bone is a self-repairing, structural tissue that has the ability to adapt its mass, shape, and composition to changes in mechanical demands without causing pain or fracture (Jee 2001; Ruff et al. 2006). There are two main types of bone tissue – cortical and trabecular (Figure 1.1). Cortical or compact bone is a dense, solid mass accounting

for nearly 80% of the skeletal mass in an adult human (Jee 2001). Cortical bone forms the outer wall of all bones and makes up the shaft (diaphysis) of all long bones. Trabecular or cancellous bone is a spongy, porous network of large plate- and rod-like elements known as trabeculae. Trabecular bone is found within the ends of long bones (metaphysis and epiphysis) and in the center of vertebrae. Cortical and trabecular bone differ in their development, architecture, function, turnover rate, frequency of age-dependent changes and fractures, and skeletal distribution (Jee 2001). In long bones, trabecular bone makes up approximately 8% of the bone mass, but has nearly ten times the surface area of cortical bone. The vertebral body consists mostly of trabecular bone (~62% of vertebral bone mass) surrounded by a denser cortical shell.

Figure 1.1. The two main types of bone.

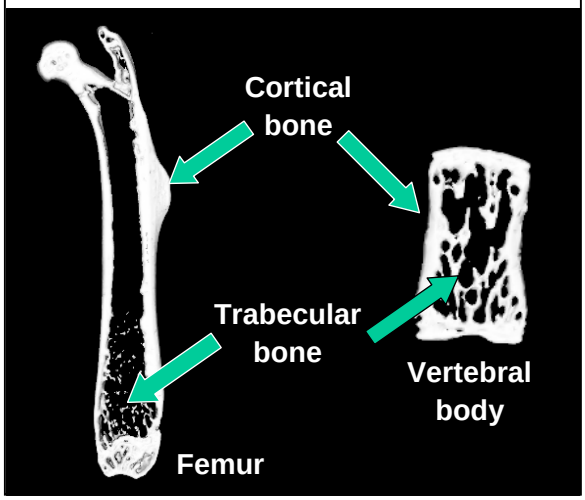

The functions of bone

Bone performs numerous functions. Bone acts as a reservoir of minerals important for the body, most notably calcium and phosphorus. The marrow, located within the medullary cavity of long bones and the spaces of trabecular bone, produces blood cells in a process called hematopoiesis. Bone buffers the blood against excessive pH changes by absorbing or releasing alkaline salts. Bone tissues also can store heavy metals and other foreign elements, removing them from the blood and reducing their effects on other tissues.

In addition to these physiological functions, bone also supports the body, protects

vital organs, and functions together with skeletal muscles, tendons, ligaments, and joints to generate movement (Currey 2002). To perform these critical mechanical functions, bones must be sufficiently stiff and strong to support the forces associated with weight bearing and joint movement. Thus, bone must be resistant to fatigue, given that the average individual takes approximately 1-3 million steps per year (Tudor-Locke et al. 2004) and bones also must be capable of withstanding enormous forces, sometimes on the order of 2-3 times body weight (Davy et al. 1988). Because bone tissue is metabolically expensive to maintain and excessive tissue is energetically demanding during movement, bone is expected to perform these functions using minimum mass (Currey et al. 1985).

The cells of bone

There are three main types of cells constituting bone – osteoclasts, osteoblasts, and osteocytes. Osteoclasts are the cells responsible for bone resorption. They are large multinucleated cells found lining surfaces undergoing bone resorption (Ducy et al. 1998; Roodman 1999). Derived from the hematopoietic stem cell lineage, osteoclasts create a locally acidic environment for the resorption of mineralized bone matrix through the creation and secretion of H^+ ions and specialized proteases.

Osteoblasts are the cells responsible for bone formation. They are derived from mesenchymal stem cells found in the stroma of bone marrow or within the layers of the periosteum (Balena et al. 1992; Aubin 1998; Karsenty 1998). Mature osteoblasts secrete a type I collagen-based extracellular matrix that undergoes mineralization (Boskey et al. 1984), leading to a composite material capable of withstanding compressive, tensile, torsional, and shearing forces (Turner 2006). The extracellular matrix also contains non-

collagenous proteins such as serum-derived proteins, proteoglycans, glycosylated proteins, and Gla proteins, which serve as regulators of mineralization and osteoblastic/osteoclastic signaling molecules (Gorski 1998).

Osteocytes are terminally differentiated osteoblasts trapped in the bone matrix and are the most abundant cell type in bone. Osteocytes have many long, slender processes encased in the lacunar-canalicular network that connect with other osteocytes, osteoblasts, bone lining cells, and the vasculature (Aarden et al. 1994; Turner et al. 1995; Jee 2001). Their functions include matrix maintenance and calcium homeostasis. Based upon their placement within the bone, their highly connected nature (Turner et al. 1995; Turner et al. 2002), and studies of osteocyte apoptosis and signaling (Tomkinson et al. 1997; Plotkin et al. 1999; Knothe Tate et al. 2004), osteocytes also are thought to act as mechanosensory receptors regulating the bone's response to the amount and distribution of strain within the bone tissue (Cowin et al. 1995; Duncan et al. 1995), fluid flow (Weinbaum et al. 1994), and tissue damage (Burr et al. 1985; Reilly 2000; Noble 2003; Noble 2005). Thus, osteocytes play a key role in the adaptive modeling and remodeling processes of bone mass including the regulation of mineral and architecure.

The growth and development of bone

The human skeleton can be divided into two subdivisions – axial and appendicular. Appendicular bones include the long and short bones of the limbs, hands, and feet. Axial bones include the flat bones of the skull and the irregular bones of the spine, ribs, and hips. The bones of these two components differ in anatomical location, function, and development.

Skeletal development begins during embryonic development as mesenchymal

condensations. These condensations form bone through two processes – intramembranous ossification and endochondral ossification. For both types of ossification, the shape and manner of growth depend on the individual bone and are genetically determined. Intramembranous ossification is involved mainly in the formation of the flat bones of the skull. A primary center of ossification appears within the mesenchymal condensation and bone is apposed. Next, trabeculae are formed by osteoblasts and interconnect to form the primary cancellous bone. Finally, cortical bone is formed when the spaces between the primary cancellous bone are filled in.

Endochondral ossification is formed from a cartilage template, or anlage. It is involved in the formation of the bones of the limbs, hips, and vertebral column. The proliferation and hypertrophy of chondrocytes (cartilage cells) form a scaffold that is subsequently calcified and replaced by primary and secondary cancellous bone. Endochondral ossification forms trabecular bone that makes up most of the ends of long bones (epiphyses and metaphyses) and the center regions of axial bones such as vertebrae. This trabecular bone has a high degree of architectural and functional complexity (Keaveny et al. 2002; Pothuaud et al. 2002). The regulation of the architecture of trabecular bone in relation to its cortical bone exterior is one focus of this dissertation.

The modulation of bone size and shape occurs through modeling and remodeling. During growth, modeling controls the size, shape, and strength of bones. Local influences modulate resorption and formation drifts that remove or add bone to create mechanically functional structures. Remodeling occurs throughout a person's life and is the process of bone turnover – resorption followed by replacement of bone. Remodeling regulates

calcium homeostasis, repairs microdamage, replaces dead tissue, and adapts micro-arhitecture to mechanical stresses. Remodeling of trabecular bone may align trabeculae with loading stresses or may perforate and remove trabeculae (Silva et al. 1997; Ciarelli et al. 2000; Huiskes 2000; Waarsing et al. 2004). Remodeling of cortical bone may thicken bone at points of maximum stress or, when mechanical loading is low, remodeling may increase cortical porosity, decrease width, and reduce strength (Frost 1983; Frost 1990; Frost 1990; Carter et al. 2001).

Phenotypic integration of bone traits

In 1881, Wilhelm Roux suggested that cells, governed by mechanical stimuli, in a self-organizational process, locally regulate formation and functional adaptation of trabecular architecture in bone (Roux 1881). Work in the last 50 years has proven that architecture is adapted to mechanical loads (Frost 1983; Frost 1990; Frost 1990; Cowin 1997; Odgaard et al. 1997) as this "functional adaptation" has been observed in the form of bone gain in the dominant arm of tennis players (Jones et al. 1977; Kannus et al. 1995; Ashizawa et al. 1999; Bass et al. 2002) or bone loss in response to the absence of gravity in space (Wronski et al. 1987; Doty 2004). Functional adaptation matches form to function through a strain-based feedback system, ensuring that structures are sufficiently stiff and strong to resist fracturing (Rubin et al. 1984; Frost 1987; Turner et al. 1998). Physical forces experienced by bone induce tissue-level strains affecting the development of trabecular architecture, peak bone mass, bone shape, matrix architecture, and the anatomical relationships within and among skeletal elements (Olson et al. 1958; Garn 1970; Cheverud 1996; Moro et al. 1996; Sumner et al. 1996; van der Meulen et al. 1996; Forwood et al. 2004; Ruff et al. 2006). The variation in bone size and shape observed

across species (Ruff et al. 2006), between populations (Ruff 2000; Stock et al. 2001), between bones (Chatterjee et al. 1999; Ruff 2003), and between sexes (Gilsanz et al. 1997; Looker et al. 2001) has been explained by the functional adaptation of structures to their particular loading environments. However, despite being a significant determinant of fracture risk, variation in bone size and shape within a single population has not been explored fully (Giladi et al. 1987; Gilsanz et al. 1995; Beck et al. 1996; Crossley et al. 1999; Duan et al. 1999; Beck et al. 2000; Szulc et al. 2006).

To understand functional adaptation of a complex, and highly adaptive system such as bone, it is important to understand the relationship among physical bone traits. Phenotypic integration refers to the interdependence among traits that contribute to the development of a functional organ or organism (Pigliucci et al. 2004). The interdependence among traits results in significant correlations among many adult skeletal traits providing multiple ways for a complex system such as bone to be sufficiently stiff and strong to support daily mechanical loads (Rauch et al. 2001). Studies of phenotypic integration have been conducted mostly in the context of evolutionary changes in skeletal shape (Olson et al. 1958). However, these studies did not consider integration in the context of skeletal fragility nor the interaction between tissue-quality and bone morphology. Further, for more complex skeletal sites such as the vertebral body, the interaction between cortical and trabecular components is not understood completely.

Recent studies indicated that phenotypic integration among cortical and trabecular traits is critical for overall strength of corticocancellous structures (Riggs et al. 2004; Duan et al. 2005; Eswaran et al. 2006; Seeman et al. 2006; Waarsing et al. 2006;

Faulkner et al. 2007; Glatt et al. 2007). During growth, the amount of load imparted to the trabecular tissue is dependent on the amount of load borne by the cortical shell. Given that physiological forces are important for the normal development of trabecular tissue, the degree of load sharing may be a critical determinant of adult bone mass and architecture. Compensatory changes with bone loss during aging also have been reported. Age-related decreases in trabecular bone volume fraction are accompanied by increases in periosteal expansion of the cortical shell (Beamer et al. 1996; Riggs et al. 2004; Glatt et al. 2007). The authors suggested that this bone remodeling is best described as "accelerated bone metabolism that resulted in fast, possibly mechanically driven, bone adaptation" (Beamer et al. 1996). As expected, the load fraction carried by the shell increased with decreasing trabecular bone volume fraction. Further, these compensatory changes occur in a sex-specific manner. Men and women lose similar amounts of bone, but women lose bone mass through loss of trabecular number and men lose bone mass through trabecular thinning (Parfitt et al. 1983; Aaron et al. 1987; Silva et al. 1997; Khosla et al. 2006). Thus, understanding the phenotypic integration among traits will improve strategies aimed at optimizing this inherent adaptive response in order to reduce fracture risk.

Prevention, Diagnosis, and Treatment of Fractures

Osteoporosis and fracture risk

Osteoporosis is a systemic skeletal disease characterized by low bone density and micro-architectural deterioration of bone tissue leading to enhanced bone fragility and an increased risk of fracture (Genant et al. 1999; NIH 2001). In the USA alone, there are

over 10 million cases of osteoporosis and more than 1.5 million individuals suffer fractures annually (NOF). The majority of fractures occur in the distal radius and proximal femur (Cummings et al. 2002). One of the main sites of osteoporotic fractures is the spinal column with approximately 700,000 osteoporotic vertebral fractures occurring each year in the USA (NOF). The loss of vertebral height and stability, risk of neurological injury, and pain that often result from vertebral fractures make osteoporosis a major clinical problem. With increasing life expectancy, the cost and number of patients with post-menopausal osteoporotic fractures is steadily increasing, driving the need for new preventative and diagnostic procedures.

Current techniques for assessing and treating fracture risk

Currently, fracture risk is well-predicted using bone mineral density (BMD) (Miller et al. 1999) and is typically measured using dual-energy x-ray absorptiometry (DXA). Because osteoporosis is associated with loss of bone mass with aging, many therapeutic strategies aim to increase trabecular bone mass during growth or to preserve trabecular bone mass during aging. Although this approach has generally been successful, there are limitations with using one global measure of bone health when it comes to identifying novel strategies aimed at reducing fracture risk (Rubin 2005). The most important limitation is that BMD does not provide a measure of the structural and compositional changes that accompany growth and aging (Duan et al. 2005). These structural and compositional changes provide critical insight into the underlying biological mechanisms responsible for reduced strength and increased fragility (Seeman et al. 2006). Thus, there is a need to supplement BMD information with additional, more detailed information about the changes in bone structure and quality that impact skeletal

strength (Faulkner et al. 2007).

Genetics of Skeletal Fragility

Fracture risk is a heritable condition (Eisman 1999; Nelson et al. 2000; Baldock et al. 2004; Duan et al. 2005; Wang et al. 2005) and there is currently a large effort to identify genes leading to increased fracture susceptibility. These studies aim to map genes that influence skeletal traits and that contribute to overall skeletal strength. Over 350 quantitative trait loci (QTL) have been mapped for bone traits, and several genes have been identified regulating BMD (Little et al. 2002; Klein et al. 2004; Edderkaoui et al. 2007). QTL identify a particular region of the genome as containing a gene(s) that is associated with the trait being measured. However, BMD, morphological traits, and compositional traits are complex and results of gene mapping studies in mice have identified QTLs on nearly all chromosomes (Shimizu et al. 1999; Drake et al. 2001; Drake et al. 2001; Yershov et al. 2001; Bouxsein et al. 2002; Klein et al. 2002; Koller et al. 2003; Robling et al. 2003; Turner et al. 2003; Volkman et al. 2003; Lang et al. 2005; Bower et al. 2006; Kenney-Hunt et al. 2006; Yu et al. 2007).

Genetic factors also regulate the relationship among traits (Seeman et al. 1996). Examinations of the functionality of a complex structure like the mouse mandible (Bailey 1986; Cheverud et al. 2004) and craniofacial traits of the rhesus macaque (Cheverud 1996) provided important insight into the genetic basis of phenotypic integration in a complex skeletal structure. Relationship QTLs suggested that phenotypic integration might arise from pleiotropy (one gene affects multiple traits). Thus, allelic variation affects multiple bone traits and this impact is mediated through multiple physiological

pathways during development. Further, these studies indicated that compensatory changes occurred within the structure, suggesting that compensation may be critical for establishing function in a complex system such as bone.

Inbred Mice as a Model to Study Genetic Basis of Skeletal Functionality and Fragility

Animal models using mice are powerful tools to identify genetic determinants of various diseases due to the ease of breeding, reproductive capacity, and availability of large numbers of genetic markers in the mouse genome. Mouse models provide the primary advantage of specific breeding to isolate QTLs and to test their effects with other genetic determinants. Inbred mice have been used to characterize genes and biological processes involved in many complex diseases including heart disease, cancer, and diabetes (Nadeau et al. 1995; Nadeau et al. 1998; Nadeau et al. 2003). Inbred mice are genetically distinct animals. Within a given inbred mouse strain, all individuals are homozygous (i.e., ~100% genetically identical at all loci) (Beck et al. 2000). Hundreds of inbred mouse strains are commercially available and provide a large degree of both genetic and phenotypic variability for many physiological systems.

Recombinant inbred (RI) mouse strains have been used to identify functional interactions among traits (Bailey 1986; Cheverud et al. 2004; Jepsen et al. 2007). RI strains are formed from an initial cross between two different inbred strains (F_1) followed by an F_1 intercross and 20 generations of strict brother-sister mating (Silver 1995). This produces a set of new inbred strains with special properties relative to each other. RI mouse strains have a unique pattern of genetic randomization between their parental strains, which creates subtle, non-pathological trait variation that can be used to measure

the tendency of different traits to co-segregate or correlate. Depending on the set of parental genes that are inherited, the RI strains build mechanically functional bones in slightly different ways. As one bone trait varies in each RI strain, other traits are expected to co-vary accordingly to achieve organ-level functionality (i.e., healthy, functional bone). Thus, traits can be examined across the panel to quantify functional (i.e., compensatory) relationships among traits.

The relatively short generation time (~10 weeks from being born to giving birth), lifespan (~16 weeks to adult maturity), and large numbers of offspring also make mouse models ideal for studying the genetic basis of complex traits during growth and with aging (Silver 1995). Further, inbred mice have proven to be reliable models for studying the growth (Price et al. 2005) and aging (Halloran et al. 2002; Glatt et al. 2007) of human bone. The age-related changes in mouse trabecular bone and the associated changes in the cortex are consistent with those observed in the human skeleton (Glatt et al. 2007). Despite the fact that mouse bone is small and does not have an extensive osteonal structure like human bone, the biological concepts learned from the mouse can be translated to the human skeleton. Although the mouse vertebral body has proportionally fewer trabeculae compared to the human vertebral body, the differences are as important as the similarities because they provide novel insight into the biology of functional adaptation. Thus, inbred mouse models provide a valuable resource to study phenotypic integration that has relevance to the human skeleton.

Systems Biology Approach to Understanding Complex Systems

Functional relationships between two traits can be examined using correlation

analysis. However, because complex systems are comprised of multiple interdependent traits, the overall organization of these interactions is better understood in the context of function and when the effects of multiple variables are taken into consideration simultaneously. Functional relationships among traits can be examined using Structural Equation Modeling (SEM), or Path Analysis (Wright 1921; Grace 2006; Jepsen et al. 2007; Sharkey et al. 2007). Structural equations are similar to multiple regression analyses. However, independent and dependent traits are selected based on *a priori* or hypothesized knowledge of how a system functions. Thus, the structural equations are specific to a particular hypothesis and not general multivariate regressions because selected traits are examined in the context of how all traits vary simultaneously to establish function.

In 1921, Sewall Wright developed and applied Path Analysis (a graphical form of SEM) to problems of inheritance (Figure 1.2). Path Analysis is a well-established and widely used multivariate analysis technique (Grace 2006) that uses conditional co-variances to test for causal relationships among traits (Wright 1921). Causality is based on the pattern of statistical dependency among traits. The directionality between two traits provides the basis for implying causal relationships (Sieberts et al. 2007). However, in cases where many models fit the same dataset, Path Analysis does not provide definitive proof of causality. Even Wright himself was aware of the limitations of Path Analysis in terms of making causal claims (Denis et al. 2006).

Figure 1.2. Path diagram representation of structural equations. x_i – independent traits; y_i – dependent traits; r_{ij} – correlation coefficient; γ_{ij}, β_{ij} – path coefficients; ξ_i – error variance.

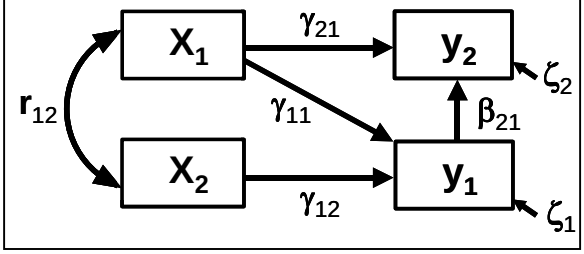

Still, models that fit the data provide evidence of functional relationships among traits and the models can be designed to test specific hypotheses regarding interactions among traits in the context of function.

Path analysis is used to examine how phenotypic integration contributes to skeletal functionality and fragility

For many conditions, genetic background plays a critical role in determining how a system will function under physiological and stressful conditions. If each trait within a system was precisely controlled by a specific set of genes, minor genetic variants affecting individual traits would have devastating effects on overall system function (Pigliucci et al. 2004). Phenotypic integration among traits allows certain systems to buffer themselves against genetic variants that alter individual traits and that would otherwise threaten functionality. Thus, although genes may not regulate all trait values, trait values may be determined in part by phenotypic integration.

Path Analysis provides an invaluable resource to understanding why certain individuals are susceptible to common health conditions like hypertension, arthritis, obesity, and osteoporosis and how genetic and environmental variants compromise the function of these complex systems. A recent examination of how the skeletal system dealt with genetic variations affecting bone slenderness revealed new insight into phenotypic integration operating in the mouse femur (Jepsen et al. 2007). Slenderness, which is a measure of bone width relative to length, is a particularly important phenotypic variation that threatens functionality. Under physiological bending and torsional loads, small reductions in bone width lead to large reductions in stiffness and strength (van der Meulen et al. 2001). Mouse femora that were slender relative to body weight established

whole-bone stiffness and strength because the narrow width was compensated by increases in cortical thickness and matrix mineralization. However, this occurred at the expense of increased brittleness as the increased mineralization led to reduced tissue-ductility. Wider (more robust) femora had thin cortices and lower mineralization. This analysis also indicated that the amount of tissue used to establish mechanical functionality was highly regulated or constrained (Currey et al. 1985; Frost 1987). Thus, phenotypic integration among external size, cortical thickness, and matrix mineralization was critical for establishing mechanical function while using minimum mass. Further, phenotypic integration in the mouse femur was critical for establishing function, but may also contribute to fracture susceptibility by giving rise to genotype-specific trait sets that are more damageable and brittle. Thus, a systems approach including Path Analysis offers a different perspective on the genetic basis of fracture susceptibility. Not all trait sets arising from phenotypic integration may perform equally well under challenging physiological conditions. Additionally, genetic or environmental perturbations that alter the processes involved in phenotypic integration could contribute to fracture susceptibility.

The possibility that slender bones, like those shown in mouse models, may be composed of more damageable material has not been considered in the human skeleton. Phenotypic integration also has not been extensively explored in corticocancellous structures. Phenotypic integration in corticocancellous sites such as the vertebral body is expected to be more complex because of functional interactions among trabecular, cortical, and compositional traits. In addition to varying the amounts of these skeletal components, phenotypic integration in corticocancellous structures also involves the

alignment and distribution of trabeculae. Therefore, to understand more completely how phenotypic integration affects the load transferring capability of complex corticocancellous structures, a new integrated approach, in addition to a systems biology approach, is needed.

Network Analysis Relates Form to Function

The science of networks gives us a different way to think about the world, and in so doing helps us solve old problems (Watts 2003). Since 1736, when Leonhard Euler realized that the problem of taking a stroll across all seven bridges in the Prussian city of Königsberg without crossing the same bridge twice could be solved with a network graph (Watts 2003), network theory has grown steadily to become a major branch of mathematics and has spilled over into sociology and anthropology, engineering and computer science, physics, biology, and economics. A network is a group of objects connected to each other in some manner. Networks represent populations of individual components that are actually doing something whether it's generating power, sending data, or even transferring loads. Network researchers are most interested in the relationships between a network's components because they affect the behavior of the system as a whole.

In network science, structure (i.e., form) always affects function. However, most networks used to describe complex systems are complex themselves. In addition to structural complexity, having many different types of nodes that are linked with different weights and directions can complicate networks. Networks are also dynamic objects because they are evolving and changing in time due to the activities or decisions of their

components. Therefore, what happens in the network and how it happens depend on the network. Further, the network in turn depends on what has happened previously. Bone networks use different combinations of trabecular bone, cortical bone, and mineral content. The way these components are combined in the connected bone network will affect the way load is transferred and will reveal biological control mechanisms that determine this structure.

Percolation theory is used to examine connectivity in dynamic systems

Percolation theory was developed during WWII by Paul Flory and Walter Stockmayer who used it to describe the polymerization process that leads to gelation (Stauffer et al. 1994). Gelation is the formation of a network of chemical bonds that spans an entire system. An example of percolation is the boiling of an egg. The egg starts out as liquid. Upon heating, the molecules bond, forming larger clusters of macromolecules. These macromolecules continue to bond until the egg becomes more solid-like (gel). Percolation theory is used to describe the phase change phenomenon when enough molecules have bonded. Figure 1.3 shows a simple graphical definition of percolation and its clusters. A fraction of squares in the lattice are filled with dots. A group of neighboring dots is defined as a cluster. When one cluster extends to opposite boundaries (i.e., from top to bottom), this cluster "percolates" through the system like water through a coffee machine. In real systems, this is not always a straight line.

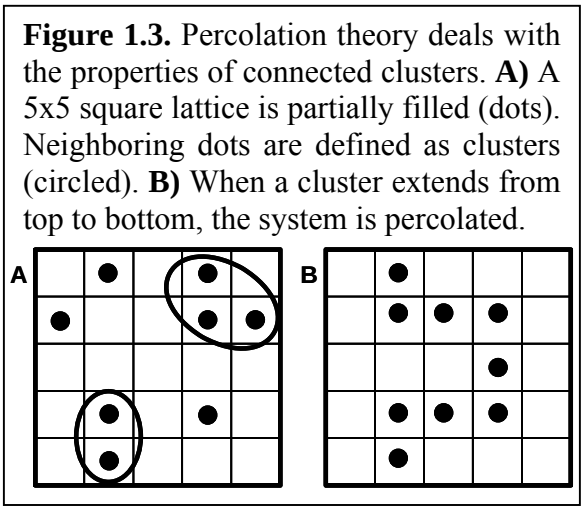

Figure 1.3. Percolation theory deals with the properties of connected clusters. **A)** A 5x5 square lattice is partially filled (dots). Neighboring dots are defined as clusters (circled). **B)** When a cluster extends from top to bottom, the system is percolated.

The corticocancellous architecture of a complex site such as the vertebra or proximal femur is a connected network of bone capable of transferring loads. The study of a network's connectivity (its ability to transfer information from point A to point B) is the focus of percolation. In bone, the transfer of load is analogous to the transfer of information. Percolation models have been used successfully to study network related phenomena including forest fires, electrical conductivity, epidemics of disease, and signal transfer in neurons (Stauffer et al. 1994; Wearne et al. 2005) and is ideally suited to the study of bone as previous data suggest that trabecular bone architecture can be modeled as a load transfer network (Tabor 2003). Thus, percolation theory offers a quantitative approach to study how different combinations of cortical and trabecular traits lead to mechanically functional structures. Developing a network approach to study corticocancellous architecture should further our understanding of the biological basis of skeletal functionality and fragility.

Summary

Understanding the basic biological principles of how bone establishes functionality is important to improving prevention, diagnosis, and treatment of fracture risk. Previous studies in inbred mice demonstrated that phenotypic integration among bone traits is critical for establishing long bone functionality by compensating for genetic and environmental variants that compromise strength. However, phenotypic integration also contributed to fracture susceptibility by giving rise to trait sets that are more damageable and brittle. It is not known whether similar compensatory mechanisms are responsible for fracture risk of long bones in the human skeleton. Further, we expect

phenotypic integration to affect all skeletal sites, including a corticocancellous site like the vertebral body. Finding that phenotypic integration gives rise to variable adult trait sets in human long bone and corticocancellous structures will provide novel insight into the genetic basis of variable bone mass and architecture as well as important diagnostic and therapeutic targets for fracture prevention. The overall goal of this dissertation is to better understand how phenotypic integration creates sets of bone traits that are functional for daily activities, but may also contribute to skeletal fragility. In Chapter 2, we successfully demonstrate that the biological concepts observed in the mouse femur can be translated to the human skeleton by testing whether phenotypic integration among morphological and compositional traits contributes to fracture susceptibility in the tibiae from young adult males and females. In Chapter 3, we shift our focus back to the mouse model in order to study more complex corticocancellous structures. We develop a novel approach using percolation theory to define the relationship between corticocancellous architecture and mechanical function in inbred mouse vertebrae. In Chapter 4, we combine the systems biology approach (Chapter 2) with the network theory approach (Chapter 3) to test whether trabecular, cortical, and compositional bone traits are functionally related in Recombinant inbred mouse vertebrae, as this would imply there is a strong biological process in bone that co-adapts traits to meet mechanical demands.

CHAPTER 2

BIOLOGICAL CO-ADAPTATION OF MORPHOLOGICAL AND COMPOSITIONAL TRAITS CONTRIBUTES TO MECHANICAL FUNCTIONALITY AND SKELETAL FRAGILITY

Reproduced from ***Bone*** 2007; 40:498-505; and ***J Bone Miner Res*** 2005; 20:1372-1380 and ***J Bone Miner Res*** 2008; 23:236-246 with permission of the American Society for Bone and Mineral Research

ABSTRACT

Biomechanical properties were assessed from tibiae of 17 adult males ages 17-46 years and 14 adult females ages 22-46 years. Tissue-level mechanical properties varied with bone size. Narrower tibiae were comprised of tissue that was more brittle and more prone to accumulating damage as compared to tissue from wider tibiae. A Path Analysis was conducted to determine whether functional interactions exist among morphological, compositional, and microstructural traits for young adult human tibiae. Data provided evidence that bone traits are co-adapted during ontogeny so that the sets of traits together satisfy physiological loading demands. However, certain sets of traits are expected to perform poorly under extreme load conditions.

Introduction: Having a narrow (i.e., more slender) tibia relative to body mass has been shown to be a major predictor of stress fracture risk. Previous data from inbred mouse strains suggested that biological processes within bone co-adapt morphological and composition traits during ontogeny to satisfy physiological loading demands. The intriguing possibility that slender bones, like those demonstrated in animal models, may be composed of more damageable material has not been considered in the human skeleton. We tested whether the relationships among morphology and tissue-level mechanical properties were the result of biological processes that co-adapt physical traits, similar to those observed for the mouse skeleton.

Materials and Methods: Cross-sectional morphology, bone slenderness, and tissue-level mechanical properties were measured from tibiae of 14 female (age 22-46 yrs) and 17 male (age 17-46 yrs) donors. Physical bone traits measured included tissue density, ash content, water content, porosity, and the area fractions of osteonal, interstitial, and

circumferential lamellar tissues. Bivariate relationships among traits were determined using linear regression analysis. Differences between males and females also were determined. A Path Analysis was conducted to test the hypothesis that slenderness is functionally related to mineralization (ash content) and the proportion of total area occupied by cortical bone.

Results: Males and females showed nearly identical tissue-level mechanical properties. However, for all body sizes, female tibiae were smaller relative to body size (i.e., less robust) compared to males. The results indicated that sex-specific growth patterns affected transverse bone size, but did not affect tissue level mechanical properties. Ash content correlated negatively with several traits including slenderness and marrow area, indicating that slender bones were constructed of tissue with higher mineralization. Path Analysis revealed that slender tibiae were compensated by higher mineralization and a greater area fraction of bone.

Conclusions: The results suggest that bone adapts by varying the relative amount of cortical bone within the diaphysis and by varying matrix composition. This co-adaptation is expected to lead to a particular set of traits that is sufficiently stiff and strong to support daily loads. However, increases in mineralization result in a more brittle and damageable material that would be expected to perform poorly under extreme load conditions. This, combined with the observation that young adult female long bones are undersized relative to body size compared to males, suggests that adult females would be expected to accumulate more damage under intense loading. Therefore, focusing attention on sets of traits and the relationship among traits may advance our understanding of how genetic and environmental factors influence bone fragility.

INTRODUCTION

Stress fractures are overuse injuries of bone that are common among elite runners and military recruits (Milgrom et al. 1985; Milgrom et al. 1989; Beck et al. 1996). Prior to injury, affected bones are typically normal with no acute injury. Morbidity from stress fractures ranges from minor pain to serious lifetime disability for the individual (Lappe et al. 2001). Stress fractures have been reported in the ribs, hip, spine, and metatarsals (Milgrom et al. 1985; Milgrom et al. 2002) but vigorous weight-bearing activities, such as running and jogging, commonly lead to stress fractures of the lower extremities, especially the tibia (Milgrom et al. 1985). During basic training, 1-5% of U.S. male military recruits sustain a stress fracture (Beck et al. 1996). However, this incidence is 2-5 times higher in female recruits (Friedl et al. 1992). Stress fractures lead to loss of manpower, valuable loss of training time, expense of medical care, and discharge of affected soldiers (Brudvig et al. 1983). A better understanding of the factors contributing to stress fractures is needed to identify new prevention strategies that will reduce fracture incidence.

A number of risk factors for stress fracture have been identified including physical fitness, external hip rotation, body height and weight, age, race, gender, muscle mass, motivation, footwear, smoking, and family history of osteoporosis (Milgrom et al. 1989; Giladi et al. 1991; Bennell et al. 1999; Lappe et al. 2001; Jones et al. 2002). One of the best predictors of stress fracture risk is bone geometry. Specifically, having a narrow (i.e., more slender) tibia relative to body mass has been shown to be a major predictor of stress fracture risk and fragility in military recruits (Giladi et al. 1987; Milgrom et al. 1989; Beck et al. 1996) as well as athletes (Crossley et al. 1999). A stress fracture is

thought to be a consequence of transiently reduced tissue strength arising from increased resorptive activity (i.e., increased porosity) that acts to repair damage induced by vigorous physical activity (Mori et al. 1993). Thus, stress fractures may be pronounced in individuals with more slender bones because smaller bone size is thought to lead to higher tissue-level stresses and thus increased damage accumulation (Milgrom et al. 1989; Beck et al. 1996). However, this postulate is based on the assumption that all bones are constructed in equivalent manners, and the contribution of variable tissue-level mechanical properties to stress fracture incidence has not been explored.

The increased risk of fracture observed for individuals with slender bones (Albright et al. 1941; Landin et al. 1983; Chan et al. 1984; Milgrom et al. 1985; Giladi et al. 1987; Gilsanz et al. 1995; Crossley et al. 1999; Beck et al. 2000; Duan et al. 2001; Kiel et al. 2001) has generally been attributed to the reduced load-bearing capacity associated with small cross-sectional size or mass (Milgrom et al. 1989; Beck et al. 1996). However, recent studies examining inbred mouse strains may help explain why bone size is a risk factor for stress fractures in the human skeleton. A comparison of adult A/J and C57BL/6J inbred mouse strains revealed that slender femora tended to have thicker cortices and higher tissue-mineral density, whereas robust femora tended to have thinner cortices and lower tissue-mineral density (Jepsen et al. 2001). The correlation between these traits provided evidence that these traits are functionally related (or interacting) in the sense that there are biological processes within bone which work to co-adapt morphologic and tissue-quality traits during ontogeny (Olson et al. 1958; Thompson 1961; Currey 1979; Carrier 1990; Ferretti et al. 1993; Papadimitriou et al. 1996). The term functional interaction is used because presumably these biological

processes ensure that the set of traits is sufficiently stiff and strong for daily loads (Moro et al. 1996; Sumner et al. 1996; Forwood et al. 2004).

A downside of these biological processes is that not all sets of traits result in equivalent failure mechanisms. For slender bones, the compensatory increases in cortical thickness and tissue-mineral density may help to increase organ-level stiffness, but the reduced tissue ductility and toughness associated with the greater tissue-mineral density (Currey 1984) may increase the risk of fracturing under extreme loading conditions, such as low-cycle fatigue (e.g., military training) and overloading (e.g., falling). We postulate that a similar reciprocal relationship between bone size and bone quality exists in the human skeleton. The intriguing possibility that slender bones, like those demonstrated in animal models, may be composed of more damageable material has not yet been considered in the human skeleton.

Understanding why females show a greater incidence of stress fractures early in life (Jones et al. 1993; Beck et al. 2000) and fragility fractures later in life (Gallagher et al. 1980; Cooper et al. 1992; Cummings et al. 2002) compared to males also may provide important insight into the biological (Duan et al. 2003) and mechanical (Winner et al. 1989) mechanisms underlying fracture risk. Sexual dimorphism is one factor that may contribute to this discrepancy (Seeman 1999; Duan et al. 2003), because bone size and shape are known determinants of bone strength (van der Meulen et al. 2001). Importantly, fracture also depends on tissue-level mechanical properties. Although it is known that sex-specific growth patterns influence bone structure, it is unclear whether variable growth patterns affect the construction of bone matrix in a way that leads to differences in tissue-level mechanical properties. The few studies that examined tissue-level

mechanical properties of long bones from adult males and females never directly tested for sex-specific differences (Currey et al. 1975; Currey 1979).

There were three major goals for this study:

1) To determine whether tissue-level mechanical properties vary with bone size in the human skeleton. In addition to tissue-level stiffness and strength, we also quantified tissue-damageability, toughness, and ductility, because these latter mechanical properties provide insight into the material response of bone when subjected to extreme load conditions such as during a fall, as well as the amount of damage accumulated within the bone when subjected to intense physical activity. Understanding why bone morphology is a risk factor for stress fractures should lead to better identification of those at risk and, ultimately, to early diagnosis, treatment, and modification of training regimens.

2) To test whether females acquire similar tissue-level mechanical properties as males by the time peak bone properties are established. We also tested whether females show a correlation between cross-sectional morphology and tissue-level mechanical properties similar to males.

3) To test whether morphological and tissue quality traits are functionally related, as this would imply there is a strong biological process in bone that co-adapts traits. We hypothesize that the morphological traits will co-vary with matrix composition and/or architectural traits that contribute to bone stiffness and strength. For slender bones, we postulate that the small cross-sectional size is compensated by higher mineralization and a proportionally greater amount of cortex. We tested this hypothesis by conducting a Path Analysis to determine whether there are functional interactions among morphological and tissue-quality traits for young adult human tibiae.

METHODS AND MATERIALS

Sample population

Tibiae of 14 female donors (12 Caucasian, 1 African-American, 1 unknown) aged 22 – 46 years (average age = 36.9 $\pm$ 8.1 yrs) and 17 male donors (15 Caucasian, 1 Hispanic, 1 African-American) aged 17 – 46 years (average age = 32.9 $\pm$ 10.4 yrs) were acquired from the Musculoskeletal Transplant Foundation (Edison, NJ, USA) and the National Disease Research Interchange (Philadelphia, PA, USA). Donor body weight and height were obtained from the source. Only donors with no known skeletal pathology were included in the study. Tibiae were freshly harvested, wrapped in wet gauze, and stored in plastic bags at –40°C.

Whole bone morphology

Tibia length (Le) was measured as the average distance between the distal articular center (the middle of the talar trochlear facet) and the two proximal articular centers (medial and lateral condyles) (Ruff 2000) using a large-capacity slide caliper with an accuracy of $\pm$2.54mm (Mantex Precision, Haglöf Inc., Madison, MS, USA). Mid-diaphyseal bone diameters in the anteroposterior ($B.Dm_{AP}$) and mediolateral ($B.Dm_{ML}$) directions at 10% intervals from 30% to 70% of the total tibia length were measured using a 300mm vernier caliper with an accuracy of $\pm$0.02mm (Fowler Company Inc., Newton, MA, USA).

Cross-sectional morphology was determined from 3-mm thick mid-diaphyseal cross-sections cut at 30, 50, and 70% of the total tibia length (Figure 2.1) using a diamond coated metallurgical saw (Model 660, South Bay Technology Inc., San Clemente, CA, USA). A calibrated image of each cross-section was obtained using a

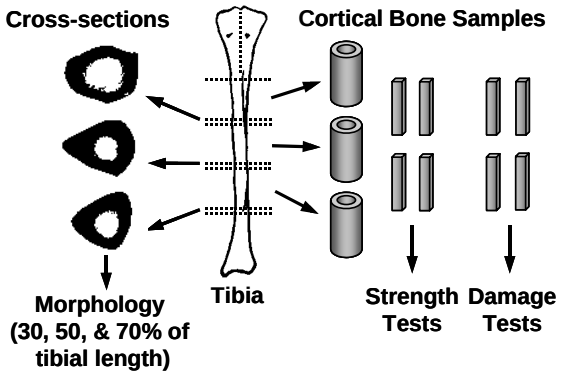

Figure 2.1. Schematic of how whole tibiae were sectioned to produce the 3mm-thick sections used for cross-sectional morphology and cortical bone samples for biomechanical testing from three diaphyseal cylindrical sections (monotonic, n = 4/tibia; damage accumulation, n = 4/tibia).

digital camera at a 0.024mm/pixel resolution. Image analysis software (IMAQ Vision Builder 6.0, National Instruments Corp., Austin, TX, USA) was used to threshold each image and quantify cortical area (Ct.Ar), total area (Tt.Ar), marrow area (Ma.Ar), polar moment of inertia (J), and cortical thickness (Ct.Th). All morphological traits were averaged over the three cross-sections for each tibia. Because the cross-section of the tibia has a non-uniform cortical thickness, the average cortical thickness was determined as 2 x Ct.Ar / (P.Pm. + E.Pm), where P.Pm and E.Pm are the periosteal and endosteal perimeters, respectively. The ratio of internal diameter to external diameter (K) has been examined previously in the context of identifying the optimal value of K that allows for minimal mass and maximal stiffness for hollow structures like long bone diaphyses (Currey et al. 1985). In this study, we tested how K varied with sex and slenderness for human tibiae. Because the non-uniform shape of the tibia diaphysis precludes measuring a single diameter directly, an estimate of the internal and external diameters was calculated for each cross-section from Ma.Ar and Tt.Ar, respectively, assuming a circular cross-section. Ct.Ar/Tt.Ar correlated negatively with K (R = -0.99, p = 0.001), as expected, indicating that the estimated internal and external diameters provided a reasonable approximation of K for the non-uniform tibia cross-sections.

Slenderness was initially calculated in the AP and ML directions as the ratio of the AP and ML section modulus values, respectively, to tibia length and body weight (Selker et al. 1989):

$$S = 1/[(J/(B.Dm/2))/(Le*BW)], \quad (1)$$

where B.Dm = bone diameter (mm), Le = tibia length (mm), and BW = body weight (kg). The section modulus has been shown to scale linearly with body mass (Selker et al. 1989). The inverse ratio was used so that a tibia with a large slenderness value is one that is thinner or gracile for the weight and height of an individual. A small slenderness value reflects a stocky or robust tibia. All morphological traits were averaged over the three cross-sections for each tibia. Slenderness was later redefined independent of body weight as the ratio of total area to tibia length (Tt.Ar/Le) for use in Path Analyses (see below).

Bone sample generation

Cortical bone samples were prepared from the diaphysis of each tibia for biomechanical testing (Figure 2.1). Three diaphyseal cylindrical sections were rough-cut into anterolateral, anteromedial, and posterior regions. From each of these regions, 1-3 prismatic beams were cut using a diamond coated metallurgical saw (Isomet, Buehler, Lake Bluff, IL, USA). The beams were machined into regular test samples using an automated CNC milling machine under constant irrigation (Modela MDX-20, Roland DGA Corp., Irvine, CA, USA). Sample width (circumferential direction) was machined to 5mm and length (longitudinal direction) was machined to 55mm for all samples. Sample height (radial direction) was 2.5mm except for 4 tibiae with thin cortices, which were machined to 2.2mm. A total of eight samples were generated from each tibia and randomly distributed to monotonic (n = 4) and damage accumulation (n = 4) test groups.

All samples were stored at –40°C in gauze saturated with phosphate buffered saline (PBS) with added calcium (Gustafson et al. 1996) and placed individually in airtight bags.

Monotonic failure properties

Tissue-level mechanical properties were assessed by loading four cortical bone samples from each tibia to failure in 4-point bending at 0.05mm/s (Figure 2.2A) using a servohydraulic materials testing system (Instron model 8872, Instron Corp., Canton, MA, USA). Specimens were submerged in a PBS solution with added calcium (Gustafson et al. 1996) and maintained at 37°C throughout all tests. Load and deflection were converted to stress and strain using the following equations which take yielding into consideration (Nádai 1950):

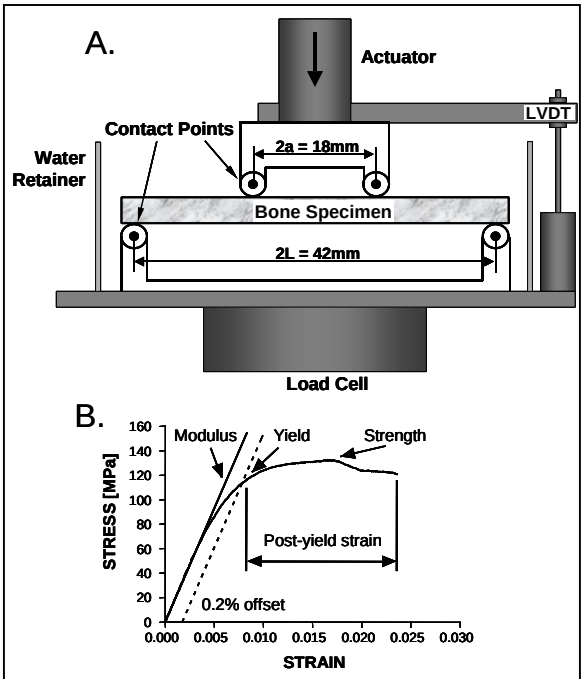

Figure 2.2. (A) Schematic of the four-point bending device shows how cortical bone samples were tested. The span between the upper contact points is 2a = 18 mm, and the span between the lower contact points is 2L = 42 mm.
(B) Typical stress-strain curve from the four-point bending monotonic tests shows how modulus, strength, post-yield strain, and total energy were calculated.

$$\sigma = 2[2M + \phi dM/d\phi]/bh^2 \quad (2)$$

$$\varepsilon = h\phi/2a = \tfrac{1}{2}\, h\Delta[(L - a)/(2a^3/3 - a^2L + L^3/3)] \quad (3)$$

where σ and ε are the stress and strain at the outer surface of the beam, M = applied moment, b = specimen width, h = specimen height, a = ½ the span between the upper two load points = 9mm, L = ½ the span between the two lower load points = 21mm, ϕ = angle

of inclination = a/ρ, and $d/d\phi$ is the derivative with respect to ϕ. The angle of inclination was written in terms of the measured deflection (Δ) by estimating the curvature (ρ) using standard beam equations. Mechanical properties were calculated from the stress-strain curves and these included modulus, strength, total energy, and post-yield strain (Figure 2.2B). Modulus was calculated from a linear regression of the initial portion of the stress-strain curve. Yield was determined using the 0.2% offset method. Post-yield strain was defined as the strain at failure minus the strain at yield. All properties were averaged over the four samples tested for each tibia.

Damage accumulation tests

Tissue damageability was assessed using a protocol designed to induce and accumulate cracks in cortical bone specimens. The accumulation of damage leads to measurable degradation of mechanical properties (Lemaãitre 1992). Therefore, the degradation of mechanical properties can be used as an index of matrix damage. Four cortical bone samples from each tibia were subjected to a fifteen cycle damage accumulation protocol (Figure 2.3A) similar to that described previously (Jepsen et al. 1997). For this protocol, "diagnostic" cycles (1, 3, 5, 7, 9, 11, 13, and 15) were interposed between "damage" cycles (2, 4, 6, 8, 10, 12, and 14). For the diagnostic cycles, the specimens were loaded in four-point bending at 0.5mm/s to 50% of the average displacement at yield (determined from the monotonic tests), held for 60 seconds, and then unloaded at 0.5mm/s. Preliminary studies indicated that this load level provided information on tissue-level mechanical properties without inducing additional damage. For the damage cycles, the specimens were loaded at 0.5mm/s to 50, 75, 100, 125, 150, 175, and 200% of displacement at yield respectively, held for 60 seconds, and then

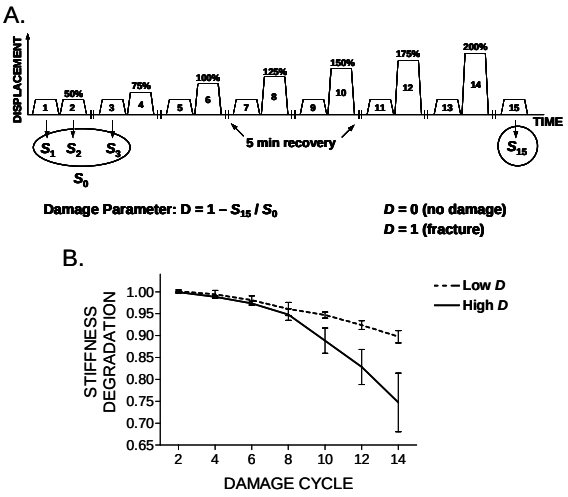

Figure 2.3. (A) A 15-cycle loading protocol was used to induce damage within machined cortical bone specimens and to measure resultant stiffness degradation. Damage was induced during cycles 2, 4, 6, 8, 10, 12, and 14 by conducting relaxation tests at increasing levels of applied displacement (expressed as a percentage of the displacement at yield). Diagnostic cycles were interposed between damaging cycles. Each damage cycle was preceded by a diagnostic cycle at 50% of displacement at yield. A 5-minute recovery period was introduced after the damage cycles to relieve residual internal stresses. **(B)** The change in stiffness calculated between sequential diagnostic tests was plotted vs. cycle number for the damage tests. The dashed curve represents a specimen showing little stiffness degradation (i.e., little damage accumulation). The solid line represents a specimen showing large stiffness degradation (i.e., more damage accumulation).

unloaded at 0.5mm/s. A 5-minute recovery period followed each damage cycle. Displacement at yield was used as a reference in the damage cycles because this parameter showed little variation among the test samples when subjected to monotonic four-point bending. The displacement at yield was 1.0mm for the samples with a height of 2.5mm and 1.07mm for the samples with a height of 2.2mm.

A mechanical measure of the amount of damage that accumulated within the test sample was quantified from the magnitude of stiffness degradation. For each diagnostic cycle, stiffness was calculated from a linear regression of the initial portion of the load-deformation curve. Specimen stiffness decreased non-uniformly with each cycle revealing increasing amounts of damage induced within each cycle and an overall damage accumulation by the end of the protocol (Figure 2.3B). At the end of the test sequence, the overall damage parameter, *D*, was calculated by comparing the stiffness of the first

and last diagnostic tests such that:

$$D = 1 - S_{15}/S_0, \quad (4)$$

where S_{15} is the stiffness of the last diagnostic cycle and S_0 is the average stiffness of the first two diagnostic cycles (S_1, S_3) and the first damage cycle (S_2).

Tissue-microstructure

To test for variation in matrix organization, bone microstructure was assessed for each sample retrieved from the damageability tests (n = 4/tibia). Samples were fixed, bulk-stained in basic fuchsin, dehydrated, and embedded undecalcified in poly-methylmethacrylate. For each sample, digital images of three transverse sections, 100μm in thickness, were taken at 10x magnification, stitched together, and traced using an interactive tablet monitor (Wacom Company, Ltd., Tokyo, Japan). Parameters measured included porosity and the area fractions of osteonal, interstitial (remodeled), and circumferential lamellar (unremodeled) tissues. Both vascular canals and resorption spaces were counted as pores. Osteonal tissue was defined as a lamellar region with a Haversian canal completely surrounded by a cement line. Data from individual test samples were averaged for each donor.

Tissue-composition

Variation in tissue-mineral density was assessed by measuring the density, ash content, and water content for each sample retrieved from the monotonic tests (n = 4/tibia). Samples were defatted using a 1:1 volume ratio of ethanol/ether for 8 hours followed by a 2:1 volume ratio of chloroform/methanol for 8 hours. The methanol residue was removed by using two changes of pure chloroform for 1 hour each. Samples were rehydrated, degassed in distilled water in a 25mm Hg vacuum for 4 hours, and then

allowed to stand at atmospheric conditions for an additional hour. Sample volume was determined using Archimedes principle by measuring the weight while the sample was suspended from a fine wire in distilled water (*submerged weight*). Samples were placed in a centrifuge for 10 minutes at 8000g with the cap of the vial closed to control humidity, and immediately weighed to obtain the *hydrated weight*. Samples were dried under vacuum at 80°C for 24 hours to constant weight and reweighed (*dry weight*). Finally, samples were ashed at 600°C for 18 hours, reweighed (*ash weight*), degassed under vacuum for 2 hours, and reweighed while suspended from a fine wire in distilled water (*submerged ash weight*). Density was calculated as (hydrated weight)/(sample volume), where sample volume = hydrated weight – submerged weight. Ash content was calculated as the ash weight normalized by the hydrated weight. Water content was calculated as (hydrated weight – dry weight) / (hydrated weight).

Statistical analysis

All data were regressed against age using linear regression analysis to identify the properties that varied significantly with age (GraphPad Prism; San Diego, CA, USA). Differences between females and males were determined using a Student's t-test with corrections applied for unequal variances (GraphPad Software, Inc; San Diego, CA USA). To determine if female and male tibiae were similarly adapted to body size, the section modulus (cross-sectional moment of inertia/bone diameter) was regressed against the product of body weight and tibia length (Ruff 2000) and the slopes were compared between sexes (ANCOVA) (GraphPad Software, Inc; San Diego, CA USA). To determine if males and females show a similar relationship between tibial cross-sectional morphology and tissue-level mechanical properties, linear regressions were performed

and slopes and intercepts between female and male regressions were compared (ANCOVA).

Since no differences were found between male and female regressions, a matrix of Pearson correlation coefficients was constructed using the combined female and male datasets. To determine whether bone morphology was related to tissue level material properties, Pearson correlation coefficients were determined between each geometrical parameter (e.g., I_{AP}, I_{ML}, J, S) and each tissue-level mechanical property (modulus, strength, total energy, post-yield strain, damageability) while taking age into consideration (Minitab, State College, PA, USA) (Di Masso et al. 1997). To test whether the morphologic traits and the tissue-level mechanical properties correlated significantly with the matrix architectural and compositional traits, Pearson correlation coefficients were calculated without correcting for age or body weight.

Path analysis

To test the hypothesis that morphological and tissue quality traits are functionally related, a Path Analysis was conducted because this allows for testing how multiple traits co-vary simultaneously (Wright 1921). Path models were constructed by specifying the directed paths among select bone traits. Directed paths identify related traits and indicate the direction of the relationship between them. The focus of this analysis is the interaction of traits and not how traits define global function. Traits were selected to test for associations between bone morphology and tissue-quality parameters. We focused on ash content given prior work in inbred mouse strains, which showed that co-variation among adult morphology and mineralization arise during post-natal growth (Price et al. 2005; Jepsen et al. 2007). Therefore, finding an association between slenderness and ash

content in the human skeleton would suggest that biological processes observed in the mouse also exist in the human skeleton. For the path model (Figure 2.4A), we postulated that relationships occur in a particular order in which slender bones (Tt.Ar/Le) are compensated by higher mineralization (ash content) and a proportionally greater amount of cortical bone. Slenderness was defined here as Tt.Ar/Le to be consistent with the studies in inbred mouse strains. Because slender tibiae tend to have a similar cortical thickness as more robust tibiae (Figure 2.4B), incorporating traits like Ct.Th or Ct.Ar into the model would not be expected to differentiate individuals with more/less bone. Rather, we used the ratio, Ct.Ar/Tt.Ar, because this trait can be related to the relative amount of tissue and it can be related to the relative expansions of the periosteal and endosteal surfaces during ontogeny. Ct.Ar/Tt.Ar also was used rather than K because the relative amount of cortical tissue can be more easily related to whole bone stiffness than the relative amount of marrow space. An arrow was also included between Ct.Ar/Tt.Ar and ash content to take into consideration the variance in ash content that was not accounted for by slenderness. Data for males and females were analyzed separately to account for the influence of dimorphic growth patterns. The generalized model (Figure 2.4A) was modified for each sex by specifying

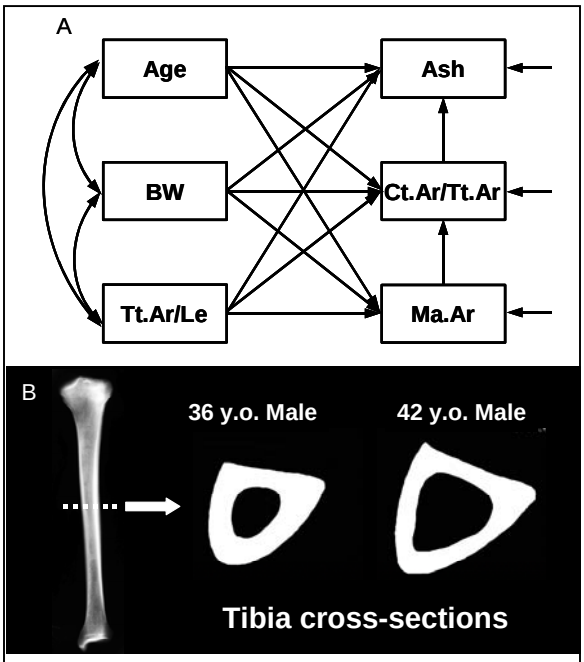

Figure 2.4. Schematic drawing of **(A)** the proposed path analysis showing all possible combinations of connections and **(B)** diaphyseal cross-sections showing the variation in size for slender (left) and robust (right) tibiae.

the minimum number of connected traits that best explained the variance in ash content and Ct.Ar/Tt.Ar.

Path coefficients, which represent the magnitude of the direct and indirect relationships between traits, were calculated using the standardized (Z-transformed) data (LISREL v.8.8; Scientific Software International, Lincolnwood, IL, USA). Male and female data were converted to Z-scores separately to eliminate size effects. Structural equations were constructed using the path coefficients to specify the interconnected relationships. Observed and model-implied covariance matrices were compared using maximum likelihood estimation and overall fit was determined by a chi-squared test. Unlike conventional null hypothesis testing, Path Analysis favors the *a priori*, theory-based model such that models are only rejected if the observed data and the expectations derived from the model do not match (i.e., if $p < 0.05$) (Grace 2006). Thus, chi-squared values with an associated *p*-value greater than 0.05 indicate that the model adequately fits the data. The Root Mean Square Error of Approximation (RMSEA) was also reported as an additional fit index. RMSEA is a measure of fit adjusted for population size and takes the number of degrees of freedom of the model into consideration (Stieger et al. 1980; MacCallum et al. 1997). For RMSEA, the *p*-value represents the significance of fit with $p < 0.05$ indicating close fit, $0.05 < p < 0.08$ indicating fair fit, and $p > 0.10$ indicating poor fit (MacCallum et al. 1997). Path Analysis as used here is similar to multivariate analysis in how the structural equations are developed. However, conventional multivariate methods seek to estimate generic fixed models (e.g., canonical correlation), and lack the flexibility required to represent the model that best matches a particular situation (i.e., directed relationships) (Grace 2006). Thus, Path Analysis allowed us to test whether

specific relationships among morphological and compositional traits exist for human tibiae.

RESULTS

Sexual dimorphism among sample population

The sample population showed broad ranges of body size, body stature, and bone morphology values (Table 2.1). Female donors were shorter than males (163 $\pm$ 6 cm vs. 178 $\pm$ 4 cm; $p < 0.0001$), but were not different in body weight (74 $\pm$ 21 kg vs. 84 $\pm$ 25 kg; $p < 0.2$). Adult females achieved a different bone size and shape compared to males: female tibiae were smaller (J, Ct.Ar, B.Dm) and more slender (S_{AP}, S_{ML}) compared to males (Table 2.1). Females and males showed similar slopes for the regression of $J/B.Dm_{AP}$ versus the product of body weight and tibia length ($p < 0.17$, ANCOVA). However, females showed a significantly smaller intercept compared to males ($p < 0.0001$, ANCOVA), indicating that, for all body sizes, female tibiae were smaller relative to body size (i.e., less robust) compared to males (Figure 2.5). Similar results were observed when using $J/B.Dm_{ML}$.

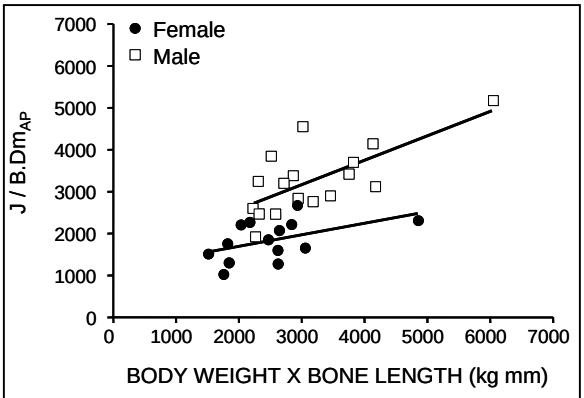

Figure 2.5. Variation in the section modulus ($J/B.Dm_{AP}$ mm^3) vs. body size (body weight x tibia length) for adult female and male tibiae.

Table 2.1. Variation in body size, body stature, and tibia morphology for young adult males and females.

PROPERTY	MALE	FEMALE	*p* -value
Age [yr]	32.9 ± 10.4	36.86 ± 8.08	0.2
Body Weight, BW [kg]	83.8 ± 25.1	73.7 ± 21.1	0.2
Body Height [cm]	177.7 ± 4.3	163.5 ± 5.9	<0.0001
Body Mass Index, BMI [kg/m^2]	26.7 ± 8.0	27.4 ± 7.2	0.8
Tibia Length, Le [cm]	38.1 ± 1.9	33.9 ± 2.8	0.0001
Cortical Area, Ct.Ar [mm^2]	355.9 ± 55.2	248.9 ± 39.9	<0.0001
AP Diameter, B.Dm$_{AP}$ [mm]	31.2 ± 2.5	26.5 ± 2.7	<0.0001
ML Diamter, B.Dm$_{ML}$ [mm]	24.3 ± 2.3	20.8 ± 2.4	0.0003
AP Moment of Inertia, I$_{AP}$ [mm^4]	34,390 ± 10,149	8,161 ± 2,691	<0.0001
ML Moment of Inertia, I$_{ML}$ [mm^4]	17,250 ± 5,945	16,615 ± 5,322	<0.0001
Polar Moment of Inertia, J [mm^4]	51,640 ± 15,886	24,776 ± 7,917	<0.0001
AP Section Modulus, J/B.Dm$_{AP}$ [mm^3]	3,279 ± 819	1,836 ± 473	<0.0001
ML Section Modulus, J/B.Dm$_{ML}$ [mm^3]	4,188 ± 907	2,352 ± 614	<0.0001
AP Slenderness, S$_{AP}$ [1/mm^2/kg]	9.9 ± 2.0	14.1 ± 4.1	0.002
ML Slenderness, S$_{ML}$ [1/mm^2/kg]	7.7 ± 1.5	11.1 ± 3.6	0.004

Modulus and strength showed little variation among individuals (coefficient of variation, COV = 9.99% and 4.84%, respectively). However, post-yield strain (COV = 21.95%), total energy (COV = 21.96%), and the damage parameter (COV = 21.13%) all showed large variability among the samples. No differences in the average tissue-level mechanical properties were observed between females and males (Table 2.2), even when corrected for differences in donor age. This included measures of stiffness (modulus), strength, ductility (failure strain, post-yield strain), toughness (energy-to-failure), and total stiffness degradation. Further, the changes in stiffness after each damage cycle were similar for males and females (Figure 2.6). These results indicated that the loading protocol induced similar amounts of damage at each load step for females and males. Thus, males and females showed similar tissue-level monotonic properties.

Table 2.2. Tissue-level mechanical properties for young adult female and male tibiae.

MECHANICAL PROPERTY	FEMALE	MALE	*p* -value
Modulus, GPa	17.5 ± 1.8	17.1 ± 1.7	0.5
Yield Strain	0.008 ± 0.0004	0.008 ± 0.0003	0.7
Yield Stress, MPa	106.2 ± 10.0	104.4 ± 7.8	0.6
Post-yield Strain	0.023 ± 0.006	0.025 ± 0.005	0.3
Failure Strain	0.031 ± 0.006	0.033 ± 0.005	0.3
Strength, MPa	133.8 ± 8.4	130.1 ± 4.2	0.2
Energy-to-Failure, MPa	3.1 ± 0.7	3.2 ± 0.7	0.3
Stiffness Degradation	0.18 ± 0.04	0.17 ± 0.03	0.6

Age-related changes for tissue-level mechanical properties and tibia size

A significant, positive correlation was observed between tibia slenderness in the AP ($R^2 = 0.31$, $p < 0.02$) and ML ($R^2 = 0.24$, $p < 0.05$) directions and age. However, I_{AP}, I_{ML}, and J did not vary with age suggesting that the variation in slenderness with age was due largely to higher body weight and BMI ($R^2 = 0.29$-0.32, $p < 0.03$) values for the older individuals. Females and males showed similar regressions for tissue modulus, strength, post-yield strain, and energy-to-failure versus age (Figure 2.7). The traits that showed a significant correlation with age were strength, post-yield strain, failure strain, energy-to-failure, *D*, and S_{AP}. This data suggested that while the tibia became more slender relative to body size with age, the cortical tissue became progressively less strong and less ductile (i.e., more brittle) with age.

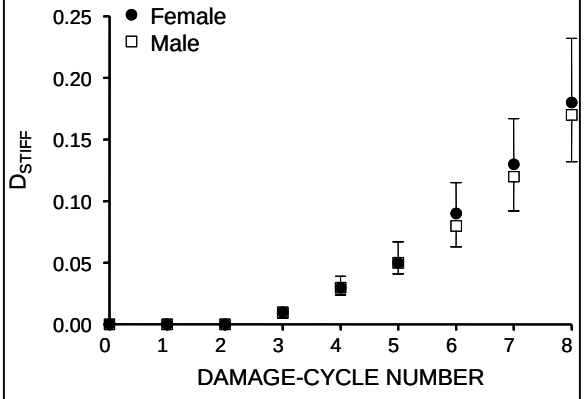

Figure 2.6. Changes in stiffness for males and females. A plot of stiffness degradation, D_{STIFF}, for each diagnostic cycle in the damage-accumulation protocol. Females and males show similar curves. Data are expressed as means ± standard deviations and were not age-corrected.

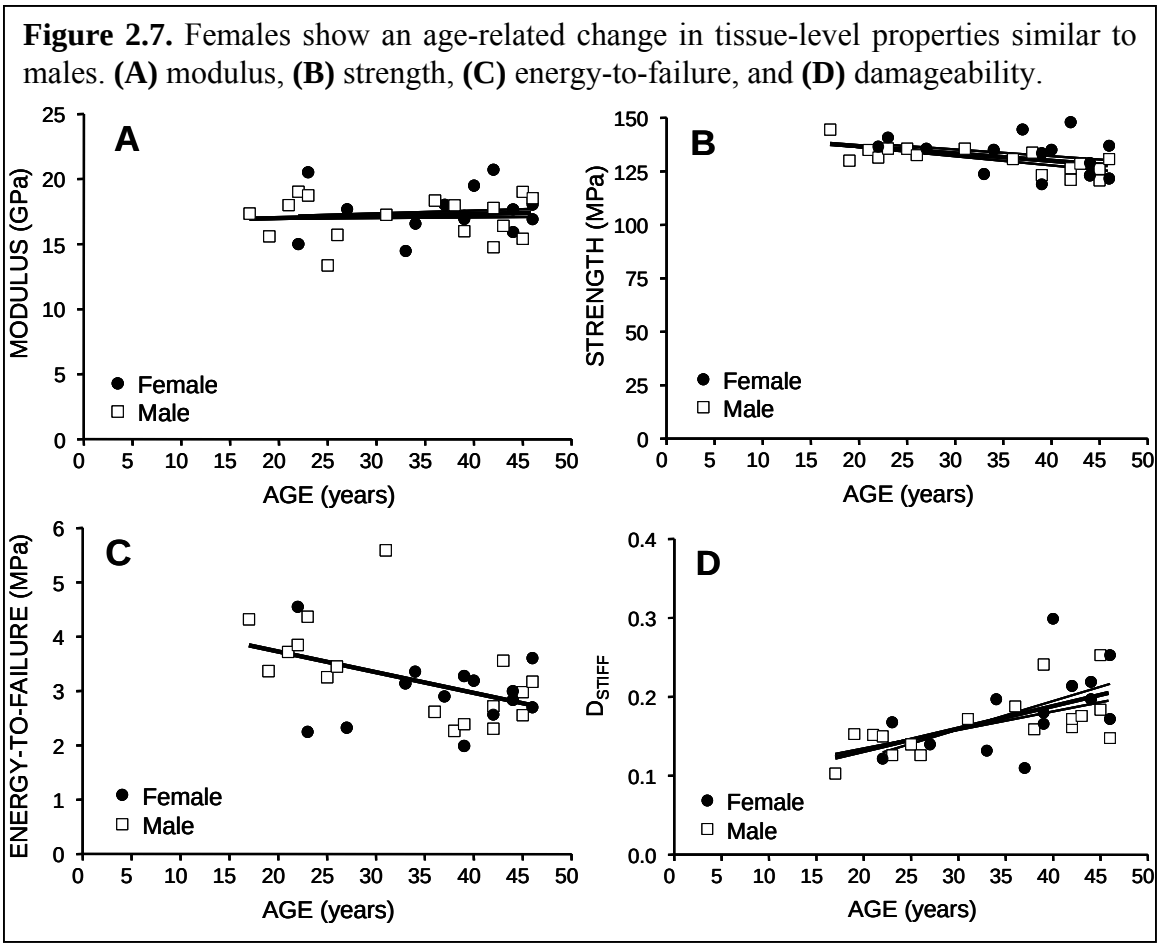

Figure 2.7. Females show an age-related change in tissue-level properties similar to males. **(A)** modulus, **(B)** strength, **(C)** energy-to-failure, and **(D)** damageability.

Correlation between bone morphology and tissue-level mechanical properties

The tissue-level mechanical properties were regressed against bone morphological traits and no significant differences in slopes were found for females and males. A correlation analysis (Table 2.3), which was conducted using the combined male and female data sets, showed that tissue-level modulus decreased with increasing bone section modulus ($J/B.Dm_{AP}$, $J/B.Dm_{ML}$), post-yield strain increased with increasing bone diameter ($B.Dm_{AP}$), and tissue-damage (*D*) increased with increasing tibia slenderness (S_{AP}, S_{ML}). The significant regressions are shown in Figure 2.8. The amount of overlap between the female and male datasets depended on whether the bone morphology traits were adjusted for body size. For unadjusted traits like diameter and J/B.Dm, the female

data simply extended the relationships observed for the males (Figure 2.8A,B). For the regression involving bone slenderness, which is adjusted for body weight and tibia length, the female data overlapped substantially with the male data (Figure 2.8C). These correlations, which were independent of age, indicated that a narrower bone was comprised of tissue that failed in a more brittle manner and accumulated more damage.

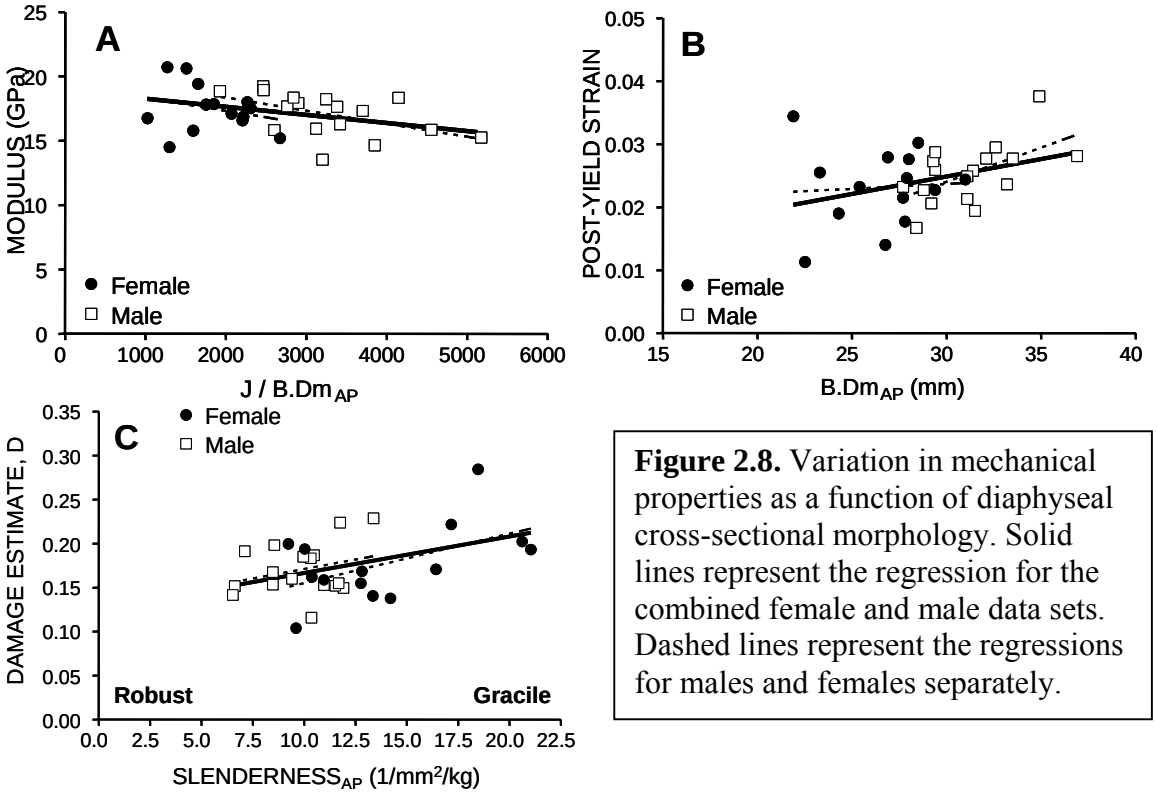

Figure 2.8. Variation in mechanical properties as a function of diaphyseal cross-sectional morphology. Solid lines represent the regression for the combined female and male data sets. Dashed lines represent the regressions for males and females separately.

Table 2.3. Correlation matrix between morphological traits and tissue-level mechanical properties. Combined male and female data sets. First row = Pearson correlation coefficient. Second row = *p*-value. Damage = Stiffness degradation. Bold entries denote significant relationships ($p \leq 0.05$).

	MODULUS	STRENGTH	PY STRAIN	ENERGY	DAMAGE
$B.Dm_{AP}$	-0.13 (0.50)	-0.15 (0.40)	**0.35** **(0.05)**	0.34 (0.06)	-0.12 (0.50)
$B.Dm_{ML}$	-0.13 (0.50)	-0.17 (0.40)	0.29 (0.12)	0.28 (0.13)	-0.03 (0.80)
Ct.Ar	-0.25 (0.20)	-0.18 (0.30)	0.31 (0.09)	0.30 (0.10)	-0.24 (0.20)
J	-0.33 (0.07)	-0.25 (0.20)	0.27 (0.14)	0.24 (0.20)	-0.24 (0.20)
J / Le	**-0.35** **(0.05)**	-0.26 (0.20)	0.26 (0.20)	0.22 (0.20)	-0.26 (0.20)
$J / Width_{AP}$	**-0.36** **(0.04)**	-0.25 (0.20)	0.22 (0.20)	0.18 (0.30)	-0.27 (0.10)
$J / Width_{ML}$	**-0.36** **(0.05)**	-0.26 (0.20)	0.24 (0.20)	0.20 (0.30)	-0.30 (0.10)
S_{AP}	0.25 (0.20)	-0.05 (0.80)	-0.10 (0.60)	-0.09 (0.70)	**0.43** **(0.02)**
S_{ML}	0.27 (0.10)	-0.04 (0.80)	-0.13 (0.56)	-0.11 (0.60)	**0.44** **(0.01)**

Correlation between tissue-level mechanical properties and tissue-quality

Significant correlations were observed between the tissue-level mechanical properties and several of the matrix compositional and micro-structural traits of the combined male and female datasets, as expected (Table 2.4). Tissue-modulus (Figure 2.9A) and strength both increased with ash content, whereas post-yield strain (Figure 2.9B) and toughness decreased. Modulus, strength (Figure 2.9C), toughness, post-yield strain all decreased with increasing porosity, whereas the damage parameter increased (Figure 2.9D). The area fraction of osteonal tissue and unremodeled tissue showed no significant correlations with any of the tissue-level mechanical properties.

Figure 2.9. Significant correlations were observed among tissue-level mechanical properties and matrix compositional and microstructural traits. Linear regressions are shown for **(A)** tissue modulus vs. ash content, **(B)** post-yield strain vs. ash content, **(C)** strength vs. porosity, and **(D)** the damage parameter vs. porosity. The thick, solid line represents the regression for the combined male and female dataset.

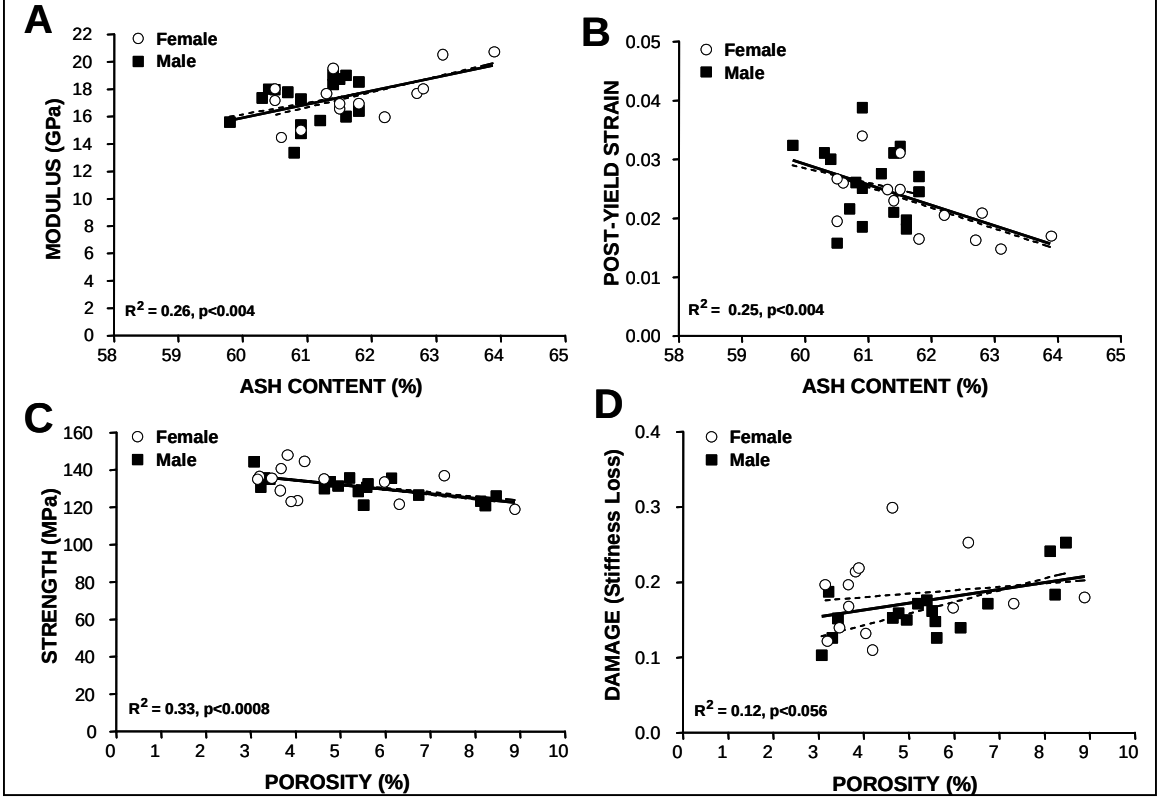

Table 2.4. Pearson correlation coefficients relating tissue microstructure and composition with tissue-level mechanical properties (combined males and females). *p*-values shown in parentheses. Bold entries denote significant relationships ($p < 0.05$).

	MODULUS	STRENGTH	PY STRAIN	ENERGY	DAMAGE
TISSUE DENSITY	0.18 (0.34)	0.10 (0.58)	-0.01 (0.95)	0.02 (0.92)	**0.37 (0.04)**
ASH CONTENT	**0.51 (0.004)**	0.3 (0.10)	**-0.50 (0.004)**	**-0.35 (0.05)**	0.21 (0.27)
WATER CONTENT	0.26 (0.16)	-0.05 (0.80)	0.01 (0.95)	-0.03 (0.88)	-0.07 (0.72)
TOTAL POROSITY	-0.17 (0.35)	**-0.57 (0.001)**	-0.23 (0.21)	-0.33 (0.07)	0.35 (0.06)
OSTEONAL TISSUE	0.17 (0.38)	-0.17 (0.35)	-0.02 (0.91)	-0.04 (0.84)	0.28 (0.12)
UNREMODELED TISSUE	-0.03 (0.86)	0.13 (0.50)	-0.10 (0.61)	-0.06 (0.76)	-0.09 (0.65)

Correlation between bone morphology and tissue-quality

Linear regression analyses conducted using uncorrected data showed significant correlations between several bone morphological traits and measures of tissue composition and microstructure (Table 2.5). Ash content correlated negatively with several traits including Tt.Ar/Le (a measure of bone slenderness) (Figure 2.10A) and Ma.Ar (Figure 2.10B), indicating that slender bones (low Tt.Ar/Le and Ma.Ar) were constructed of tissue with a higher degree of mineralization. Total porosity correlated negatively with Ct.Ar/Tt.Ar and positively with K, indicating that tibiae with a proportionally larger amount of cortex relative to overall bone size showed a reduced amount of porosity. K was similar ($p < 0.88$, t-test) for males (0.61 ± 0.04) and females (0.61 ± 0.03) and the overall range was 0.56 – 0.70. The amount of unremodeled tissue decreased with Tt.Ar/Le, indicating that smaller bones tended to have more unremodeled tissue.

Figure 2.10. Relationships between bone morphology and matrix composition and microstructural traits. Linear regressions are shown for **(A)** ash content vs. Tt.Ar/Le (slenderness) and **(B)** ash content vs. marrow area. The thick, solid line represents the regression for the combined male and female dataset.

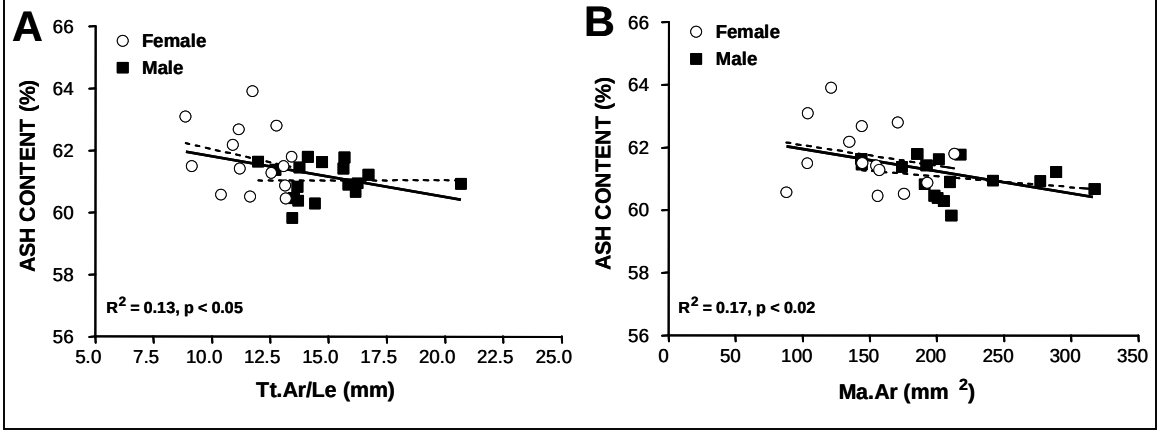

Table 2.5. Pearson correlation coefficients relating tissue microstructure and composition with physical bone traits (combined male and female datasets). *p*-values shown in parentheses. Bold entries denote significant relationships ($p < 0.05$).

	Tt.Ar	Ct.Ar	Ma.Ar	Tt.Ar/Le	Ct.Ar/Tt.Ar	K	I_{AP}	$I_{AP}/(B.Dm_{AP}/2)$
Tissue density	-0.21 (0.26)	-0.24 (0.20)	-0.14 (0.45)	-0.16 (0.40)	-0.07 (0.71)	0.06 (0.75)	-0.25 (0.18)	-0.26 (0.17)
Ash content	**-0.43 (0.02)**	**-0.38 (0.03)**	**-0.42 (0.02)**	**-0.36 (0.05)**	0.17 (0.37)	-0.17 (0.38)	**-0.37 (0.04)**	**-0.38 (0.04)**
Water content	0.20 (0.29)	0.25 (0.17)	0.09 (0.63)	0.14 (0.47)	0.10 (0.59)	-0.10 (0.60)	0.24 (0.20)	0.21 (0.26)
Total porosity	0.23 (0.22)	0.10 (0.58)	**0.37 (0.04)**	0.29 (0.11)	**-0.46 (0.01)**	**0.45 (0.01)**	0.20 (0.17)	0.14 (0.45)
Osteonal tissue	0.04 (0.82)	-0.06 (0.73)	0.18 (0.33)	0.06 (0.74)	-0.32 (0.08)	0.31 (0.09)	0.04 (0.85)	-0.02 (0.91)
Unremodeled tissue	**-0.38 (0.03)**	-0.29 (0.11)	**-0.45 (0.01)**	**-0.40 (0.03)**	0.33 (0.08)	-0.33 (0.07)	-0.33 (0.07)	-0.29 (0.11)

Path analysis

Path Analysis was conducted to test whether the tissue-quality traits were functionally related to the morphological traits. For males, the final path model included all traits from the generalized model (Figure 2.4A), but with 4 fewer connections (Figure 2.11A). The chi-square ($\chi^2 = 4.2$, $p < 0.52$) and RMSEA ($p = 0.00$) values both indicated that there was an excellent fit between the data and the path model. The large path coefficients between body weight and Ma.Ar and between age and ash content indicated that body weight and age were important covariates for the males. Holding these covariates fixed revealed that bone slenderness (Tt.Ar/Le) was functionally related to ash content and the relative amount of cortical tissue (Ct.Ar/Tt.Ar). The path coefficients were calculated based on Z-transformed data and thus reflect the number of standard deviation changes in a trait arising from a 1 standard deviation change in slenderness. The path coefficients among the morphological traits were large, as expected. When all direct and indirect paths were taken into consideration, a 1 standard deviation decrease in

Tt.Ar/Le was associated with a 0.76 standard deviation increase in Ct.Ar/Tt.Ar. This indicated that more slender bones tended to have a cortex that occupied proportionally more space. This path model accounted for 65% of the variation in Ma.Ar and 92% of the variation in Ct.Ar/Tt.Ar. Furthermore, there was a large path coefficient between Ct.Ar/Tt.Ar and ash content. Although the direct path between slenderness and ash content showed a weak coefficient of -0.13, when the indirect paths through Ct.Ar/Tt.Ar and Ma.Ar were considered the relationship between slenderness and ash content was negative with an overall path coefficient of -0.41. Using this path model, 48% of the variation in ash content among the males was explained based on bone morphology. The path model thus indicated that slender male tibiae were compensated by a higher degree of mineralization and a proportionally greater amount of cortex.

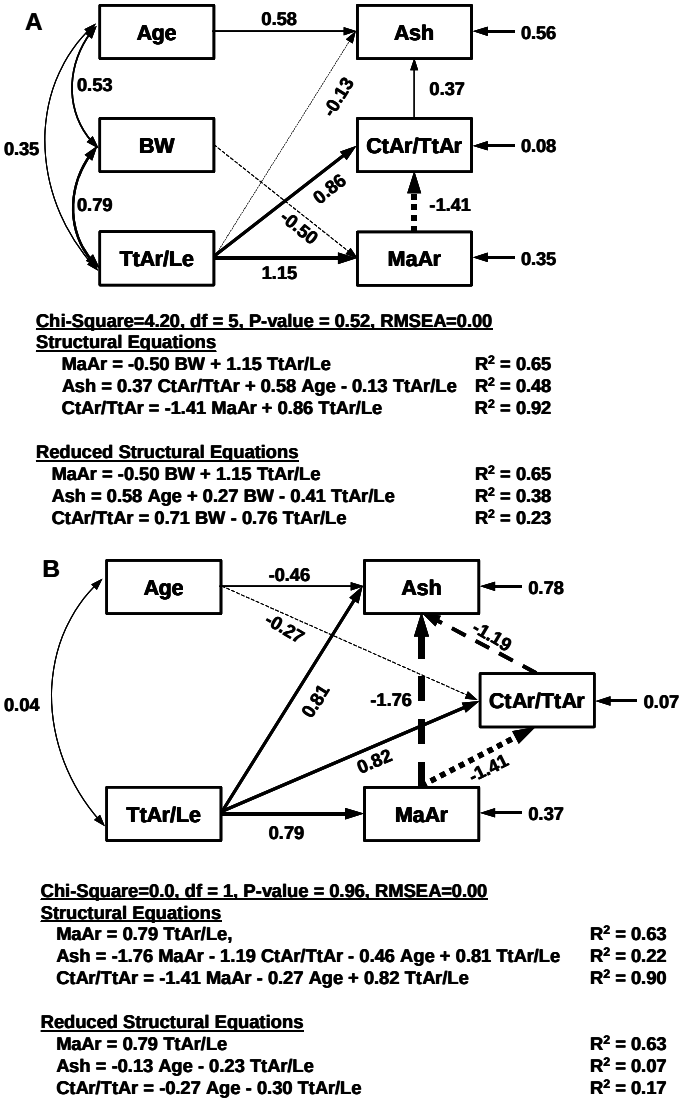

Figure 2.11. Path analysis (with least number of variables and connections) showing traits, connections between traits, and path coefficients for **(A)** males and **(B)** females.

For females, the general path model (Figure 2.4A) was modified substantially to arrive at a model that adequately fit the data. The final path model for females (Figure 2.11B) was different than the males. Body weight had only a minor influence on the relationships among traits and consequently this variable was removed from the path model. The path coefficients among Tt.Ar/Le, Ma.Ar, and Ct.Ar/Tt.Ar were large and accounted for 63-90% of the variation in Ma.Ar and Ct.Ar/Tt.Ar, similar to that observed for the males. Unlike the males, a connection between Ma.Ar and ash content was required for the female data and the path coefficient was quite large (-1.76). When the path model for the males was run with this connection, the path coefficient between Ma.Ar and ash content was only 0.07 and there was a decrease in the overall fit of the model. This indicated that this path was unique for the female data. This model explained 22% of the variation in ash content among the females, which was only half of that explained for the males. Nevertheless, when age was held constant, a 1 standard deviation decrease in Tt.Ar/Le was associated with a 0.23 standard deviation increase in ash content and a 0.30 standard deviation increase in Ct.Ar/Tt.Ar. Thus, like the males, slender female tibiae were also associated with a higher degree of mineralization and a proportionally greater amount of cortical bone.

The Path Analysis was repeated by replacing Ct.Ar/Tt.Ar with K. This analysis resulted in nearly identical path coefficients and had the same explanatory power for ash content. The only difference was the path coefficients immediately connecting with K were opposite in sign to those determined for Ct.Ar/Tt.Ar, as expected (data not shown).

DISCUSSION

Morphological and tissue-level mechanical traits are related

Tissue-level mechanical properties, including measures of fragility and damageability, were assessed for cortical bone samples that were machined from the diaphyses of young adult male and female tibiae. The current results, and those of others, indicated that not all cortical tissue was constructed in the same manner. The mechanical properties of cortical tissue vary with age (Currey et al. 1975; Burstein et al. 1976; Currey 1979; McCalden et al. 1993), across species (Currey 1979), among bones of the same individual (Papadimitriou et al. 1996), and among anatomical sites within the same bone (Riggs et al. 1993; Skedros et al. 2003). Here we showed that the average mechanical properties of cortical tissue also varied as a function of the overall size of the bone. Positive correlations were observed between measures of bone size ($B.Dm_{AP}$) and measures of tissue ductility (post-yield strain, total energy) and negative correlations were observed between bone size (moment of inertia, section modulus) and tissue modulus. This coupling between bone morphology and tissue-level mechanical properties has been attributed to an adaptive response of bone (Currey 1979; Ferretti et al. 1993; Jepsen et al. 2001). The goal of this adaptive response is to ensure that morphology and quality together meet mechanical demands. This coupling was observed when comparing bones subjected to widely varying mechanical demands from different species (Currey 1979) and has also been used to explain the maturation of bone during growth (Brear et al. 1990; Carrier et al. 1990; Heinrich 1999; Ferretti et al. 2003). Our current results suggested that this coupling might also exist for a particular bone (tibia) within the same species (human). Additional studies are needed to determine if similar relationships

between morphology and quality exist for other long bones (e.g., femur, humerus, and radius).

The variation in long bone slenderness has been attributed to genetic and environmental factors influencing growth and development (Christian et al. 1989) and has been implicated as a risk factor for osteoporotic fracture (Kiel et al. 2001). The data provide a new paradigm that also may explain why military recruits (Giladi et al. 1987; Milgrom et al. 1989; Beck et al. 1996) and athletes (Crossley et al. 1999) with narrow bones show a higher incidence of stress fractures compared to individuals with wide bones. Individuals with narrow tibiae were previously thought to show increased fatigue damage during intense training because the smaller bone size would lead to an overload situation (i.e., higher tissue level stresses) (Milgrom et al. 1989; Beck et al. 1996; Crossley et al. 1999). This interpretation was based on the assumption that tissue mechanical properties did not vary among individuals. However, the current results indicated that tissue-level mechanical properties do vary among individuals. Specifically, the data suggest that there are at least two important tissue-level mechanical property variations that need to be considered to understand why bone size is a risk factor for stress fractures. Narrower tibiae were comprised of tissue that was more brittle (low total energy) and was prone to accumulate more damage compared to tissue from wider tibia. Having tissue that is more or less damageable may be inconsequential during day-to-day activities. However, tissue-level mechanical properties like total energy and ductility become particularly important in defining the response of bone to an extreme loading condition, such as that expected during military training or during a fall. Total energy defines the amount of energy required to break a bone (important during a fall) and

ductility and damageability define the amount of damage accumulated under overload or repetitive loading (important during military training). Further, tissue stresses would be expected to remain higher for narrow tibiae loaded in bending or torsion. Moment of inertia is related to the external diameter raised to the fourth power. Because whole bone stiffness and strength are correlated with moment of inertia (Selker et al. 1989; van der Meulen et al. 2001), a bone with a large external diameter should also show large overall stiffness and strength values. However, the ~30% variation in tissue modulus (Table 2.2) did not fully compensate for the ~100% variation in the moment of inertia or the section modulus (Table 2.1) (van der Meulen et al. 2001). Thus, *in situ* damage accumulation may elicit a biological response (remodeling) that, coupled with the higher tissue stresses, exacerbates the fatigue process (Mori et al. 1993; Burr et al. 1997). Consequently, individuals with narrow tibia may be at higher risk of stress fractures because of higher *in vivo* tissue stresses (overloading) coupled with tissue that is more prone to accumulating damage.

The relationship between morphology and tissue-level mechanical properties observed in the human skeleton was consistent with that observed for the mouse skeleton (Jepsen et al. 2001). In both the mouse and human skeletons, genetic heterogeneity leads to variability in adult bone morphology and tissue level mechanical properties. A comparison of femora from A/J and C57BL/6J (B6) inbred strains showed that A/J femora were more slender than B6 as a result of the two strains having similar bone lengths, but A/J having a significantly smaller cross-sectional size and shape (Jepsen et al. 2001). Despite the difference in bone size, the two strains showed similar whole bone stiffness values. The variability in bone slenderness was inversely related to mineral

content suggesting that bone morphology and mineral content were coordinately regulated so whole bone stiffness appropriately matched the mechanical demands imposed by weight bearing. However, as a result of regulating mineral content to match bone size, A/J femora failed in a brittle manner and showed poor fatigue properties. In the human skeleton, smaller bones were stiffer and less ductile. Thus, a reciprocal relationship was observed between bone stiffness and ductility for both skeleton systems. This reciprocal relationship has been extensively reported for cortical bone (Currey 1984), and it is thought to be a result of the nature of the compositional and structural factors that can be modulated on a biological level (Portigliatti Barbos et al. 1984; Martin et al. 1993; Skedros et al. 2003; Skedros et al. 2004) . Although variation in mineral content may have explained the differences in brittleness for the mouse skeleton, we expect that the human skeleton will be more complex and that the variation in tissue-level mechanical properties will be a consequence of variable composition (mineral, collagen, water) as well as microarchitecture (lamellae, osteon size, porosity).

The calculated bending modulus and strength values, which were determined from machined bone samples and were thus quantified in a manner that was independent of bone size, were consistent with bone tensile properties (Burstein et al. 1976), as expected. Test samples were randomly selected in order to obtain representative mean values for each tibia and the variation in mechanical properties within each tibia was similar to the variability observed across tibiae. Thus, we believe that the mean values reported here represent the generalized tissue-level mechanical behavior for each tibia.

Compared to back-calculating tissue-level mechanical properties from whole bone failure tests, the current method of measuring tissue-level mechanical properties directly

from machined samples provided a broader range of mechanical properties that were needed to better understand why bone size is a risk factor for stress fractures. The mechanical properties included measures of ductility (i.e., post-yield strain, total energy) as well as an independent measure of damageability (i.e., the damage parameter). These properties were chosen since they were relevant for understanding the material response of bones subjected to the vigorous, repetitive loading associated with military training and running. Post-yield strain and total energy represent measures of tissue ductility and were assessed to discriminate between ductile and brittle failure modes. Materials that fail in a brittle manner show low post-yield strain and total energy values. Variation in the ductility of cortical bone arises from differences in the initiation, accumulation, propagation, and coalescence of damage in the form of microcracks (Currey et al. 1992; Cowin 2001). Variation in the damage parameter reflected differences in the amount of damage accumulated within the tissue and/or differences in the way damage degraded tissue stiffness. The damage parameter correlated negatively with post-yield strain and total energy (R^2 = 0.22-0.25, $p < 0.05$) indicating that cortical tissue that failed in a brittle manner also tended to have higher tissue damageability or, accumulate more damage. Although the *ex vivo* bending tests do not necessarily reflect the *in vivo* loads imposed on the tibia (Lanyon et al. 1975; Ruff 1984; Selker et al. 1989; Burr et al. 1996), the bending loads were expected to induce a combination of tensile, compressive, and shear damage (Boyce et al. 1998) that may be sufficiently complex to represent a generalized variation in bone quality among human tibiae. Further, the bending formula that was used to convert load and deflection to stress and strain, because it accounted for nonlinear effects (Nadai 1950), provided a more appropriate estimate of bending strength compared to

standard beam theory (Burstein et al. 1972).

Sexual dimorphism affects tibia morphology but not tissue-level mechanical properties

The data indicated that the tibial diaphyses of females and males were composed of material having similar tissue-level mechanical properties, and that the mechanical properties degraded with age at similar rates over the age range of 17-46 years. Further, males and females showed a similar relationship between tissue-level mechanical properties and cross-sectional morphology. These data suggested that the genetic (Iscan et al. 1984; Turner et al. 1990; Wiren et al. 2004) and environmental (Gordon et al. 1994) factors contributing to sex-specific growth patterns affected adult tibial cross-sectional size and shape, but did not affect bone matrix construction, mineralization, and organization in a way that significantly affected tissue-level mechanical properties.

Our data confirm that males and females achieve similar adult tissue-level mechanical properties during growth, which has only been assumed in prior analyses (Ruff 2000). Prior studies reported mechanical property values for young adults, but did not directly compare data for females and males (Currey et al. 1975; Currey 1979). Because the bone samples used in this study were machined from within the middle of the cortex, the tissue that was added to the subperiosteal or subendosteal surfaces during and after puberty was likely not tested in our study. Thus, the current data could not be used to determine if sex-specific differences in tissue-quality exist following puberty. This data reflects the tissue properties established early in life, plus the modifications to these properties associated with osteonal-remodeling and cortical drift (Enlow 1963) during the ensuing years.

The data may also help explain why age is another risk factor for stress fractures

(Brudvig et al. 1983; Shaffer et al. 1999). Although the current data were collected by cross-sectional means, the mechanical property versus age regressions implied that *in situ* tissue-level mechanical properties begin to decline early in adulthood for males and females, even before bone loss becomes measurable (Parfitt 1984). This was consistent with previous studies (Melick et al. 1966; Currey et al. 1975; Burstein et al. 1976; Burstein et al. 1976; McCalden et al. 1993) and indicated that cortical bone becomes less ductile (i.e., more brittle) and weaker with age and that these changes began early in life. Stiffness and strength typically increase until about 30 years of age and then decline slowly thereafter (Currey et al. 1975). In contrast, the post-yield behavior of bone degrades rapidly with age, and this loss in ductility is a primary reason why bone tissue becomes progressively more brittle (McCalden et al. 1993) and shows lower impact strength (Currey 1979). The decline in tissue-level strength, ductility, and damageability have been attributed to age-related changes in ash content (Currey 1979), osteonal remodeling (Evans et al. 1970), collagen quality (Wang et al. 2002; Wang et al. 2003), mineral density distribution (Reid et al. 1987), and porosity (Currey 1979; McCalden et al. 1993). Thus, even in the young adult age range, the amount of damage accumulated under vigorous loading regimens would be expected to increase with age. Beyond 50 years of age, the mechanical properties of females and males may follow different degradation pathways associated with sex-specific bone loss patterns (McCalden et al. 1993). This variation in tissue ductility may increase the susceptibility of stress fracture risk for recruits that enter into military training at an older age.

The similarity in tissue-level mechanical properties for adult men and women may be explained based on early transverse bone-growth patterns. During pre-pubertal

growth, the periosteal and endosteal surfaces of female and male long bone diaphyses follow nearly identical expansion rates (Garn 1970). Despite the dimorphic transverse bone-growth patterns arising during puberty (Garn 1970), the long bones of both sexes appear to be constructed in a way so that by 20 years of age bone size is properly adapted to satisfy loading demands associated with body weight (Moro et al. 1996; Sumner et al. 1996; Ruff 2003; Forwood et al. 2004). Whole bone stiffness and peak tissue strains are thus kept at proper levels (Frost 1987) during growth simply by depositing enough tissue on the periosteal and endosteal surfaces to keep pace with weight gain. Thus, because there is no discrepancy in the relationship between bone size and body size during growth, males and females can construct the tibia with similar tissue-level mechanical properties without a loss in mechanical function.

The relationship between bone size (section modulus) and body size (body weight x tibia length), which was established previously by Ruff (Ruff 2000) and was based on the resistance of bone to bending loads, was significantly different between males and females (Table 2.1, Fig. 2.5). Similar differences were observed by others (Geusens et al. 1991; Looker et al. 2001; Duan et al. 2003; Nieves et al. 2005). Given that adaptive factors appear to match bone size to body size during growth (Moro et al. 1996; Sumner et al. 1996; Ruff 2003; Forwood et al. 2004), this difference suggests that these adaptive factors no longer work the same way when men and women reach adulthood. This latent difference in bone adaptation may be due to differences in post-pubescent endocrine factors that regulate the relative amounts of bone added to the periosteum versus the endosteum (Duan et al. 2003). Thus, adult females would be expected to accumulate more damage under intense loading compared to males and this may be a contributing

factor to the larger stress fracture incidence for female athletes and military recruits (Friedl et al. 1992; Beck et al. 1996).

Morphological and tissue-quality traits are functionally related

The bivariate analysis confirmed the hypothesis that morphological traits correlate or co-vary with matrix compositional and microstructural traits in the human skeleton. The Path Analysis further revealed that the relationship between bone slenderness and ash content observed in the bivariate correlation analysis was actually part of a larger association that involved the relative size of the marrow space and thus the proportion of the diaphysis that was occupied by cortical tissue (i.e., the inverse of K). These associations were independent of body weight, age, and sex. Path Analysis, which is based on conditional covariances (Wright 1921), provides a rigorous statistical approach to reveal relationships among physical bone traits when co-factors such as age and body size can obscure these relationships. Age and body size were easily corrected in the current study because the physical traits (e.g., Tt.Ar, Ct.Ar, ash content, porosity) varied linearly with each co-factor for this young-adult population (data not shown).

The functional relationships between bone morphology and mineralization observed in this study are consistent with prior work comparing various bones subjected to radically different mechanical loading environments from different species (Currey 1979). These functional interactions have also been reported for long bones and vertebrae from genetically distinct inbred mouse strains (Tommasini et al. 2005; Jepsen et al. 2007), phalangeal segments from the brown bat (Papadimitriou et al. 1996), and during long bone growth (Carrier 1983; Brear 1990; Heinrich 1999). Our path model focused primarily on ash content (Jepsen et al. 2001) as a measure of matrix composition, because

this particular trait is an important determinant of tissue-level stiffness and ductility. However, it is entirely possible that variation in tissue stiffness could arise by variation in other matrix components, such as collagen architecture and porosity (Currey 1988; Martin et al. 1989), and these factors could be incorporated into similar path models. When body size and age were taken into consideration, slender tibiae were also found to have less porosity and a greater area fraction of unremodeled tissue compared to more robust tibiae. The negative correlation between bone slenderness and the area fraction of unremodeled tissue is consistent with the findings of Ural and Vashishth who examined bone samples over a much larger age-range and showed that slender tibiae contain a greater amount of interstitial tissue compared to more robust tibiae (Ural et al. 2006). A lower amount of remodeling may partly explain the increase in ash content in smaller bones. Because ash content is a tissue averaged measure of the amount of mineral packed into the matrix, further examination using backscatter electron (BSE) or FTIR imaging is needed to more comprehensively assess the heterogeneity of tissue mineral content, its association with organic matrix constituents, and its contribution to material stiffness.

Functional interactions among traits provide new insight into biological control mechanisms in bone

The results of the Path Analysis show that associations between morphology and tissue-level mechanical properties arise in part because of variation in matrix composition. Path Analysis differs from multiple regression analysis in many ways (Grace 2006), but one important aspect here is that connections among traits are specified in a particular way to reveal order and thus should be traceable to a biological mechanism. Although the biological nature of co-adapted traits in bone is not fully

understood, finding that morphological and compositional traits were functionally related provides further evidence that biological controls exist in bone whereby mechanical functionality is established during ontogeny by adapting a set of traits so together they satisfy physiological loading demands (Carrier 1983). For long bones, the set of traits are expected to result in a structure that is sufficiently stiff for daily loading demands (Moro et al. 1996; Sumner et al. 1996; Forwood et al. 2004). Transgenic mouse strains provided evidence that alterations in an extracellular matrix protein can elicit adaptive responses to possibly compensate for the changes in tissue-quality (Bonadio et al. 1993). Although the mouse and human skeletons differ in scale and microstructure, the basic concept that traits are co-adapted to create a mechanically functional structure appears to translate from the mouse to the human skeleton.

The generalized path model (Figure 2.4A) was constructed based largely on *a priori* knowledge of how biological processes define bone size and shape during growth for the human (Garn 1970) and mouse skeletons (Price et al. 2005; Jepsen et al. 2007). Thus, the functional interactions among traits observed in the adult skeleton are a manifestation of biological processes that exist during ontogeny. We expect that the biological mechanism(s) responsible for these functional interactions will be determined by additional research examining skeletal growth patterns (Price et al. 2005). Variation in size and shape among individuals reflects the various genetic and environmental factors that promote or inhibit periosteal expansion relative to longitudinal growth. If bone did not possess biological processes to co-adapt traits, there would be little chance of observing any consistent relationship among traits for the unrelated individuals examined in the current study. Thus, the current data suggest that these individuals share common

biological controls during ontogeny. Although it is not entirely clear how co-adapted traits arise, one theory suggests that co-adapted traits are a consequence of genes affecting hormonal regulation, which have pleitropic effects (Sinervo et al. 2002). It is expected that having the biological processes to co-adapt skeletal traits was fixed in the genome during evolution, since these processes would be expected to increase fitness and survival by allowing for multiple ways to grow structures that match daily loading demands (Olson et al. 1958; Cheverud 1996). This would have the effect of dampening the deleterious effects of the environmental (Sinervo et al. 2002) and genetic (Wright 1921) factors that promote a slender bone phenotype. The biological paradigm that traits are co-adapted is not limited to bone, but has also been observed for the heart (Nadeau et al. 2003).

Interactions among physical traits contribute to mechanically functional structures

The data provide important new insight into how mechanically functional structures are constructed. The results suggested that bone adapts in at least two ways. First, the negative association between Tt.Ar/Le and Ct.Ar/Tt.Ar suggests that bone adapts by varying the relative amount of cortical bone within the diaphysis. This negative correlation indicates that marrow size is proportionally smaller in slender bones compared to robust bones. The relationship between external and internal diameters (K) has been examined previously in the context of identifying the optimal value of K that allows for minimal mass and maximal stiffness for a hollow structure (Currey et al. 1985). Prior work compared inter and intra-species effects, but there are no data on how K varies with bone slenderness. For slender bones, adapting by reducing marrow size (lower K) would maximize the amount of bone within the diaphysis to increase overall

stiffness. For robust bones, this adaptive response would minimize the amount of bone to reduce overall mass. This adaptive process would require that the relative expansion rates of the endosteal and periosteal surfaces are coupled and thus biologically controlled during ontogeny (Price et al. 2005).

Second, the negative association between Tt.Ar/Le and ash content suggests that bone also adapts by varying matrix composition. This negative correlation is consistent with the idea that increasing the amount of mineral incorporated within the matrix will result in a compensatory increase in tissue-stiffness that could partly compensate for the reduced cross-sectional size of a slender long bone. This adaptive mechanism would require that osteoblasts, or possibly osteocytes, sense their environment and modulate matrix composition. The biological control mechanisms that regulate mineral content are not fully understood, but it is clear that matrix mineralization varies among bones with different functions (Currey 1979). The association between slenderness and mineralization may act to further increase global stiffness and strength beyond that which can be accommodated by morphological variation. This is particularly important since addition of bone to the endosteal surface, although useful, presents a limitation to how much compensation can occur solely on a morphological basis. Thus, matrix-level adaptations may be needed to further increase global stiffness and strength.

As illustrated in Figure 2.12, the two adaptive processes have an important effect on whole bone stiffness and strength. Whole bone stiffness under bending loads is proportional to the tissue-modulus (E) times the rectangular moment of inertia (I) and failure load is proportional to tissue-strength times Section Modulus (I/R). If biological processes did not co-adapt traits, then a slender bone with the same length, K, and

mineral content (and thus tissue-modulus and tissue-strength) as a robust bone would have approximately 30-40% reductions in whole bone stiffness and failure load and

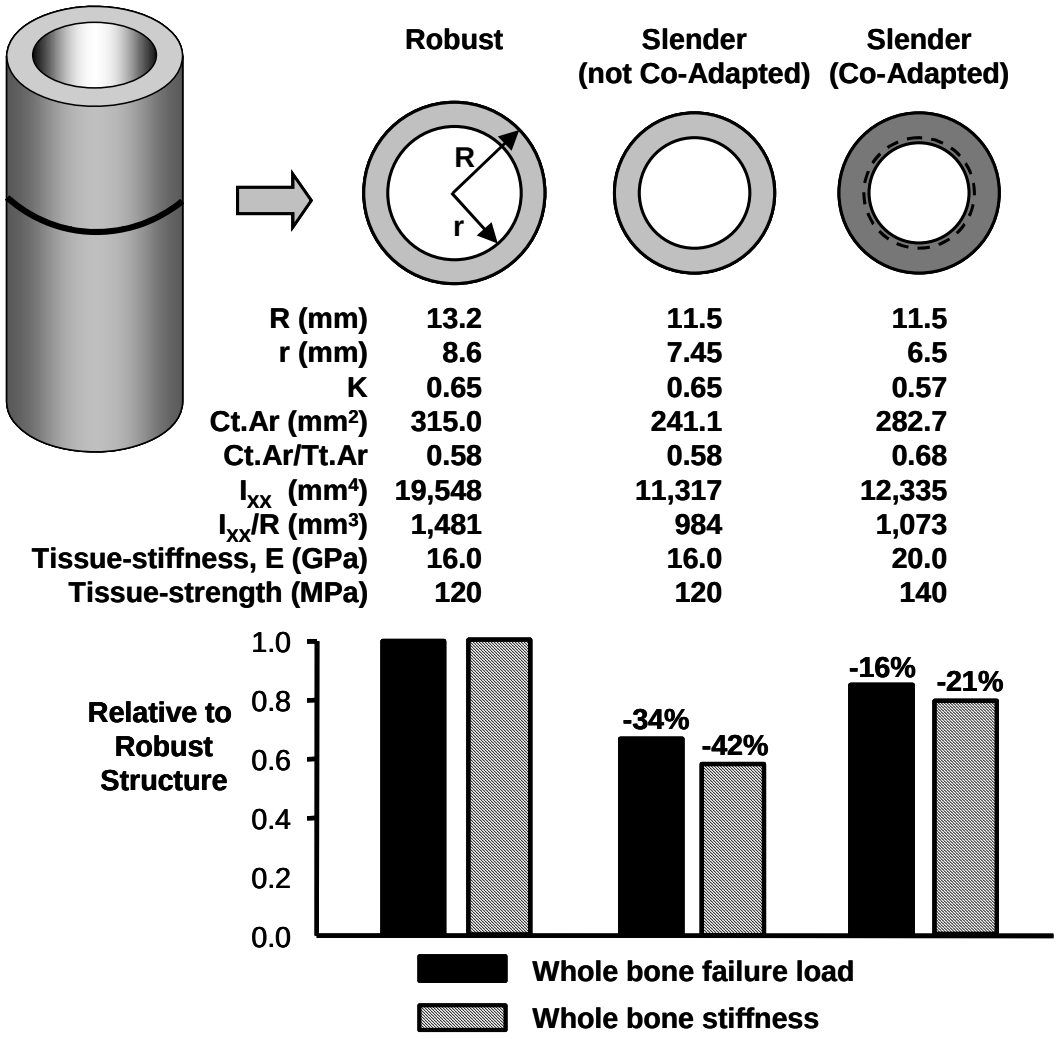

Figure 2.12. Schematic illustration of how co-adaptation of morphological and composition traits acts to increase overall stiffness and failure load of a slender cylindrical structure. The slender structure, without co-adapted traits, has the same tissue modulus (E), K, and Ct.Ar/Tt.Ar as the robust structure, but this results in a dramatically lower stiffness and failure load. The slender structure with co-adapted traits has a slightly smaller marrow area (lower K, higher Ct.Ar/Tt.Ar) and larger tissue-modulus and tissue strength compared with the robust structure. These small changes increase the stiffness and failure load of the slender bone so that they are closer to the robust structure.

would likely be under-designed for normal daily loading conditions. For slender bones, relatively subtle increases in endosteal bone and mineral content (tissue-modulus),

consistent with the current dataset and indicative of biological processes that co-adapt traits, have the benefit of increasing overall stiffness and failure load closer to that of the robust bone. Further, co-adaptation of traits in slender bones does not result in greater cortical area relative to body weight compared to robust bones. Consequently, there does not appear to be a metabolic cost associated with this co-adaptation.

Interactions among physical traits contribute to increased risk of stress fractures

We studied the tibia diaphysis from young adult males and females because bone slenderness in this age group is correlated with increased risk of stress fractures in athletes (Crossley et al. 1999) and military recruits (Milgrom et al. 1989; Beck et al. 1996). Individuals with slender bones, which are measured clinically as diaphyses with a small cross-sectional size for a given length and metaphyses with lower bone mass, show low BMD and a higher fracture incidence throughout life compared to individuals with robust bones (Giladi et al. 1987; Milgrom et al. 1989; Gilsanz et al. 1995; Beck et al. 1996; Crossley et al. 1999; Duan et al. 1999; Beck et al. 2000; Skaggs et al. 2001). The increased fracture risk of slender bones has typically been attributed to the reduced load carrying capacity associated with the small cross-sectional size and mass (Milgrom et al. 1989; Beck et al. 2000). However, the current data may provide new insight into this problem. Our data showed that slender bones were compensated by increased ash content and a proportionally greater amount of cortical tissue. Although this co-adaptation has the benefit of ensuring a particular set of traits is sufficiently stiff and strong to support daily loads, the downside is that not all sets of traits result in equivalent failure mechanisms. For slender bones, the combination of a thicker cortex and higher mineral content may help to increase organ-level stiffness, but the reduced tissue ductility and toughness that

were associated with the greater ash content may increase the risk of fracturing under extreme loading conditions, such as low-cycle fatigue (e.g., military training) and overload (e.g., falling). Thus, this co-adaptation, because it involves matrix mineralization, appears to result in the development of preferred sets of adult traits within the context of extreme load conditions.

Sexual dimorphism contributes to differences in functional interactions among bone traits

Although the overall relationship among Tt.Ar/Le, Ct.Ar/Tt.Ar, and ash content was similar for males and females, Ma.Ar proved to be a strong covariate for ash content in the Path Analysis for females but not males. This is consistent with dimorphic growth patterns after puberty, in which the endosteum switches from expansion to infilling for females. In males, the marrow space continues to expand in proportion to periosteal expansion. Prior work showed that females prone to stress fractures had more narrow tibiae and thinner cortices compared to females that did not develop stress fracture (Beck et al. 2000). Having slender bones plus thinner cortices may indicate that for these individuals there was a lack of infilling or lack of co-adaptation between periosteal and endosteal surface movements during growth.

Limitations

There are several limitations to this study worth addressing. First, the difficulty in acquiring tibiae from healthy men and women in the 20-40 year age range limited the number of samples for this study. Nevertheless, this did not affect the comparison of mechanical and morphological properties between sexes, but it may have resulted in not seeing more significant correlations between morphology and tissue-quality (Table 2.5). Second, tissue-damageability was based on measures of degradation of stiffness and

relaxation. Future work will determine if the type, distribution, and quantity of damage is different for females and males. In addition, our measure of tissue-damageability relates to the progressive accumulation of damage prior to failure (Jepsen et al. 1997; Jepsen et al. 1999), and may not reflect how damage accumulates under long-term fatigue loading. Third, the relationship between the cross-sectional size of the tibia and body size did not take into account load sharing between the tibia and the fibula. Fourth, our analysis does not take into consideration differences in the amount or type of loading, which have been shown to play important roles in the development of bone size and shape (Taaffe et al. 1995). Finally, our analysis, which assumes that randomly acquired tibial samples provide a representative view into bone biology, does not take into account lean muscle mass, which may be better correlated with bone size and shape than overall body weight (Petit et al. 2005). However, after adjusting the body weight values of the current study by the average lean mass values for males and females of similar ages reported previously (Horber et al. 1997), female tibiae remained significantly more slender compared to males. Thus, these limitations do not appear to affect the primary outcomes of this study, which are that males and females have similar tissue-level mechanical properties and also show a similar correlation between bone size and tissue-quality.

Summary

The results of this study identified functional interactions among physical bone traits suggesting that bone possesses important biological processes that co-adapt morphological and compositional traits so the set of traits results in a structure sufficiently stiff for daily activities. These results have important clinical implications because bone functionality and bone biology may be better understood based on

knowledge of sets of traits rather than a single complex trait such as bone mass. Variation in the ability of bone to co-adapt traits would be expected to lead to under- and over-designed structures. The downside of co-adapting matrix composition is that increases in mineralization result in a more brittle and damageable material that would be expected to perform poorly under extreme load conditions. Thus, for more slender bones, reduced tissue ductility and toughness associated with greater ash content may increase the risk of fracturing from low-cycle fatigue (e.g., military training) and overload (e.g., falling). Therefore, rather than using complex traits or a series of unrelated traits, clinical assessment of fracture risk may benefit from knowledge of sets of traits and the functional interactions among the traits.

ACKNOWLEDGMENTS

The authors thank Haviva Goldman, PhD and Mitchell B. Schaffler, PhD for their suggestions in establishing the histological protocols. The authors thank the U.S. Department of Defense (DAMD17-01-1-0806) and the National Institutes of Health (AR44927) for their support of this research. Samples were acquired through the Musculoskeletal Transplant Foundation (Edison, NJ, USA) and the National Disease Research Interchange (Philadelphia, PA, USA).

CHAPTER 3

PERCOLATION THEORY RELATES CORTICOCANCELLOUS ARCHITECTURE TO MECHANICAL FUNCTION IN VERTEBRAE OF INBRED MOUSE STRAINS

Reproduced from ***Bone*** 2008; 42:743-750

ABSTRACT

Complex corticocancellous skeletal sites such as the vertebra or proximal femur are connected networks of bone capable of transferring mechanical loads. Characterizing these structures as networks may allow us to quantify the load transferring behavior of the emergent system as a function of the connected cortical and trabecular components. By defining the relationship between certain physical bone traits and mechanical load transfer pathways, a clearer picture of the genetic determinants of skeletal fragility can be developed. We tested the hypothesis that the measures provided by network percolation theory will reveal that different combinations of cortical, trabecular, and compositional traits lead to significantly different load transfer pathways within the vertebral bodies among inbred mouse strains. Gross morphologic, micro-architectural, and compositional traits of L5 vertebrae from 15 week old A/J (A), C57BL/6J (B6), and C3H/HeJ (C3H) inbred mice (n=10/strain) were determined using micro-computed tomography. Measures included total cross-sectional area, bone volume fraction, trabecular number, thickness, spacing, cortical area, and tissue mineral density. Two-dimensional coronal sections were converted to network graphs with the cortical shell considered as one highly connected node. Percolation parameters including correlation length (average number of connected nodes between superior and inferior surfaces), chemical length (minimum number of connected nodes between surfaces), and backbone mass (strut number) were measured. Analysis of the topology of the connected bone networks showed that A and B6 mice transfer load through trabecular pathways in the middle of the vertebral body in addition to the cortical shell. C3H mice transfer load primarily through the highly mineralized cortical shell. Thus, the measures provided by percolation theory provide a quantitative

approach to study how different combinations of cortical and trabecular traits lead to mechanically functional structures. The data further emphasize the interdependent nature of these physical bone traits suggesting similar genetic variants may affect both trabecular and cortical bone. Therefore, developing a network approach to study corticocancellous architecture during growth should further our understanding of the biological basis of skeletal fragility and, thus, provide novel engineering approaches to studying the genetic basis of fracture risk.

INTRODUCTION

Growth and development greatly affect peak adult bone properties, which are important determinants of fracture risk early in life and skeletal fragility late in life. Bone mineral density (BMD), which is a measure of the amount of bone, is an important clinical tool used to diagnosis fracture risk. However, to study how cancellous architecture arises during growth, multiple measures of bone architecture and tissue quality must be examined rather than simply the amount of bone. Advances in our understanding of genetic variation in growth and development offer insight into the degree of integration among skeletal features that highlights the flaws in analytical approaches that attempt to reduce the skeleton into discrete, supposedly independent traits, each with its own adaptive story (Pearson et al. 2004). Prior work examining details of trabecular bone architecture revealed that differences in mechanical properties could be explained by regional variation in trabecular architecture (Beamer et al. 1996; Ritzel et al. 1997; Tabor 2003). However, these studies failed to reveal fully how the entire bone structure is designed (or adapts) to handle the transfer of loads because they focused on a region of interest (ROI) of cancellous bone and did not consider the critical interactions of cortical bone with the flow of stress or were incomplete in that they did not include the variability in material quality. Therefore, a new integrated approach is needed to understand more completely how the underlying biological processes during growth and development determine the load transferring capability of complex corticocancellous structures.

Network science offers an approach that can help shed new light on an old problem (Watts 2003). In networks, structure almost always affects function. Researchers

are most interested in the relationships between a network's components because they affect the behavior of the system as a whole. Networks are dynamic, yet robust; maintaining a given function despite adaptive changes in their components with time. The study of a network's connectivity (its ability to transfer information from point A to point B) is the focus of percolation theory. The main objectives of percolation theory are to characterize the distribution of cluster sizes in the network and to determine how the transfer of information depends on network architecture (Watts 2003). Although it was originally developed to answer questions in organic chemistry, percolation models have been used successfully to study network related phenomena including forest fires, electrical conductivity, epidemics of disease, and signal transfer in neurons (Stauffer et al. 1994).

The corticocancellous architecture of a complex skeletal site such as the vertebra or proximal femur is a connected network of bone capable of transferring mechanical loads, which is the "information" transferred through the network. The adaptive nature of these networks results in bone structures similar in mechanical function, but different in design. Previously, percolation theory has been used in the description of age-related changes of mechanical competence in an ROI of normal and osteoporotic trabecular bone (Tabor 2003). A network percolation model can also be used to study how genetic differences in bone growth affect mechanical function. Genetic variation gives rise to variation in the biological activity of each cell population leading to mechanically functional bone networks built with different combinations of trabecular bone, cortical bone, and mineral content. Bone has an inherent adaptive response to modify the apposition, resorption, and mineralization processes that determine bone structure and

tissue-quality to meet mechanical demands (Ferretti et al. 1993). For example, inbred mice have the capability of modulating compositional and morphological bone traits to meet mechanical demands associated with weight bearing (Jepsen et al. 2001; Jepsen et al. 2003). The coupling between bone morphology and tissue quality appears advantageous for ensuring that adequate whole-bone stiffness is achieved for day-to-day activity (i.e., create a functional skeleton). However, the disadvantage is that the tissue-quality factors that tend to make bone stiff also tend to make bone less ductile, less tough, and more damageable (Currey 1984). Thus, understanding the design principles of a functional skeleton and understanding the relationships among skeletal traits are important in determining how genetically varying growth patterns lead to skeletal fragility. Characterizing a complex corticocancellous structure as a connected network allows us to 1) analyze quantitatively the load transferring behavior of the emergent system as a function of the connected components and 2) quantify how the structure evolves over time – specifically, how the biological processes modulate the structure to meet mechanical demands during growth and development.

By defining the relationship between certain morphological traits and mechanical load transfer pathways, a clearer picture of the genetic determinants of skeletal fragility can be developed. To develop the network theory, we made use of the variability in structure-function relationships observed among three inbred mouse strains (Tommasini et al. 2005). Previous work showed that these inbred strains built vertebrae with different combinations of cortical, trabecular, and compositional traits (Tommasini et al. 2005). Here, we tested the hypothesis that the measures provided by percolation theory will reveal that these different combinations of traits lead to significantly different load

transfer pathways within the vertebral bodies among these inbred mouse strains. We used percolation theory to analyze samples from a prior study (Tommasini et al. 2005) and compared indices related to load transfer among inbred mouse strains. Further, we identified which mechanical properties were predicted by percolation parameters.

MATERIALS AND METHODS

Data on vertebrae of inbred mice

In a previous study, female A/J (A, $n = 10$), C57BL/6J (B6, $n = 10$), and C3H/HeJ (C3H, $n = 10$) inbred mice were purchased from Jackson Laboratory (Bar Harbor, ME, USA) at 4 weeks of age (Tommasini et al. 2005). The Committee on Animal Care and Use approved the handling and treatment of mice. Mice were killed at 15 weeks of age and gross morphologic, micro-architectural, and compositional traits of L5 vertebral bodies were determined using a desktop micro-Computed Tomography (micro-CT) system (GE eXplore Locus SP Specimen Scanner; GE Healthcare, London, Ontario, Canada) (Tommasini et al. 2005). Overall measures included the total cross-sectional area (Tt.Ar = cortical bone + trabecular bone + marrow) and the total bone area (B.Ar = cortical bone + trabecular bone). Cortical bone traits included the area of cortical bone (Ct.Ar) and the second area (polar) moment of inertia (Ct.J). Measures of trabecular morphology included trabecular bone volume fraction (Tb BV/TV), trabecular number (Tb.N), trabecular thickness (Tb.Th), and trabecular separation (Tb.Sp). TMD also was calculated from the micro-CT images as described previously (Tommasini et al. 2005). TMD is the average mineral value of the bone voxels alone, expressed in hydroxyapatite equivalents. It should be noted that mice were analyzed at 15 weeks of age so the results

reflect genetic differences in the growth and development of mechanically functional vertebrae (Price et al. 2005; Tommasini et al. 2005).

Whole-bone mechanical properties of intact L5 vertebrae (n=10/genotype) were measured previously by compressing the vertebral body with a 3-mm-diameter platen (Tommasini et al. 2005). Mechanical properties, included failure load (F_u), stiffness (S), and total displacement (Δ_T) as a measure of ductility. Failure load was defined as the highest load preceding a rapid decrease in the measured load. Total deflection was measured using a custom optical strain measuring system as described previously (Tommasini et al. 2005).

The network model and percolation parameters

The network design, or topology, determines the structural stability, dynamic behavior, robustness, and attack tolerance of the structure (Barbasi 2002). Thresholded micro-CT images from the previous study were used to assess the network topology of the vertebral bodies. Using an iterative thinning algorithm (Matlab, The Mathworks Inc., Natick, MA, USA), two-dimensional (2D) coronal sections (two per bone) were skeletonized and nodes and branches were identified (Figure 3.1A,B). These 2D sections were taken for each bone at approximately 1/3 and 2/3 of the anteroposterior width of the vertebral body (~0.35mm apart). The skeleton graphs were converted into network maps by considering the cortical surface as one highly connected node or hub (Figure 3.1C). The degree distribution is a function describing the total number of nodes in a network with a given number of connections to other nodes (Barbasi 2002). The degree distribution of a random network follows a bell curve, in which most nodes have the same number of links, and nodes with a very large number of links do not exist (Figure

3.1D). In contrast, the power law degree distribution of a scale-free network predicts that most nodes have only a few links, held together by a few highly connected hubs (Figure 3.1D). The distinction between scale-free and random networks is important because it provides context into how to build a functional skeleton and how to assess the deleterious effects of bone loss on mechanical behavior more accurately. Based on the prominence of the cortical shell, the scale-free network topology was applicable for the mouse vertebrae.

Figure 3.1: Conversion of 2D vertebral images into network maps. **(A)** Two-dimensional coronal sections were **(B)** skeletonized and nodes were identified. **(C)** The skeleton graphs were converted into network maps by considering the cortical surface as one highly connected node or hub (large circles). **(D)** Graphical representation of random (no hub) and scale-free (cortical hub) networks.

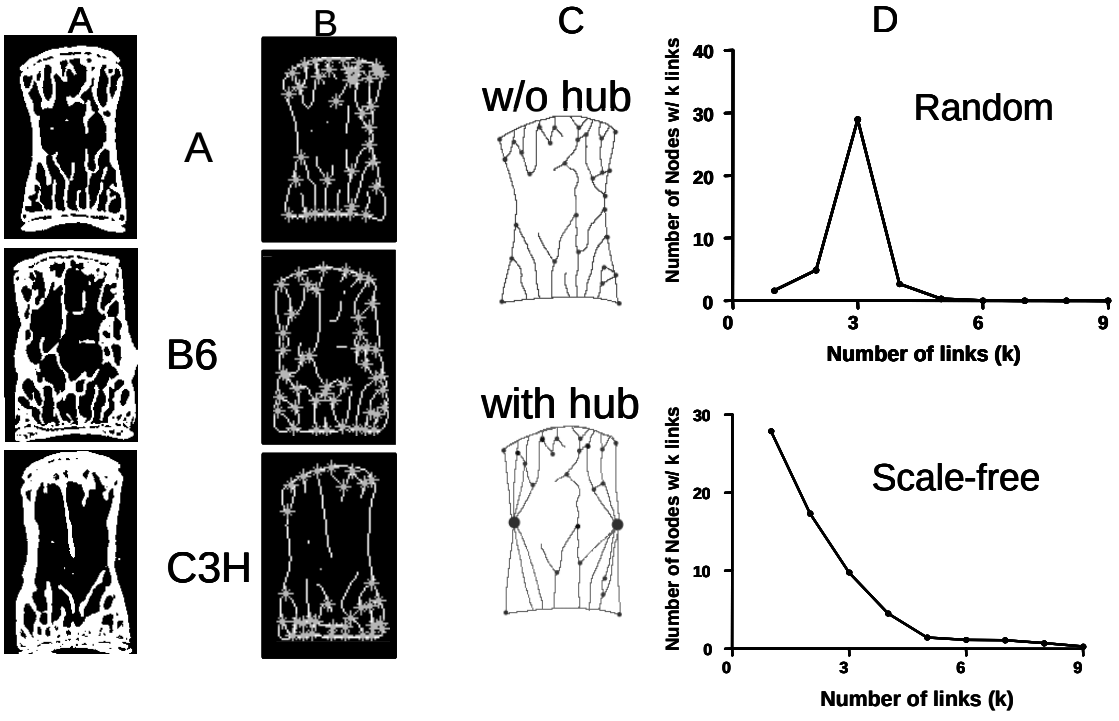

Further, despite analyzing 2D images where trabecular connections segment the cortex, we chose to view the system as a scale-free network, which is more representative of the 3D vertebral body structure because a continuous cortical shell acts as a network hub connected to many trabecular struts.

The percolation model was intended to interpret the relationship between network structure and mechanical function. Adult, functional bones are assumed to contain percolating clusters or else they would not be able to transfer load. Percolation theory deals with the number and properties of the connected clusters, which are made up of free, or dead ends (non-loaded segments) and a **backbone**. In terms of vertebral bone architecture, the backbone defines the pathways that transfer load between superior and inferior surfaces and consists of single connected segments and multi-connected segments.

An algorithm was developed to calculate simple percolation parameters (Matlab, The Mathworks Inc., Natick, MA, USA). The inputs into the algorithm are the set of nodes with their connected neighboring nodes and the starting and end points or surfaces. The only predefined rules for our network are that information can only travel from the superior surface toward the inferior surface (thus load applied to the superior surface can only travel to connected nodes in the network located either horizontal to or below) and the information is self-avoiding (information cannot travel to a node it has been to previously). The **correlation** and **chemical path** lengths measure the load sharing capacity of the network, which is expected to vary with genetic background (Figure 3.2). The chemical length (ChemL) is the distance of the shortest path in which the percolating network connects opposite boundaries. The correlation length (CorrL) is the average distance between connected opposite boundaries. For bone architecture, path distance is a measure of the number of nodes, or intersections of connected bone struts, between boundaries. Size and geometry also play an important role in a network's ability to transfer information. The percolation model refers to these characteristics as **mass**.

Backbone mass (BboneMass) was defined as the number of connected struts comprising the dead ends and the cortical and trabecular components of the backbone.

Figure 3.2: Structures **A** and **B** have similar bone volume fractions yet vastly different network topologies for transferring load from top to bottom. Load applied to the top surface can only travel to connected nodes (open circles) in the network located either horizontal to or below and cannot travel to a node it has been to previously. Compared to structure **B**, structure **A** has higher correlation length (average number of nodes crossed along paths connecting top and bottom surface; CorrL) and chemical length (fewest number of nodes crossed along paths connecting top and bottom surface; ChemL). Thus, structure **A** has a higher load sharing capacity.

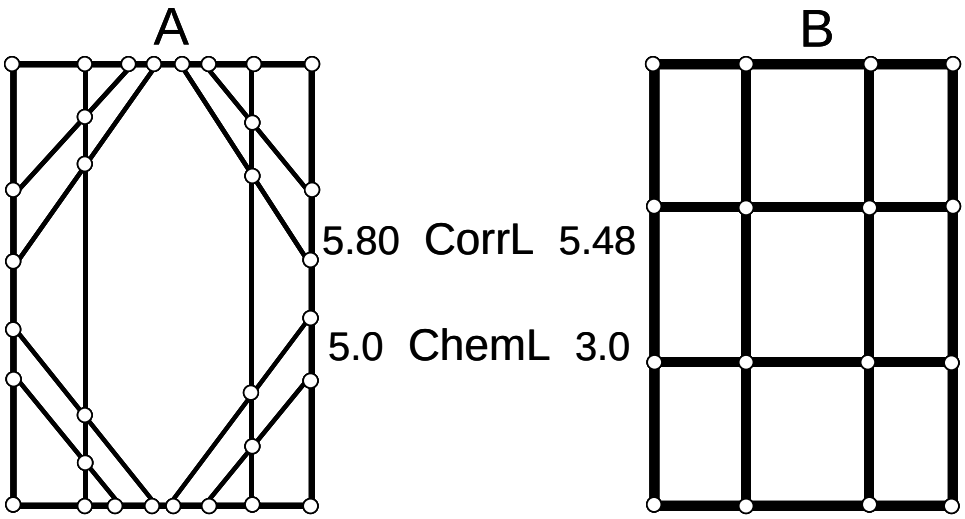

Previous work showed genetic variation in the combination of trabecular and cortical traits in the construction of mechanically functional vertebrae (Tommasini et al. 2005). To test how these different combinations influence network behavior (mechanical load transfer) the ratio of cortical nodes to trabecular nodes (Ct:Tb Nodes) and the ratio of trabecular struts and cortical struts (Tb:Ct Struts) was calculated. The percentage of existing links connected to the cortex was then calculated (%hub).

Statistical analysis

Differences in percolation parameters among A, B6, and C3H were determined using a one-way analysis of variance (ANOVA) and a Tukey's posthoc test (GraphPad Prism; San Diego, CA, USA). Relationships between percolation parameters and bone

morphology and composition were determined within each genotype and across genotypes by combining individual data from all three strains and calculating correlation coefficients between each percolation parameter (CorrL, ChemL, BboneMass, Tb:Ct Struts, Ct:Tb Nodes, %hub) and each morphological and compositional trait (Tb BV/TV, Tt.Ar, Ct.Ar, TMD, etc.) (Minitab, State College, PA, USA). When a large number of non-independent tests are conducted, the likelihood that at least one will achieve statistical significance on the basis of chance alone increases. To correct this, permutation tests were used to establish a threshold for statistical significance in the correlation analyses (Churchill et al. 1994). A copy of the analytical program used for this study is available at http://www.jax.org/staff/churchill/labsite under the data sets link (Nadeau et al. 2003). The average threshold values for all 3 strains were $r = 0.67$ for $p < 0.10$ and $r = 0.61$ for $p < 0.05$. After correcting for multiple comparisons, many significant relationships remained. Multiple linear regression analyses were then conducted to 1) determine inter-strain variation in percolation parameters explained by a combination of trabecular, cortical, and compositional traits and 2) identify mechanical properties that are explained by a combination of percolation parameters.

RESULTS

Genetic variation in network structure

The results of the network analysis and the previous structure-function study showed that all three inbred strains constructed mechanically functional vertebrae in different ways (Table 3.1). Percolation measures revealed that significant differences existed in the way the three inbred mouse strains constructed the bone network of the

vertebral body. B6 vertebrae had significantly higher correlation lengths ($p < 0.001$) than A and C3H meaning the B6 connected network was bigger (i.e., more paths shared the load between surfaces). The chemical length (shortest path of load transfer) of B6 mice was also significantly higher than A and C3H ($p < 0.001$). These results were not surprising since B6 had the highest Tb BV/TV and thus, more of the load could be shared through trabeculae in the middle of the vertebral body compared to A and C3H.

Table 3.1. Inter-strain differences in vertebral body network architecture. [a, b, c] Significantly different from A, B6, or C3H, respectively ($p < 0.05$). Data shown as mean + standard deviation.

Physical Bone Traits	***A***	***B6***	***C3H***
Tt.Ar (mm^2)	$1.4 \pm 0.07^{b,c}$	$1.6 \pm 0.05^{a,c}$	$1.7 \pm 0.13^{a,b}$
B.Ar (mm^2)	$0.49 \pm 0.06^{b,c}$	0.64 ± 0.06^{a}	0.63 ± 0.08^{a}
Ct.Ar (mm^2)	0.28 ± 0.02^{c}	0.30 ± 0.03^{c}	$0.43 \pm 0.03^{a,b}$
Tb BV/TV (%)	19.2 ± 2.9^{b}	$26.6 \pm 2.6^{a,c}$	16.5 ± 3.8^{b}
Tb.Th (mm)	0.038 ± 0.003^{c}	0.041 ± 0.004^{c}	$0.047 \pm 0.006^{a,b}$
TbN (1/mm)	$6.2 \pm 0.4^{b,c}$	$7.8 \pm 0.04^{a,c}$	$4.0 \pm 0.5^{a,b}$
Tb.Sp (mm)	0.17 ± 0.03^{c}	0.10 ± 0.01^{c}	$0.42 \pm 0.11^{a,b}$
TMD (mg/cm^3)	$770.4 \pm 8.9^{b,c}$	$735.1 \pm 19.2^{a,c}$	$821.7 \pm 9.2^{a,b}$
Mechanical Properties			
F_U (N)	$19.2 \pm 3.1^{b,c}$	28.5 ± 2.5^{a}	29.7 ± 6.5^{a}
Stiffness (N/mm)	464 ± 166^{c}	443 ± 158^{c}	$1{,}192 \pm 301^{a,b}$
Δ_T (mm)	0.13 ± 0.05^{b}	$0.19 \pm 0.05^{a,c}$	0.07 ± 0.06^{b}
Percolation Measures			
Correlation length	5.43 ± 1.36^{b}	$9.06 \pm 2.29^{a,c}$	4.27 ± 0.47^{b}
Chemical length	2.47 ± 0.44^{b}	$3.98 \pm 1.09^{a,c}$	2.17 ± 0.44^{b}
Backbone mass	35.65 ± 8.27^{b}	$58.25 \pm 12.47^{a,c}$	27.35 ± 3.88^{b}
Ct:Tb Nodes	0.82 ± 0.17^{c}	0.54 ± 0.15^{c}	$1.28 \pm 0.67^{a,b}$
% of links to hub	26.2 ± 5.6^{b}	$21.6 \pm 2.5^{a,c}$	29.8 ± 6.5^{b}
Tb:Ct Struts	16.83 ± 4.13^{b}	$28.13 \pm 6.23^{a,c}$	12.43 ± 1.70^{b}

Differences in the reliance on the cortex were made clearer by comparing cortical and trabecular components of the network. The ratio of cortical to trabecular nodes in the C3H vertebrae was significantly higher than A ($p < 0.01$) and B6 ($p < 0.001$). There was no significant difference between A and B6. Thus, C3H vertebrae relied heavily on the

cortex to transfer load from superior to inferior surfaces. B6 had the lowest reliance on the cortical hub with a lower percentage of existing links connected to the cortical hubs compared to A ($p < 0.05$) and C3H ($p < 0.001$). The number and type of struts that were used by each inbred strain to carry load also differed. B6 mice had significantly higher backbone mass than A and C3H ($p < 0.001$). This was mainly due to a higher contribution from trabecular struts in B6 vertebrae, which had a significantly higher ratio of trabecular to cortical struts than A and C3H ($p < 0.001$).

Variation in network structure is dependent on variation in vertebral architecture

All percolation parameters were measured independent of bone size, shape, and mineralization. However, these traits were statistically related to trabecular, cortical, and compositional components of the mouse vertebra. Pearson correlation coefficients determined for each genotype separately revealed that correlations between percolation parameters and physical bone traits were consistent within genotypes (data not shown). The univariate analysis performed across genotypes by combining the datasets revealed that percolation parameters were significantly correlated to physical bone traits specifying trabecular architecture (Tb BV/TV, connectivity, Tb.N, Tb.Sp) and composition (TMD) (Table 3.2). According to Pearson correlation coefficients, percolation parameters also were significantly related to cortical bone area (Ct.Ar). However, the correlation coefficients were slightly below the threshold determined from permutation tests for $p < 0.05$.

Table 3.2. Correlation coefficients for percolation parameters and trabecular, cortical, and compositional traits. Pearson correlation coefficients are shown. *p*-value in parentheses. Bold values significant ($p < 0.05$) above threshold of $\pm$0.61 determined by permutation tests.

	Weight	B.Ar	Tb BV/TV	NNd:NTm	Tb.Th	Tb.Sp	Tb.N	Ct.Ar	Ct.J	Tt.Ar	TMD
CorrL	-0.27	0.30	**0.78**	**0.74**	-0.05	**-0.63**	**0.79**	-0.39	-0.22	-0.04	**-0.74**
	(0.15)	(0.11)	**(0.00)**	**(0.00)**	(0.80)	**(0.00)**	**(0.00)**	(0.03)	(0.25)	(0.84)	**(0.00)**
ChemL	-0.28	0.27	**0.71**	**0.67**	-0.03	-0.52	**0.72**	-0.33	-0.16	-0.06	**-0.72**
	(0.14)	(0.16)	**(0.00)**	**(0.00)**	(0.80)	(0.00)	**(0.00)**	(0.03)	(0.39)	(0.75)	**(0.00)**
Bbone	-0.26	0.31	**0.85**	**0.80**	-0.04	**-0.67**	**0.85**	-0.41	-0.23	-0.09	**-0.79**
Mass	(0.17)	(0.10)	**(0.00)**	**(0.00)**	(0.84)	**(0.00)**	**(0.00)**	(0.03)	(0.22)	(0.63)	**(0.00)**
Ct:Tb	0.14	-0.11	**-0.76**	**-0.64**	0.09	**0.75**	**-0.80**	0.53	0.44	0.31	0.73
Nodes	(0.45)	(0.56)	**(0.00)**	**(0.00)**	(0.64)	**(0.00)**	**(0.00)**	(0.00)	(0.02)	(0.10)	(0.00)
% links	0.25	-0.12	-0.59	-0.55	0.12	0.52	**-0.62**	0.36	0.28	0.22	0.54
to hub	(0.18)	(0.54)	(0.00)	(0.00)	(0.54)	(0.00)	**(0.00)**	(0.05)	(0.14)	(0.24)	(0.00)
Tb:Ct	-0.25	0.30	**0.85**	**0.79**	-0.05	**-0.68**	**0.86**	-0.42	-0.24	-0.10	**-0.80**
Struts	(0.18)	(0.11)	**(0.00)**	**(0.00)**	(0.80)	**(0.00)**	**(0.00)**	(0.02)	(0.20)	(0.60)	**(0.00)**

Table 3.3. Multivariate analysis comparing percolation parameters with morphological and compositional bone traits. Multiple linear regression analysis was conducted to determine the amount of inter-strain variation in correlation length (CorrL), chemical length (ChemL), backbone mass (BboneMass), the ratio of cortical to trabecular nodes (Ct:Tb Nodes), and the ratio of trabecular to cortical struts (Tb:Ct Struts). The constants or traits shown in bold depict terms in the regression model showing significant ($p < 0.05$) or borderline significant ($p < 0.1$) contributions. R^2 values were adjusted for number of independent variables.

Equation	R^2*-adj*
CorrL = 0.2 – 0.8 Tb BV/TV + 1.5 TbN – 0.1 TMD + 13.4 CtAr + 0.1 Weight	0.617
ChemL = 13.7 – 9.8 Tb BV/TV 0.6 TbN – 0.02 **TMD** + 11.5 **CtAr** + 0.05 Weight	0.562
BboneMass = -29 – 50 Tb BV/TV + 12.4 **TbN** – 0.06 TMD + 120 **CtAr** + 0.7 Weight	0.777
Ct:Tb Nodes = 3.9 – 9.0 **Tb BV/TV** + 0.1 TbN + 3.8 **CtAr** – 0.04Weight	0.681
%hub = **1.3** – 0.14 Tb BV/TV – 0.04 TbN – 0.001 TMD + 0.001 CtAr + 0.01 Weight	0.331
Tb:Ct Struts = -16.4 – 24.4 TbBV/TV + 6.2 **TbN** – 0.03 TMD + 58.3 **CtAr** + 0.4Weight	0.774

Independent of the relationships observed within strains, no relationship observed across the strains was unexpected based on geometry and mathematical dependency. Simple correlation analysis does not convey the nature of these relationships. Therefore, a multivariate analysis was used to investigate how these correlations relate to the mechanical functionality of a structure. Multiple linear regression analyses (Table 3.3) revealed that a combination of cortical, trabecular, and compositional traits were needed

to achieve 60-80% explanatory power for percolation parameters including correlation and chemical length for all three strains simultaneously.

Genetic variation in mechanical properties is dependent on network structure

Multivariate regression analyses (Table 3.4) examining percolation parameters and whole bone mechanical properties across all three strains revealed that a combination of percolation parameters accounted for >60% of the variation in vertebral stiffness. However, combinations of percolation parameters explained only ~20% of failure load and ~40% of total displacement. Thus, the data revealed that combinations of cortical and trabecular morphology and composition contribute to genetic variation in bone network structures and, specifically, to variation in whole bone vertebral stiffness.

Table 3.4. Multivariate regression analysis comparing whole mechanical properties with percolation parameters. Multiple linear regression analysis was conducted to determine the amount of inter-strain variation in stiffness, strength (F_U), and total displacement (Δ_T) using percolation parameters including correlation length (CorrL), chemical length (ChemL), backbone mass (BboneMass), the ratio of cortical to trabecular nodes (Ct:Tb Nodes), the percentage of links to the cortical hub (%hub), and the ratio of trabecular to cortical struts (Tb:Ct) as predictors. The constants or traits shown in bold depict terms in the regression model showing significant ($p < 0.05$) or borderline significant ($p < 0.1$) contributions. R^2 values were adjusted for number of independent variables.

Equation	R^2	R^2-*adj*
Stiff = 27 + 49 CorrL – 184 **ChemL** + 78.9 BboneMass + 555 **Ct:Tb Nodes** + 883 %hub – 158 Tb:Ct Struts	0.633	0.504
F_U = **16.8** + 0.04 CorrL – 1.33 ChemL + 1.20 BboneMass + 10.1 **Ct:Tb Nodes** – 25.5 %hub – 2.02 Tb:Ct Struts	0.21	0.000
Δ_T = **0.22** – 0.005 CorrL + 0.03 ChemL – 0.02 BboneMass – 0.04 Ct:Tb Nodes – 0.32 %hub + 0.04 Tb:Ct Struts	0.414	0.254

DISCUSSION

Networks reveal functional interactions among sets of traits

The results of this study confirmed the hypothesis that percolation theory revealed that different combinations of cortical and trabecular morphological and compositional traits contribute to genetic variation in bone network structures and, ultimately, to variation in whole bone mechanical properties. Therefore, load transfer pathways are under genetic control. The data were also consistent with results from previous studies using standard reductionist methods that characterized the quantity of cortical and trabecular traits separately (Turner et al. 2000; Turner et al. 2001; Tommasini et al. 2005). The percolation parameters quantified differences in the way load is transferred from superior to inferior surfaces in the inbred mouse vertebral body. B6 vertebrae had higher trabecular BV/TV and thinner cortices, which combined to produce larger networks that shared the load among paths within the trabecular bone of the vertebral body. In contrast, C3H vertebrae had lower trabecular BV/TV, but a higher amount of cortical bone as evidenced by higher reliance on the cortex in load transfer networks. Turner et al. suggested that the lack of trabecular bone in C3H mice could be the result of mechanical adaptation to thicker cortices due to a possible stress shielding effect (Turner et al. 2000). We believe these interactions among traits are part of a larger biological paradigm (Jepsen et al. 2007). The network approach presented here was not meant to replace standard reductionist approaches to understanding the structure-function relationships, but to supplement them.

By providing simple quantitative measures of how bone is constructed to transfer load, the current data may provide new insight into skeletal fragility. The correlations

among morphological and compositional traits suggest that physical bone traits are coordinated (or are co-adapted) so the set of traits result in vertebrae that are sufficiently stiff for daily loading demands (Tommasini et al. 2005; Jepsen et al. 2007). However, not all sets of traits resulted in equivalent failure mechanisms. In C3H vertebral bodies, decreased BV/TV was compensated by increases in tissue mineral content and the reliance on the cortical shell in its load transfer network. Although the observed co-adaptation of traits had the result of ensuring that C3H vertebrae were sufficiently stiff and strong for daily loading, the combination of thicker cortices and higher mineralization reduced tissue-ductility. Thus, consistent with previous work examining factors that contribute to skeletal fragility (Duan et al. 2001; Jepsen et al. 2001; Seeman 2001; Jepsen et al. 2003; Currey 2005; Price et al. 2005; Tommasini et al. 2007), the co-adaptation of traits may result in the development of sets of traits preferred over others and increase fracture risk under extreme load conditions (Jepsen et al. 2007).

Assessment of physical bone traits that determine mechanical strength of corticocancellous bone has largely centered on BMD or trabecular bone volume fraction (Beamer et al. 1996; Klein et al. 2001; Turner et al. 2001). BMD, which is a successful clinical tool for diagnosing fracture risk, is highly heritable (Giguere et al. 2000), making it a good candidate for use as a surrogate measure of fracture risk in many genetic analyses. Recent studies have shown that the contribution of the cortical shell to mechanical function should not be overlooked (Silva et al. 1997; Yamauchi et al. 2004; Tommasini et al. 2005; Sornay-Rendu et al. 2007). Quantitative trait loci (QTLs) regulating complex properties like bone strength, fragility, and BMD have been identified (Klein et al. 1998; Beamer et al. 1999; Orwoll et al. 2001; Yershov et al. 2001; Li et al.

2002). However, few studies have been conducted with knowledge of the relationships among genes, cellular processes, growth patterns, physical traits, and mechanical functions (Yershov et al. 2001; Leamy et al. 2002; Li et al. 2002; Mohan et al. 2003; Li et al. 2007). The current data may provide new insight into this problem. Using a single complex trait such as BMD or BV/TV as the sole phenotypic marker in genetic analyses may be insufficient because of the complex relationship between mechanical properties and the underlying bone traits. The cortical, trabecular, and mineral components of the inbred mouse vertebral body are functionally dependent. Based on three distinct inbred mouse strains, the data suggest that individual strains do not inherit a single trait but a set of traits that determines whether bone will be 1) stiff, strong, and tough or 2) stiff, strong, and brittle. These sets of traits reflect the organ-level mechanical functionality of adult bone. Future work will focus on the biological processes that establish this functionality.

Not all load transfer pathways are equal

The results of the multivariate analysis, which showed that percolation parameters accurately explained stiffness but not F_U and Δ_T, also were consistent with the idea that structures are built to be sufficiently stiff for physiological loading demands. Network topology independent of vertebral size, amount of bone, and composition is sufficient to explain stiffness. However, global failure strength and ductility may depend on local failures in the network's ability to transfer load, which depend on the morphology and composition of the particular pathway. Additionally, not all pathways are used equally in the transfer of mechanical load. Thus, more information about the structure and how load is shared throughout the network may be needed to explain why the topological measures alone were poor predictors of F_U and Δ_T.

Fortunately, network science provides the foundation for future analyses studying the "fitness" or significance of certain pathways relative to the global structure (Barbasi 2002; Watts 2003). Individual trabecular struts and cortices can be assigned fitness values based on their combination of morphological and compositional traits. Different genotypes are expected to use unique combinations of high-fitness load pathways. Based on the data in the present study, C3H vertebrae had fit pathways with a combination of thick, highly mineralized struts (Table 3.1; Figure 3.1A) oriented in the direction of loading whereas B6 and A had fit pathways that were thinner and angled into the cortex compared to the direction of loading (connecting load to cortical boundaries). Knowledge of the failure mechanism of the most used load transfer pathways along with the morphology and composition of the specific paths would be expected to improve the explanatory power for global strength and ductility. Other factors contributing to the lower explanatory power for these regressions include 1) underestimation of F_U of C3H vertebral bodies due to brittle failure mode; 2) variation in other matrix components (Martin et al. 1989; Viguet-Carrin et al. 2006); and 3) architectural traits not measured in this study that could contribute to variation in more complex mechanical properties such as F_U and Δ_T (Fyhrie et al. 1994; Keaveny et al. 2002). The multivariate analyses performed here lay the groundwork for future analyses aimed at identifying other factors contributing to whole-bone mechanical properties and the direction of causality among these traits (Li et al. 2006).

Networks are dynamic objects, evolving during growth due to the activities of their components

One of the challenges to a complete understanding of the biological basis of

Wolff's law lies in understanding how architectural changes with growth (and aging) relate to mechanical function. Network science eliminates some of the shortcomings of reductionist techniques (BV/TV, Ct.Th, etc.) by revealing a way to quantify how bone cells establish and maintain a mechanically functional, connected structure throughout life. Fitness, or the probability of a structure to survive, provides a way to test the hypothesis that skeletal architecture changes to meet mechanical demands (Ruimerman et al. 2005; Glatt et al. 2007). To satisfy mechanical demands during growth, osteoblasts and osteoclasts are expected to arrange and maintain trabecular struts with the highest fitness relative to load transfer through the whole bone and remove struts that have low fitness or are unloaded. Paths with the highest fitness (i.e., critical to load transfer) would be hypothesized to be the pathways that are retained throughout growth. Thus, this analysis is in line with the idea that mechanical stresses (i.e., fluid flow) on osteocytes are critical for cells to remain viable and for individual bone components to adapt as part of the global structure (Wang et al. 2005).

The observed relationships among adult bone shape and quality were determined by genetic variation in cellular activity on trabecular and cortical bone surfaces. However, how the cells use available resources to shape the network to share loads is still not fully understood. The functional interaction between cortical and trabecular morphology appears to be an important biological paradigm for vertebrae. Genetic or environmental perturbations that alter these functional interactions during growth would be expected to lead to loss of function and/or suboptimal adult bone quality (Jepsen et al. 2007). The traditional approach of relating individual adult bone traits (BMD, etc.) to QTLs or cellular processes may be improved further by examining how sets of traits

develop during growth. Thus, improving our knowledge of the biological control mechanisms coordinating the set of trabecular and cortical traits during growth may provide new targets for genetic analyses as well as new strategies for building more robust bones.

Together with knowledge of mechanical environment, network topology also provides context not only about its transfer capacity in particular directions (normal physical activity versus a fall), but also how to improve the assessment of the deleterious effects of bone loss on mechanical behavior. We found that the vertebrae of three distinct inbred mouse strains could be described as a scale-free network based on the prominence of the cortical shell (Figure 3.1D) (Akhter et al. 2000; Turner et al. 2000; Klein et al. 2001; Tommasini et al. 2005). If osteoclastic resorption does not discriminate between nodes, but affect small nodes and large hubs with the same probability (i.e., random loss of bone struts due to uniform trabecular thinning), small nodes are far more likely to be dismantled in scale-free networks since there are many more of them (Barbasi 2002). Thus, the critical threshold below which a connected system is virtually unharmed is higher in scale-free networks because the existence of hubs keeps the network together. However, when the largest nodes of a scale-free network are removed (i.e., directed bone loss), there is a critical point beyond which the network breaks apart. Computational models of 3D networks have shown that trabecular perforation leads to the most significant loss of stiffness and strength compared to uniform thinning (Silva et al. 1997; Guo et al. 2002; Liebschner et al. 2005). Therefore, the network topology of adult corticocancellous structures impacts the severity of changes in mechanical integrity due to bone loss. Thus, we expect similar analyses of human bone to be valuable because

bone loss appears to be directed and not random (Singh et al. 1970; Ciarelli et al. 2000; Mosekilde et al. 2000).

This simple 2D analysis shows promise for future 3D analyses, which are used to assess 3D structures such as neural networks. Challenges that make 3D analysis of bone slightly more difficult than neural networks include proper classification of the vertical shell and the complexity of the loads experienced by corticocancellous structures such as the proximal femur. Currently, 3D algorithms are being developed on 3D models and bone volumes.

Summary

The results of this study demonstrate that measures provided by percolation theory provide additional insight into the contribution of genetically determined bone traits to variation in whole bone mechanical function. The network-based approach developed here introduces a shift in the perspective of bone as a highly organized, aligned, and adapted structure. Specifically, percolation parameters present a new way to attack the challenge of associating the architecture of corticocancellous structures, such as the proximal femur and vertebral body, with mechanical function. Although previous studies were successful in identifying structure-function relationships, the biologically significant aspect of Wolff's law has not been presented (Cowin 2001). This study showed that mechanically functional bone networks are built with different genetically determined combinations of trabecular bone, cortical bone, and mineral content. The data suggest the coordination of the biological activity of each cell population solves the global problem of mechanical functionality by creating and maintaining connected structures throughout life. Therefore, developing a network approach to study

corticocancellous architecture during growth should further our understanding of the biological basis of Wolff's law and, thus, provide novel engineering approaches to studying the genetic basis of fracture risk.

ACKNOWLEDGMENTS

The authors thank the National Institutes of Health (NIH AR44927; MH071818; NCRR 1S10RR014801) for their support of this research.

CHAPTER 4

PHENOTYPIC INTEGRATION OF TRABECULAR AND CORTICAL BONE TRAITS CONTRIBUTES TO GENETIC VARIATION IN MECHANICAL FUNCTIONALITY OF ADULT MOUSE VERTEBRAE

ABSTRACT

Prior studies in young adult mouse and human skeletons suggest that long bones possess biological processes which co-adapt morphological and compositional traits in a particular way to satisfy mechanical demands. However, it is not known whether similar phenotypic integration mechanisms exist in more complex corticocancellous sites. The goal of this study was test whether trabecular, cortical, and compositional bone traits are functionally related, as this would imply there is a strong biological process in bone that co-adapts traits.

Micro-architectural traits were assessed from L4 vertebrae from 20 female AXB/BXA Recombinant Inbred (RI) mouse strains (age=16 weeks) using micro-CT. Whole-bone mechanical properties were measured from vertebral body compression tests. A Path Analysis was conducted to test the hypothesis that phenotypic integration among cortical, trabecular, and compositional traits compensates for genetic variants affecting skeletal size and mass.

Path Analysis revealed that phenotypic integration among trabecular, cortical, and compositional traits plays a key role in achieving organ-level mechanical functionality. Smaller vertebrae relative to body size achieved stiffness sufficient for mechanical functionality by increasing tissue mineral density and the relative amounts of cortical and trabecular bone.

Without this phenotypic integration, smaller vertebrae relative to body size would be unable to support daily loads. However, because mineralization is involved, phenotypic integration may lead to a set of traits that is functional for daily loading, yet susceptible to fracture under extreme loading (i.e., fall). Thus, improved understanding of

the biological processes that contribute to phenotypic variation may provide a novel approach to identifying sets of traits that better predict fracture risk.

INTRODUCTION

Functional (i.e., compensatory) interactions among bone traits play a critical role in determining normal mechanical function. However, little is known about the nature of this phenotypic integration in the context of genetic variants affecting skeletal size, mass, and quality, which are key determinants of bone functionality and fracture susceptibility (Albright et al. 1941; Giladi et al. 1987; Milgrom et al. 1989; Gilsanz et al. 1995; Beck et al. 1996; Vega et al. 1998; Duan et al. 1999; Duan et al. 2001; Duan et al. 2001). In long bones, phenotypic integration of morphologic and compositional bone traits is critical in establishing mechanically functional structures by compensating for genetic variants leading to slender phenotypes. However, phenotypic integration also contributes to fracture susceptibility by giving rise to genotype-specific trait sets that are more damageable and brittle (Jepsen et al. 2007; Tommasini et al. 2008). Thus, improved understanding of the biological processes that contribute to phenotypic integration may provide a novel approach to identifying sets of traits that better predict fracture risk.

We expect phenotypic integration is not limited to long bone, but is a general paradigm affecting all skeletal sites including more complex corticocancellous structures. Most fractures typically occur in metaphyseal regions such as the distal radius, proximal femur, and vertebral body (NOF). There is growing evidence indicating that sets of interdependent morphological and compositional traits, in addition to BMD, provide more accurate predictions of fracture risk in more complex corticocancellous sites (Faulkner et al. 2007). Previous work in inbred mouse vertebrae showed that individual strains do not inherit a single bone trait, but a set of trabecular, cortical, and compositional traits that reflect the organ-level mechanical functionality of adult

vertebrae (Tommasini et al. 2005). Although never formally tested, other studies also have speculated that similar co-adaptive mechanisms observed in long bones exist in corticocancellous structures (Waarsing et al. 2006; Glatt et al. 2007).

One challenge to understanding the genetic basis of skeletal fragility in corticocancellous structures is understanding how the interdependence of physical bone traits affects the biomechanical roles of the cortical and trabecular components. Previous studies have generally segregated cortical and trabecular traits and have not considered that phenotypic values of trabecular architecture may depend on cortical traits. Adult trait correlations among cortical and trabecular traits arise because of functional interactions during growth. Bone cells work in a coordinated manner to construct a functional structure designed to share load among its components with limited available resources (amount of tissue is limited to minimize mass) (Currey et al. 1985; Frost 1987). As the relative amounts of cortical and trabecular tissue vary in a structure, the load sharing of these components varies (Silva et al. 1997; Eswaran et al. 2006). Because vertebrae are primarily loaded in compression, external size (cross-sectional area) is a critical phenotypic trait. Genetic controls determining bone size relative to body weight are expected to influence the biomechanical roles of the components during growth and ultimately the observed adult trait interactions. For example, if cortical thickness increases in response to genetic variants decreasing external size (similar to long bones), then stress shielding during growth would be expected to lead to decreased trabecular bone volume fraction in adult vertebrae (Figure 4.1).

Figure 4.1. Schematic illustrating proposed interdependence of cortical and trabecular traits during growth. If cortical thickness increases in response to genetic variants decreasing external size (similar to long bones), then stress shielding during growth would be expected to lead to decreased trabecular bone volume fraction in adults.

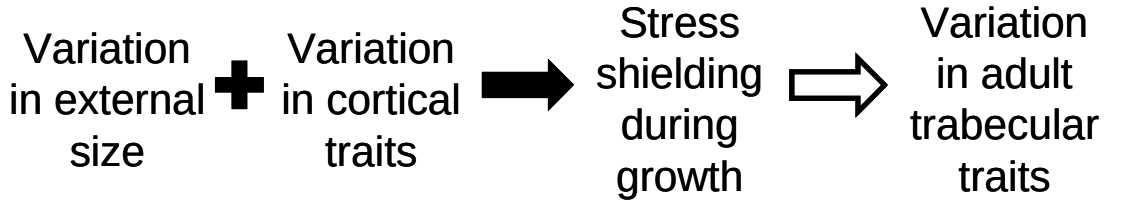

A systems biology approach provides insight into future studies assessing skeletal health (Jepsen et al. 2007). By viewing bone as a set of interdependent traits, we can learn new associations among physical bone traits that can be translated to the human skeleton (Tommasini et al. 2008) and that can be used to refine genetic analyses identifying genes that are directly involved in regulating bone strength. The goal of this study was to test whether trabecular, cortical, and compositional bone traits are functionally related, as this would imply there is a strong biological process in bone that co-adapts traits in corticocancellous structures. We postulate that the cortical and trabecular bone traits will co-vary with matrix composition contributing to bone stiffness and strength. We tested this hypothesis using a panel of AXB/BXA Recombinant Inbred (RI) Mouse Strains. The unique pattern of randomization of A/J and C57BL/6J genomic regions among the RI panel creates subtle, non-pathological trait variation that can be used to measure the tendency for different traits to co-vary and to study the biology of complex traits (Nadeau et al. 2003).

MATERIALS AND METHODS

Recombinant inbred mouse strains

Female AXB/BXA recombinant inbred (RI) mice derived from A/J and C57BL/6J (B6) progenitor strains were examined in this study. RI strains have a unique pattern of genetic randomization between their parental strains that creates subtle, non-pathological trait variation that can be used to measure the tendency for different traits to co-segregate or correlate (Nadeau et al. 2003). If the RI strains share common biological controls regulating trait co-variation, then the RI strains will build mechanically functional bones in slightly different ways depending on the set of A/J and B6 genes that were inherited (Figure 4.2). Traits can be examined across the panel as a powerful experimental model to quantify functional relationships among traits (Nadeau et al. 2003; Li et al. 2006).

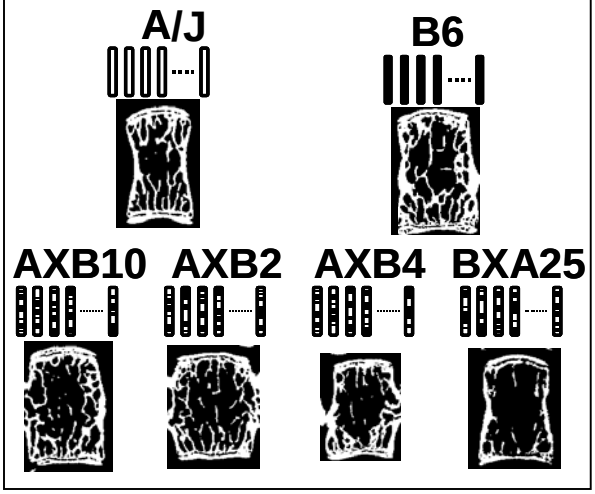

Figure 4.2. Coronal sections of vertebral bodies showing widely varying architectures among A/J, B6, and representative AXB/BXA RI strains.

A/J, B6, and 20 AXB/BXA RI strains (n = 10/genotype) were bred at The Jackson Laboratory (Bar Harbor, ME, USA) and shipped to the Mount Sinai School of Medicine (New York, NY, USA) at 3.5 weeks of age. The Institutional Animal Care and Use Committee approved the handling and treatment of mice. To standardize environmental conditions, mice were fed a standard rodent chow (Purina Rodent Chow 5001) and water *ad libitum*, subjected to a 12-h light:dark cycle, and raised with approximately 5 mice/cage in the same room. Mice were killed at 16 weeks of age because previous

studies showed that growth-related changes in traits slowed prior to this age (Price et al. 2005). Caudal lumbar vertebral segments, including L4-L6, were harvested and stored frozen in PBS with added calcium (Gustafson et al. 1996) at –20°C.

Physical bone traits

Micro-architectural traits and tissue mineral density (TMD) were measured using an eXplore Locus SP Pre-Clinical Specimen Micro-Computed Tomography (micro-CT) system (GE Healthcare, London, Ontario, Canada). The L4 vertebrae were scanned at 16μm voxel resolution. Vertebral bodies were isolated for analyses and cortical bone was segmented manually from trabecular bone (Figure 4.3) (Tommasini et al. 2005). Trabecular and cortical morphometry, including trabecular bone volume fraction (BV/TV), trabecular thickness (Tb.Th), trabecular number (Tb.N), trabecular separation (Tb.Sp), cortical area (Ct.Ar), and cortical thickness (Ct.Th), were assessed using MicroView Advanced Bone Analysis (v. 2.1; GE Healthcare). Vertebral body size was measured in two-dimensions as total cross-sectional area (Tt.Ar) averaged for all transverse sections per bone and in three-dimensions as total vertebral volume (Tt.V = total bone volume (Tt.BV) + marrow volume). The relative amount of cortical area (RCA) was calculated as Ct.Ar/Tt.Ar. TMD was calculated from the micro-CT images by converting the gray-scale output of bone voxels in Hounsfield units (HU) to mineral values (mg/cc of hydroxyapatite) through the use of a calibration phantom containing air, water, and hydroxyapatite (SB3:Gamex RMI, Middleton, WI, USA). TMD is defined as the average bone voxel HU value divided by the average HU value of the hydroxyapatite phantom multiplied by 1130 mg/cc (hydroxyapatite physical density). The same calibration phantom was included in all scans to adjust mineral density measurements for

the variability in X-ray attenuation inherent to independent scan sessions (Jepsen et al. 2007). Trabecular TMD (Tb.TMD), cortical TMD (Ct.TMD), and total TMD (Tt.TMD) were calculated.

Figure 4.3. Cortical bone was segmented manually from trabecular bone in micro-CT images of L4 vertebral bodies. Trabecular traits included BV/TV, Tb.N, Tb.Th, Tb.Sp, and Tb.TMD. Cortical traits included Ct.Ar, Ct.Th, and Ct.TMD.

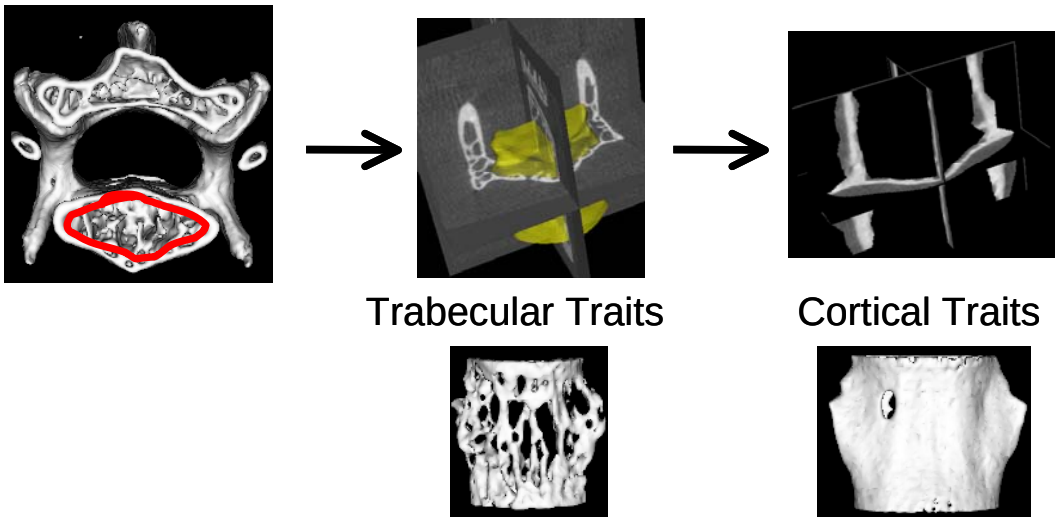

Network model and percolation parameters

The network topology of the vertebral bodies was assessed from the thresholded micro-CT images as described previously (Tommasini et al. 2008). Measures provided by network percolation theory provide an integrative and quantitative approach to study how different combinations of cortical and trabecular traits lead to mechanically functional structures. The corticocancellous architecture of the vertebral body was treated as a connected network whose function is to transfer mechanical load from superior to inferior surfaces (i.e., compressive loads). Two-dimensional (2D) coronal sections (two per bone) were skeletonized and nodes and branches were identified using an iterative thinning algorithm (Matlab, The Mathworks Inc., Natick, MA, USA). These 2D sections were taken from each bone at approximately 1/3 and 2/3 of the anteroposterior width of the

vertebral body. The skeleton graphs then were converted into network maps by considering the cortical surface as one highly connected node or hub.

Next, the algorithm calculated simple percolation parameters as described previously (Tommasini et al. 2008). The inputs into the algorithm are the set of nodes with their connected neighboring nodes and the starting and end points or surfaces. Thus, the network inputs did not take trabecular or cortical morphology into consideration. The only predefined rules for our network are that information can only travel from the superior surface toward the inferior surface (i.e., load applied to the superior surface can only travel to connected nodes in the network located either horizontal to or below) and the information is self-avoiding (i.e., information cannot travel to a node it has been to previously). The **correlation** and **chemical path** lengths measure the load sharing capacity of the network, which is expected to vary with genetic background. The chemical length (ChemL) is the number of nodes along the shortest path of the percolating network that connects opposite boundaries. The correlation length (CorrL) is the average number of nodes along all paths between connected opposite boundaries. To test how genetic variation in the combination of trabecular and cortical traits influences network behavior (i.e., load transfer) CorrL, ChemL, the number of load transfer paths (# paths), the number of nodes (# nodes), and the percentage of existing links connected to the cortex (%hub) were calculated.

Whole-bone mechanical properties

Whole-bone mechanical properties of intact L4 vertebrae (n=10/genotype) were measured by compressing the vertebral body with a 3mm diameter platen as described previously (Tommasini et al. 2005). Mechanical properties, including failure load (F_U)

and stiffness (S), were measured using a servohydraulic materials testing machine (Instron model 8872; Instron Corp., Canton, MA, USA). F_U was defined as the highest load preceding a rapid decrease in the measured load.

Co-variation among adult traits

Co-segregation of traits following genetic randomization can be examined using correlation analysis. Trait means and standard deviations were calculated for each AXB/BXA RI strain. Linear regressions between each of the traits were conducted across the RI panel using the mean values for each RI strain. Pearson correlation coefficients were calculated for all trait-trait comparisons to test whether the morphologic traits, mechanical properties, and network parameters correlated significantly with the architectural and compositional traits. The correlation matrix retained the magnitude and direction of each correlation coefficient. Statistically significant correlations were identified by establishing a threshold correlation magnitude determined using permutation tests (Churchill et al. 1994; Nadeau et al. 2003), which corrected for multiple comparisons and established the maximum correlation coefficient that arises when the bone traits are randomly arranged across the RI panel.

Narrow Sense Heritability

The narrow sense heritability, h^2, estimates the proportion of phenotypic variation attributable to additive genetic effects. h^2 was determined for all traits and mechanical properties using the method described by Belknap (Belknap 1998). For the RI panel, h^2 was determined as $V_A / (V_A + V_E)$, where V_A is the additive genetic component of variance, V_E is the environmental component of variance, and $V_A + V_E$ is the phenotypic variance, V_P. The value of h^2 was estimated using the R^2 value from a one-way ANOVA

by RI strain.

Path Analysis

Path Analysis is a multivariate analysis that allows for testing how multiple traits co-vary simultaneously. Path Analysis also offers the flexibility required to represent user-defined models based on hypotheses that best match a particular situation (i.e., directed relationships) (Wright 1921; Grace 2006; Jepsen et al. 2007; Sharkey et al. 2007). Thus, Path Analysis allowed us to test whether specific functional relationships among trabecular, cortical, and compositional bone traits exist for the AXB/BXA RI mouse vertebrae. Trait values were converted to Z-scores as $\text{Z-score}_i = (x_i - x_{\text{ref}})/\text{SD}_{\text{ref}}$, where x_i is the trait value for each mouse and x_{ref} and SD_{ref} are the mean and standard deviation, respectively, calculated using the average values for all 20 AXB/BXA RI strains. This Z-transformation standardizes the variables so each trait shows a mean of zero and a standard deviation of one.

Path coefficients, which represent the magnitude of the direct and indirect relationships between traits, were calculated using the Z-transformed data (LISREL v.8.8; Scientific Software International, Lincolnwood, IL, USA). Structural equations were constructed using the path coefficients to specify the interconnected relationships. Observed and model-implied covariance matrices were compared using maximum likelihood estimation and overall fit was determined by a chi-squared (χ^2) test. Unlike conventional null hypothesis testing, Path Analysis favors the *a priori*, theory-based model such that models are only rejected if the observed data and the expectations derived from the model do not match (i.e., if $p < 0.05$) (Grace 2006). The Root Mean Square Error of Approximation (RMSEA) was also reported and is a measure of fit

adjusted for population size and degrees of freedom (df) (Stieger et al. 1980; MacCallum et al. 1997). For RMSEA, the *p*-value represents the significance of fit with $p < 0.05$ indicating close fit, $0.05 < p < 0.08$ indicating fair fit, and $p > 0.10$ indicating poor fit (MacCallum et al. 1997). Preferred models should meet certain standards including: 1) it should have at least 1 df; 2) the p-value associated with χ^2 should be greater than 0.05; 3) individual path coefficients should be significantly different from 0 based on a t-test; 4) path coefficients should be greater than 0.05; 5) a substantial proportion of phenotypic variance of the endogenous variables (i.e., R^2-values associated with structural equations) should be explained by the model (Li et al. 2006).

Path model to test for phenotypic integration among traits: Phenotypic integration among physical bone traits is critical in establishing mechanical functionality by compensating for genetic variants that would otherwise threaten functionality. A path model was constructed to test whether a) genetic variants affecting vertebral size relative to body weight and b) genetic constraints imposed on the amount of tissue that can be used to construct functional vertebrae together determine the distribution of tissue types in functional vertebrae (Figure 4.4). To test the hypothesis that functional interactions among cortical, trabecular, and compositional traits compensate for genetic variants affecting skeletal size and mass, independent variables in the model included body weight, total vertebral volume (Tt.V), and total bone volume (Tt.BV). Dependent variables included the relative

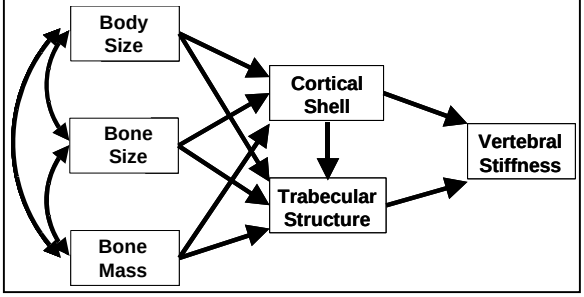

Figure 4.4. The proposed path model specified paths among select bone traits related to biological processes involved in the formation and resorption of bone tissue.

amounts of cortical area (RCA), trabecular bone volume (BV/TV), and total tissue mineral density (Tt.TMD). These traits were selected because functional interactions among the set of cortical (RCA), trabecular (BV/TV), and compositional (Tt.TMD) bone traits during growth and development collectively define adult whole-bone stiffness and strength. Further, these particular bone traits were used to construct the path model because they move us one step closer to the underlying biological processes involved in the formation and resorption of bone tissue during growth and development (RCA – periosteal and endosteal activity; BV/TV – endosteal activity; Tt.TMD – mineralization; Tt.V – growth plate biology and periosteal expansion) and the interactions among them.

Path model to test for robustness of interactions among cortical and trabecular traits:

A separate Path Analysis was performed to specifically examine the interactions among cortical and trabecular traits. To study this specific co-variation, we focused on a phenotype that, if it were not compensated, would lead to an under-designed (i.e., weaker) structure. For femora, this phenotypic trait was bone slenderness, which is largely genetically determined (Jepsen et al. 2007). For the vertebral body, total cross-sectional area (Tt.Ar) is a critical phenotypic trait, because the structure is loaded primarily in compression, and stiffness and strength are related to external size. Thus, genetic variants affecting Tt.Ar must be compensated by variation in other traits or the structure will be under-designed relative to body weight (Figure 4.1). Simplified Path Models were developed that removed the biological constraints imposed on the amount of bone tissue (Tt.BV). The models tested the specific nature of the cortical and trabecular trait relationships for the adult vertebrae of the AXB/BXA RI strains. The first model tested the hypothesis that cortical traits determine trabecular traits. Independent

variables included body weight, Tt.Ar, cortical area (Ct.Ar), and the cortical tissue mineral density (Ct.TMD). Dependent variables included trabecular thickness (Tb.Th), number (Tb.N), and tissue mineral density (Tb.TMD). The second model tested the reverse hypothesis, that trabecular traits determine cortical traits. Independent variables included body weight, Tt.Ar, and Tb.TMD. Dependent variables included Ct.Ar and Ct.TMD.

Model selection methods include Akaike's information criterion (AIC), which provides a penalized likelihood statistic for model comparison (Akaike 1973; Li et al. 2006). CAIC is an adjustment of AIC to correct for bias in small sample sizes and is recommended for our models because the ratio of the sample size to the number of estimable parameters is less than 40 (Burnham et al. 1998). A model with the smallest value of AIC or CAIC among several candidate models is preferred. The expected value of the cross-validation index (ECVI) also estimates the overall error and predictive validity of a model (Browne et al. 1993).

Path model to test for functional interactions among physical bone traits and network topology: A path model was constructed to test how the phenotypic integration among physical bone traits contributes to the variation in network topology. Correlation length (CorrL), the number of paths (#paths), and the percentage of links to the cortical shell (%hub) were added to the model testing the interactions among trabecular (BV/TV), cortical (RCA), and composition (TMD) traits. This model describes how the amount and the distribution of trabecular and cortical tissue specifically are arranged to transfer compressive loads. A separate model was constructed to test how the genetic variants affecting skeletal size and mass directly affect the percolation parameters. Independent

variables in the model included body weight, total vertebral volume (Tt.V), and total bone volume (Tt.BV). Dependent variables included the correlation length (CorrL), the number of paths (# paths), and the percentage of links to the cortical shell (% hub).

RESULTS

Variation in physical bone traits, mechanical properties, and network topology among AXB/BXA RI mouse strains

Randomization of A/J and B6 genomic regions resulted in wide variation in vertebral size, composition, and network architecture among the RI strains (Table 4.1). The mean values were normally distributed across the RI panel for all bone traits ($p > 0.1$, Kolmogorov-Smirnov test). Mean values of each trait revealed that the size and architecture of the RI vertebral bodies ranged from being smaller in overall size than A/J with thin cortices and lower BV/TV, to larger in volume compared to B6 vertebrae with thicker cortices and higher BV/TV. Body weight and Tt.TMD varied within and beyond the values of the A/J and B6 progenitor strains. Whole-bone stiffness (S) and strength (F_U) also showed wide variation among the RI strains. Percolation parameters ranged within and beyond the values for the A/J and B6 inbred strains (Table 4.2).

Table 4.1. Variation in vertebral body size, morphology, composition, and whole-bone stiffness and strength among 16-week old female A/J, B6, and AXB/BXA RI strains. Data shown as mean ± standard deviation.

	n	BW (g)	Height (mm)	Tt.V (mm^3)	Tt.Ar (mm^2)	BV/TV	Tb.N (mm^{-1})	Tb.Th (mm)	Tb.Sp (mm)	Tb.TMD (mg/cc)	Ct.Th (mm)	Ct.Ar (mm^2)	Ct.TMD (mg/cc)	Tt.TMD (mg/cc)	RCA	*S* (N/mm)	F_U (N)
A/J	10	18.7	1.9	2.45	1.4	0.20	4.97	0.040	0.16	680.6	0.09	0.34	871.4	802.9	0.24	171.1	17.4
		1.7	0.1	0.21	0.1	0.02	0.31	0.002	0.01	22.4	0.00	0.02	16.9	35.2	0.01	82.5	4.4
B6	10	20.6	2.2	3.3	1.7	0.25	5.91	0.040	0.13	691.5	0.10	0.42	891.3	811.7	0.25	161.0	24.5
		0.9	0.1	0.18	0.1	0.02	0.47	0.001	0.01	22.8	0.01	0.02	22.6	31.6	0.01	65.9	3.6
AXB1	9	20.8	2.2	2.83	1.4	0.17	4.28	0.040	0.20	682.5	0.09	0.35	925.9	844.1	0.24	102.8	21.6
		1.0	0.1	0.16	0.1	0.01	0.31	0.001	0.02	12.9	0.01	0.03	31.8	143.8	0.02	41.5	4.0
AXB2	10	20.1	1.8	2.46	1.5	0.21	5.27	0.040	0.15	663.4	0.09	0.36	867.3	786.1	0.24	110.0	22.2
		1.1	0.1	0.22	0.1	0.02	0.31	0.002	0.01	50.7	0.01	0.03	57.0	42.9	0.02	43.1	4.2
AXB4	10	15.9	1.7	1.68	1.1	0.17	4.55	0.037	0.18	616.7	0.08	0.27	821.4	753.3	0.25	65.7	14.1
		1.3	0.1	0.14	0.1	0.02	0.61	0.002	0.03	35.6	0.01	0.02	28.7	36.9	0.02	30.4	5.9
AXB5	9	19.3	2.0	2.26	1.3	0.14	3.62	0.039	0.24	651.8	0.08	0.31	831.0	776.3	0.24	75.2	13.9
		1.1	0.1	0.1	0.1	0.01	0.17	0.002	0.01	45.1	0.00	0.03	58.1	41.0	0.01	39.8	3.3
AXB6	10	24.0	2.3	3.41	1.6	0.22	4.97	0.044	0.16	722.6	0.10	0.41	927.6	849.4	0.25	150.0	29.5
		1.8	0.2	0.56	0.2	0.04	0.54	0.004	0.03	70.7	0.01	0.06	89.3	57.0	0.02	51.6	7.9
AXB8	9	17.6	2.1	2.56	1.4	0.13	3.63	0.039	0.24	592.8	0.08	0.3	851.7	775.5	0.22	98.9	12.7
		2.9	0.2	0.23	0.1	0.00	0.4	0.002	0.02	43.4	0.00	0.02	77.7	57.2	0.01	61.9	2.4
AXB10	9	21.4	2.0	2.94	1.6	0.25	5.68	0.043	0.13	699.7	0.09	0.37	895.8	811.4	0.23	122.0	24.2
		1.6	0.1	0.22	0.1	0.05	0.54	0.004	0.02	43.1	0.01	0.04	36.2	77.0	0.03	44.5	9.4
AXB12	9	19.8	2.0	2.78	1.6	0.21	5.15	0.040	0.15	635.3	0.07	0.32	814.5	735.8	0.21	89.6	15.0
		1.6	0.1	0.26	0.1	0.01	0.31	0.001	0.01	20.8	0.00	0.02	36.0	52.8	0.01	38.5	4.2
AXB13	10	19.0	2.0	2.67	1.5	0.21	5.25	0.041	0.15	662.8	0.08	0.35	844.0	774.7	0.24	113.5	19.2
		1.4	0.1	0.23	0.1	0.01	0.12	0.001	0.01	16.2	0.00	0.02	27.6	39.2	0.02	48.0	6.3
AXB15	10	24.8	2.3	3.52	1.7	0.20	4.74	0.042	0.17	680.3	0.09	0.4	892.3	813.1	0.24	111.5	21.4
		1.4	0.1	0.31	0.1	0.01	0.14	0.001	0.01	57.1	0.01	0.02	29.7	37.2	0.02	53.2	6.5
AXB18	10	18.7	2.1	2.84	1.5	0.15	4.3	0.036	0.20	557.4	0.07	0.3	795.0	714.2	0.20	65.3	10.5
		2.8	0.2	0.56	0.2	0.02	0.67	0.001	0.03	54.3	0.01	0.04	71.5	47.4	0.01	33.5	4.4
AXB19	10	22.9	2.0	2.94	1.6	0.18	4.66	0.039	0.18	650.9	0.09	0.37	886.9	808.4	0.24	151.2	17.8
		1.8	0.4	0.73	0.2	0.02	0.61	0.002	0.02	35.9	0.01	0.02	42.3	58.9	0.02	61.6	4.6
AXB20	10	15.2	1.9	3.42	1.4	0.18	4.82	0.037	0.17	561.1	0.07	0.28	778.7	694.0	0.20	80.9	11.4
		2.7	0.2	0.42	0.1	0.02	0.32	0.002	0.02	39.8	0.01	0.02	65.9	61.4	0.01	32.3	2.5
AXB23	10	20.5	1.9	2.55	1.4	0.25	5.67	0.043	0.13	718.8	0.09	0.36	892.8	824.6	0.25	128.4	23.0
		0.9	0.1	0.09	0.1	0.01	0.25	0.002	0.01	39.3	0.00	0.01	37.5	36.8	0.01	31.9	3.5
AXB24	9	19.9	2.2	2.94	1.5	0.27	6.32	0.043	0.12	729	0.09	0.36	885.7	816.5	0.25	163.9	24.9
		0.6	0.1	0.21	0.1	0.02	0.6	0.002	0.01	18.5	0.01	0.02	35.4	37.3	0.01	131.1	6.7
BXA7	10	23.1	2.1	3.35	1.8	0.15	3.58	0.042	0.24	685.4	0.10	0.45	891.6	830.1	0.25	131.1	21.8
		1.1	0.1	0.31	0.1	0.03	0.6	0.001	0.05	21.5	0.01	0.04	24.0	35.2	0.01	36.5	4.9
BXA14	10	23.3	2.2	3.18	1.5	0.25	5.75	0.044	0.13	708	0.09	0.37	887.8	814.5	0.25	139.3	29.0
		1.8	0.1	0.22	0.1	0.01	0.19	0.001	0.01	34.1	0.00	0.02	41.3	35.7	0.01	36.9	3.8
BXA17	10	22.6	2.2	3.09	1.5	0.25	5.97	0.042	0.13	666.6	0.08	0.35	846.3	769.2	0.23	140.5	25.0
		1.0	0.1	0.28	0.1	0.03	0.58	0.001	0.02	33.5	0.01	0.02	50.0	53.2	0.02	46.3	5.2
BXA25	10	24.1	2.1	3.08	1.6	0.28	6.31	0.044	0.11	734.6	0.10	0.42	930.9	849.1	0.26	163.2	30.6
		1.7	0.0	0.15	0.1	0.01	0.16	0.002	0.00	15.3	0.01	0.03	17.0	35.5	0.01	72.0	8.0
BXA26	10	17.9	1.9	2.4	1.4	0.19	4.8	0.040	0.17	657.7	0.09	0.35	864.4	791.1	0.25	146.9	19.2
		1.3	0.0	0.21	0.1	0.01	0.24	0.001	0.01	28.7	0.00	0.02	47.3	39.9	0.01	67.6	2.6
Mean		**20.5**	**2.0**	**2.8**	**1.5**	**0.21**	**5.01**	**0.041**	**0.17**	**665.9**	**0.09**	**0.36**	**867.9**	**791.6**	**0.24**	**121.9**	**20.4**
StDev		**2.6**	**0.2**	**0.44**	**0.2**	**0.04**	**0.82**	**0.003**	**0.04**	**49.4**	**0.01**	**0.04**	**41.4**	**43.2**	**0.02**	**49.8**	**4.9**

Co-segregation of physical bone traits across the AXB/BXA RI panel

A correlation analysis using the mean values for each RI strain was performed to identify physical bone traits that co-segregated (correlated) in a significant manner (Table 4.3). Permutation tests for 20 AXB/BXA RI strains and 20 traits indicated that a correlation coefficient of 0.69 corresponded to a significance level of $p < 0.10$, a

Table 4.2. Variation in network topology quantified by percolation theory among 16-week old female A/J, B6, and AXB/BXA RI strains. Data shown as mean ± standard deviation.

	n	CorrL	ChemL	# paths	# nodes	%hub
A/J	10	8.44 1.70	2.44 0.50	112.45 68.15	48.23 9.34	22.1% 9.0%
B6	10	11.36 2.71	2.35 0.51	340.67 383.35	64.57 9.35	17.5% 2.3%
AXB1	9	8.91 2.35	2.67 0.59	108.33 113.54	45.11 12.76	22.5% 5.6%
AXB2	10	8.83 2.79	2.60 0.62	113.85 83.71	49.90 17.21	19.7% 2.7%
AXB4	10	6.63 1.12	2.18 0.50	51.29 33.14	36.21 7.98	20.4% 3.0%
AXB5	9	6.09 1.58	2.34 0.70	31.84 20.78	27.56 7.94	27.0% 6.2%
AXB6	10	10.36 3.14	2.64 1.00	388.56 580.83	60.15 15.58	19.9% 5.6%
AXB8	9	5.96 1.74	2.32 0.81	60.67 18.78	29.74 6.80	25.8% 5.4%
AXB10	9	10.49 2.80	2.51 0.67	263.15 287.73	63.85 17.31	16.9% 3.0%
AXB12	9	9.23 1.55	2.55 0.43	125.64 69.57	53.43 8.94	18.5% 3.4%
AXB13	10	10.12 2.55	2.35 0.62	236.28 447.21	56.78 8.73	18.9% 2.7%
AXB15	10	11.40 2.74	2.49 0.49	326.82 201.45	60.45 12.07	19.4% 2.0%
AXB18	10	7.57 1.44	2.39 0.59	58.32 33.84	40.01 10.46	25.3% 7.3%
AXB19	10	7.40 1.65	2.54 0.43	54.16 31.39	41.26 7.72	22.9% 4.9%
AXB20	10	7.63 1.90	2.39 0.51	64.54 61.98	39.54 15.52	25.1% 7.1%
AXB23	10	9.91 1.66	2.44 0.50	190.77 161.38	56.63 9.59	19.0% 3.9%
AXB24	9	11.27 1.94	2.44 0.62	348.56 275.55	70.79 14.66	17.7% 2.2%
BXA7	10	6.12 1.52	2.68 0.96	39.24 24.99	29.22 8.96	26.6% 9.5%
BXA14	10	11.24 3.06	2.20 0.49	380.80 598.55	64.69 15.42	19.8% 3.4%
BXA17	10	11.97 2.72	2.30 0.62	779.69 1450.13	74.89 17.65	17.5% 2.4%
BXA25	10	12.36 3.75	2.40 0.51	878.91 1186.63	74.27 11.75	16.3% 3.5%
BXA26	10	8.43 1.67	2.40 0.51	155.68 65.50	51.54 8.99	18.5% 3.0%
Mean **StDev**		9.17 2.02	2.44 0.14	232.28 228.03	51.77 14.40	20.8% 3.3%

correlation coefficient of 0.72 corresponded to $p < 0.05$, and a correlation coefficient of 0.77 corresponded to $p < 0.01$. The analysis revealed that 37% (70 out of 190) of the correlations examined were significant ($r > \pm 0.72$, $p < 0.05$). Thus, many physical bone traits co-varied after genetic randomization. Narrow sense heritability values, h^2, were significant for all traits (Table 4.3). Trabecular and cortical morphological traits varied in h^2 from 0.54 – 0.83. Mineral density and mechanical properties ranged from 0.30 – 0.58. Percolation parameters varied from 0.09 – 0.75.

The data indicated that all RI strains built functional vertebrae with stiffness and strength values proportional to body weight (BW vs. S, $r = 0.64$; BW vs. F_U, $r = 0.76$). Relationships between certain traits such as Tb.N and BV/TV ($r = 0.97$) and Tb.N and Tb.Sp ($r = -0.99$) were expected based on geometric scaling and mathematical relationships. Most percolation parameters correlated with morphology as expected. CorrL, # paths, # nodes, and % hub were significantly correlated with trabecular morphology (BV/TV, Tb.N, Tb.Sp). Percolation parameters were also significantly related to stiffness and strength. ChemL did not

significantly correlate with any parameter and had the lowest h^2. This was a result of defining the cortical shell as a hub, which resulted in small variation in ChemL among the RI strains since each vertebral body had the same shortest load transfer path between

Table 4.3. Pearson correlation coefficients relating vertebral body morphology, composition, whole-bone mechanical properties, and network topology. Narrow sense heritability (h^2) on the diagonal. Bold values significant ($p < 0.05$) above threshold of $\pm$72 determined by permutation tests. All h^2 values are significant ($p < 0.001$).

	BW	**Tt.V**	**Tt.Ar**	**BV/TV**	**Tb.N**	**Tb.Th**	**Tb.Sp**	**Tb. TMD**	**Ct. TMD**	**Ct.Ar**	**Ct.Th**	**RCA**	**Tt. TMD**	***S***	F_U	**CorrL**	**ChemL**	**# paths**	**# nodes**	**%hub**
Body Weight	$h^2 = 0.76$																			
Tt.V	**0.85**	$h^2 = 0.67$																		
Tt.Ar	**0.78**	**0.90**	$h^2 = 0.67$																	
BV/TV	0.44	0.34	0.29	$h^2 = 0.83$																
Tb.N	0.29	0.22	0.17	**0.97**	$h^2 = 0.82$															
Tb.Th	**0.73**	0.58	0.54	**0.79**	0.63	$h^2 = 0.68$														
Tb.Sp	-0.29	-0.22	-0.18	**-0.96**	**-0.99**	-0.63	$h^2 = 0.80$													
Tb. TMD	0.71	0.48	0.44	**0.72**	0.55	**0.96**	-0.54	$h^2 = 0.50$												
Ct. TMD	**0.75**	0.56	0.49	0.45	0.28	**0.76**	-0.28	**0.86**	$h^2 = 0.35$											
Ct.Ar	**0.86**	0.78	**0.85**	0.42	0.24	**0.78**	-0.24	**0.77**	**0.80**	$h^2 = 0.75$										
Ct.Th	**0.77**	0.57	0.59	0.50	0.31	**0.85**	-0.31	**0.89**	**0.91**	**0.92**	$h^2 = 0.72$									
RCA	0.50	0.16	0.14	0.38	0.23	0.69	-0.22	**0.82**	**0.80**	0.64	**0.86**	$h^2 = 0.54$								
Tt. TMD	**0.73**	0.51	0.45	0.41	0.22	**0.77**	-0.21	**0.89**	**0.98**	**0.80**	**0.93**	**0.86**	$h^2 = 0.39$							
S	0.64	0.57	0.53	0.68	0.58	**0.76**	-0.55	**0.77**	**0.73**	**0.74**	**0.79**	0.62	**0.72**	$h^2 = 0.30$						
F_U	**0.76**	0.59	0.52	**0.79**	0.65	**0.93**	-0.64	**0.91**	**0.83**	**0.78**	**0.87**	**0.72**	**0.80**	**0.81**	$h^2 = 0.58$					
CorrL	0.57	0.54	0.41	**0.91**	**0.87**	**0.76**	**-0.88**	0.66	0.47	0.46	0.48	0.29	0.40	0.60	**0.77**	$h^2 = 0.67$				
ChemL	0.40	0.47	0.64	-0.06	-0.16	0.24	0.12	0.28	0.46	0.55	0.40	0.12	0.41	0.22	0.21	-0.02	$h^2 = 0.09$			
# paths	0.56	0.48	0.33	**0.77**	**0.73**	0.64	-0.68	0.56	0.42	0.44	0.49	0.35	0.38	0.61	**0.73**	**0.84**	-0.17	$h^2 = 0.39$		
# nodes	0.51	0.47	0.36	**0.95**	**0.92**	**0.75**	**-0.92**	0.65	0.43	0.42	0.45	0.29	0.37	0.65	**0.76**	**0.98**	-0.06	**0.84**	$h^2 = 0.75$	
%hub	-0.32	-0.18	-0.18	**-0.88**	**-0.87**	-0.65	**0.90**	-0.60	-0.38	-0.30	-0.39	-0.35	-0.33	-0.54	-0.65	**-0.84**	0.07	-0.67	**-0.89**	$h^2 = 0.56$

superior and inferior surfaces – through the cortex. Unexpected relationships such as the relationship between body weight and Tb.Th and the relationships between Tb.Th and

cortical traits were also observed. However, the correlation analysis does not convey the specific nature of these relationships.

Phenotypic integration among trabecular, cortical, and compositional traits

A path model (Figure 4.5), which tested whether phenotypic integration of cortical, trabecular, and compositional traits arises from genetic variants affecting body weight and vertebral size, and constraints imposed on the amount of tissue that can be used to construct functional vertebrae, fit the data extremely well (χ^2 = 9.11; p = 0.76; RMSEA = 0.000). The structural equations derived from the model explained 61-96% of the variation in adult Tt.TMD, RCA, and BV/TV (Figure 4.5). The structural equations indicated that if the total amount of tissue used to construct vertebrae is constrained (i.e., fixed Tt.BV) for a given body weight (i.e., fixed weight), a mouse showing a 1-SD decrease in Tt.V (i.e., small vertebral size relative to body size) would also show a 0.76-SD increase in Tt.TMD [0.38 (direct) + -1.42 x 0.80 (indirect)], a 1.42-SD increase in RCA, and a 1.25-SD increase in BV/TV [-1.78 (direct) + -1.42 x -0.37 (indirect)]. The path analysis also confirmed that cortical and trabecular bone traits were functionally related (Figure 4.5). Path coefficients reflect the strength of association among traits (line thickness). In particular, the proportional amount of cortical

Figure 4.5. Path model showing how functional interactions among cortical and trabecular traits compensate for genetic variants affecting vertebral size.

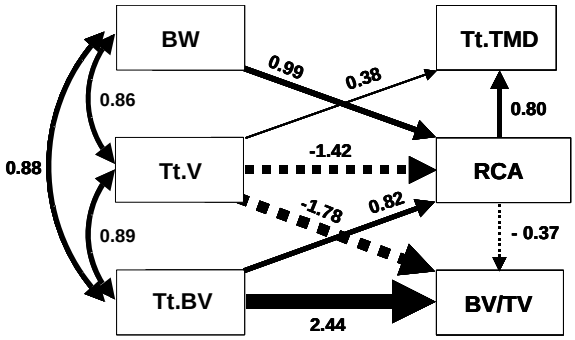

Chi-sq=0.38, df=4, p-value=0.98, RMSEA=0.000

Structural Equations (Z-transformed data)

Tt.TMD = 0.80 RCA + 0.38 TtV R^2 = 0.89
RCA = 0.99 BW - 1.42 TtV + 0.82 TtBV R^2 = 0.61
BV/TV = -0.37 RCA -1.78 TtV + 2.44 TtBV R^2 = 0.96

Reduced Structural Equations (Z-transformed data)

Tt.TMD = 0.79 BW - 0.76 TtV + 0.66 TtBV R^2 = 0.64
RCA = 0.98 BW - 1.42 TtV + 0.82 TtBV R^2 = 0.61
BV/TV = -0.36 BW - 1.25 TtV + 0.66 TtBV R^2 = 0.91

bone (RCA) was negatively related (-0.37) to the proportional amount of trabecular bone (BV/TV) and positively related to Tt.TMD (0.80). Thus, holding all other variables fixed, a 1-SD increase in RCA would result in a 0.37-SD decrease in BV/TV and a 0.80-SD increase in Tt.TMD.

Phenotypic integration among physical bone traits contributes to network topology

Including select percolation parameters to the path model (Figure 4.6) revealed that network topology was related to the phenotypic integration among physical bone traits. The structural equations derived from the path model showed that the functional interactions among Tt.TMD, RCA, and BV/TV explained 87% of correlation length (CorrL), 71% of the number of load transfer paths (# paths), and 77% of the percentage of connections to the cortical shell (%hub) (Figure 4.6). These results indicated that the functional interactions among trabecular, cortical, and composition traits influence how the architecture is designed to transfer load. Thus, the co-adaptation of traits in response to genetic variants affecting skeletal size and mass (Figure 4.5) occurs in a manner that creates functional load transfer networks. Mean trait values co-varied among the RI

Figure 4.6. Path model showing how interactions among trabecular and cortical traits influence network topology.

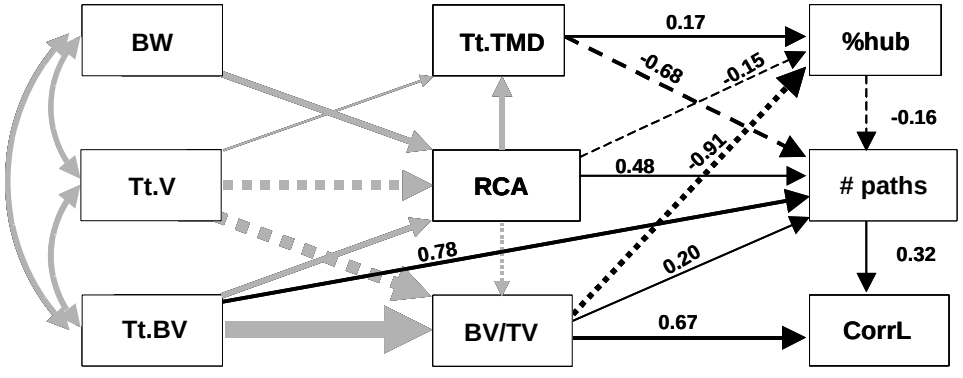

Chi-sq=17.59, df=15, p-value=0.29, RMSEA=0.104

Structural Equations (Z-transformed data)

CorrL = 0.67 BV/TV + 0.32 #paths R^2 = 0.87

#paths = 0.20 BV/TV + 0.48 RCA - 0.68 TtTMD R^2 = 0.71

%hub = -0.91 BV/TV - 0.15 RCA + 0.17 TtTMD R^2 = 0.77

Reduced Structural Equations (Z-transformed data)

CorrL = -0.67 BW - 1.03 TtV + 1.90 TtBV R^2 = 0.78

#paths = -0.19 BW - 0.61 TtV + 1.47 TtBV R^2 = 0.64

%hub = 0.31 BW + 1.22 TtV - 1.95 TtBV R^2 = 0.70

strains such that smaller vertebrae relative to body size achieve mechanical functionality by increasing the number of load transfer paths through trabeculae in the center of the vertebral body. Therefore, %hub decreases and CorrL (i.e., load sharing capacity of the network) increases.

The Path analysis also showed that network measures provided by percolation theory co-adapt in direct response to genetic variants affecting skeletal size and mass (Figure 4.7). Removing the physical bone traits (BV/TV, RCA, Tt.TMD) from the path model and directly linking body weight, vertebral size (Tt.V), and the total amount of bone tissue (Tt.BV) to percolation parameters (CorrL, # paths, % hub) resulted in a significant fit between the model and the data (χ^2 = 0.05; p = 0.83; RMSEA = 0.000). The reduced structural equations revealed that the same relationship between changes in skeletal size and mass and network topology existed as in the model that included the physical bone traits (Figure 4.6). Variation in body weight, Tt.V, and Tt.BV accounted for 81% of the variation in CorrL, 68% of the variation in # paths, and 66% of the variation in %hub (reduced structural equations, Figure 4.7). Further, smaller vertebrae relative to body size achieved mechanical functionality by increasing the number of load transfer paths through trabeculae in the center of the vertebral body.

Figure 4.7. Path model showing how network topology is directly related to variation in skeletal size and mass.

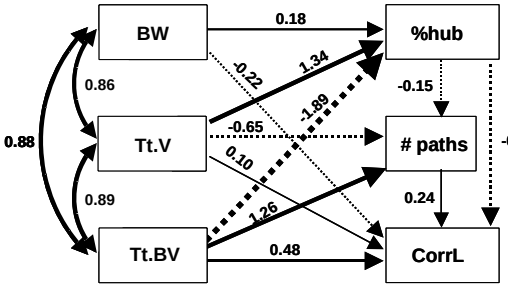

Chi-sq=0.05, df=1, p-value=0.83, RMSEA=0.000

Structural Equations (Z-transformed data)
CorrL = 0.24 #paths - 0.48 %hub - 0.22 BW + 0.10 TtV + 0.48 TtBV R^2 = 0.92
#paths = -0.15 %hub - 0.65 TtV + 1.26 TtBV R^2 = 0.69
%hub = 0.18 BW + 1.34 TtV - 1.89 TtBV R^2 = 0.66

Reduced Structural Equations (Z-transformed data)
CorrL = -0.32 BW - 0.75 TtV + 1.76 TtBV R^2 = 0.81
#paths = -0.03 BW - 0.86 TtV + 1.55 TtBV R^2 = 0.68
%hub = 0.18 BW + 1.34 TtV - 1.89 TtBV R^2 = 0.66

Phenotypic integration among physical bone traits contributes to whole-bone stiffness and strength

The structural equations derived from the path model showed that the functional interactions among Tt.TMD, RCA, and BV/TV explained 66% of adult stiffness and 91% of adult strength (Figure 4.8). These results indicated that mean trait values co-varied among the RI strains such that smaller vertebrae relative to body size achieve mechanical functionality by increasing Tt.TMD and the relative amounts of cortical and trabecular bone.

Figure 4.8. Path model showing how phenotypic integration among cortical, trabecular, and compositional traits contribute to mechanical properties.

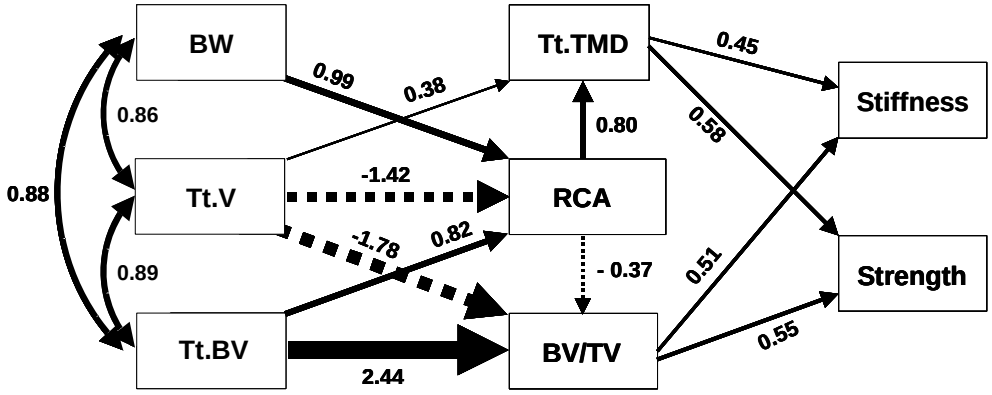

Chi-sq=9.11, df=13, p-value=0.76, RMSEA=0.000

Structural Equations (Z -transformed data)
Tt.TMD = 0.80 RCA + 0.38 TtV R^2 = 0.89
RCA = 0.99 BW – 1.42 TtV + TtBV R^2 = 0.61
BV/TV = -0.37 RCA – 1.78 TtV + 2.44 TtBV R^2 = 0.96

Structural Equations (Z -transformed data)
Stiff = 0.51 BV/TV + 45 Tt.TMD R^2 = 0.66
Strength = 0.55 BV/TV + 0.58 TMD R^2=0.91

Functional interactions among cortical and trabecular traits

We expect that genetic variants affecting the size and quality of the cortical shell during growth will influence adult trabecular bone mass and architecture (Figure 4.1). The Path Analysis using only adult traits (Figure 4.5) suggested that trabecular mass and mineralization depend on cortical traits. The inclusion of arrows from RCA to Tt.TMD and BV/TV were critical for the model to fit the data. Reversing the direction of one of

these arrows or removing one of these arrows decreased the goodness of fit, suggesting that the relative amount of cortical bone used to construct vertebrae dictated the amount and composition of trabecular bone in the adult structure. Path models were constructed to test the robustness the relationship between cortical and trabecular traits. Total vertebral body cross-sectional area (Tt.Ar) and body weight were included to take body size into consideration. Goodness-of-fit statistics indicated that both models fit the data (Table 4.4). Model selection statistics (Table 4.4) indicated that the model with the trabecular traits determining the cortical traits (Figure 4.9B) is slightly preferred over the other model (Figure 4.9A). However, caution is recommended in this interpretation because the physical traits are the result of multiple causal effects, some of which may be influenced by unobserved factors.

Table 4.4. Model comparison for relationship between cortical and trabecular traits. χ^2 – goodness-of-fit. RMSEA – root mean square error of approximation. df – degrees of freedom. ECVI – expected value of the cross-validation index. AIC – Akaike's information criterion. CAIC – corrected AIC.

Model Direction	χ^2	df	*p*-Value	RMSEA (90% CI)	ECVI (90% CI)	AIC	CAIC
Ct → Tb	2.05	5	0.84	0 (0.0 – 0.20)	3.40 (3.40 – 3.61)	48.1	94.0
Ct ← Tb	0.13	1	0.72	0 (0.0 – 0.49)	2.73 (2.73 – 2.97)	40.1	80.0

Figure 4.9. Path models testing the robustness of the functional interactions among cortical and trabecular traits. **(A)** Variation in cortical traits dictates the observed variation in trabecular traits. **(B)** Variation in trabecular traits dictates observed variation in cortical traits.

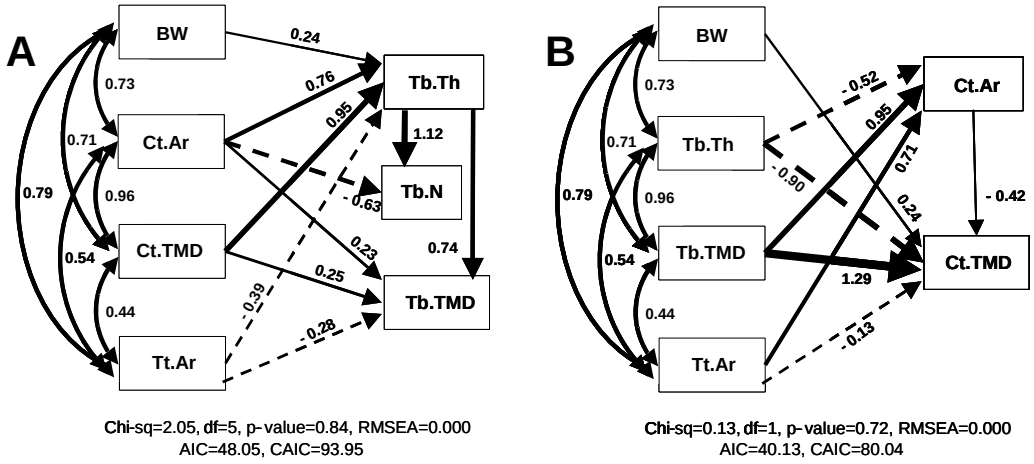

DISCUSSION

Phenotypic integration provides insight into the biological basis of skeletal functionality and fragility

The data showed that phenotypic integration among trabecular, cortical, and compositional traits plays a key role in achieving organ-level mechanical functionality. The Path models presented here also provide insight into the genetic basis of skeletal fragility by suggesting that the co-variation observed among adult traits is a result of biological processes that co-adapt traits. Based on the RI analysis, smaller vertebrae relative to body size achieve stiffness sufficient for mechanical functionality by increasing TMD and the relative amounts of cortical and trabecular bone. The data suggest that there is tremendous order in the way a functional bone is constructed. Bone is constructed not with a random set of traits, but with a highly integrated set of traits with the aim to transfer load as efficiently as possible (i.e., using limited available resources). Without this phenotypic integration, smaller vertebrae relative to body size would be unable to support daily loads (i.e., not functional). However, because mineralization is involved, phenotypic integration may lead to a set of traits that is functional for daily loading, yet susceptible to fracture under extreme loading (i.e., fall). This is consistent with previous work examining phenotypic integration in the mouse and human skeletons that offered a different perspective on how fracture susceptibility may arise: 1) some sets of traits arising from phenotypic integration may be susceptible to fracture under challenging physiological conditions, 2) genetic or environmental variants that disrupt the biological processes involved in phenotypic integration would be expected to affect functionality (Jepsen et al. 2007; Tommasini et al. 2008).

Systems biology approach identified functionally related traits

Assessment of physical bone traits that determine mechanical strength of corticocancellous bone largely centers on bone mineral density (BMD) of individual components (i.e., trabecular BV/TV). However, few studies are conducted with knowledge of the relationships among genes, cellular processes, physical traits of cortical *and* trabecular bone, and mechanical function. Prior studies reported functional relationships among physical bone traits using correlation analysis (Turner et al. 2000; Rosen et al. 2001; Tommasini et al. 2005; Ng et al. 2007). In the current study, the observed trait correlations in the bivariate analysis did not fully describe the relationship between traits. However, in a complex system such as bone, the overall nature of the interactions of multiple traits in the context of function is better understood through a systems biology approach (Nadeau et al. 2003). The Path analysis explained how the bone traits interact and how the interactions define mechanical functionality. For example, the bivariate analysis (Table 4.3) revealed a positive relationship between BV/TV and Tt.V. The Path analysis showed that, in the context of weight and amount of bone, Tt.V and BV/TV had a net *negative* relationship (Figure 4.5). Thus, the systems biology approach revealed the compensatory nature of the relationship between traits that was not evident from the bivariate analysis.

Network theory approach quantified how architecture was arranged to perform mechanical function

Although traditional measures of cortical and trabecular bone adequately characterize the phenotypes of each bone type, knowledge of the trait values themselves does not fully reveal how function is established for each genotype. This requires

knowledge of how the trabecular and cortical traits interact to transfer mechanical load. We previously developed novel traits based on percolation theory to quantify the architecture of the vertebral body in an integrative way (Tommasini et al. 2008). The percolation parameters provided quantitative measures of the load transferring behavior of the developing system as a function of the connected cortical and trabecular components. The Path analysis indicated that phenotypic integration among cortical and trabecular traits responds to genetic variants affecting skeletal size and mass in a manner that creates functional load transfer networks. Together, the network and systems biology approaches integrated traditional measures of the amount and distribution of bone tissue (e.g., BV/TV, Tb.N, TbTh, Ct.Th) with connectivity in the context of mechanical function.

The observed relationships among adult physical bone traits were determined by genetic variation in cellular activity during growth. During growth, bone cells arrange and maintain trabeculae to satisfy normal physiological loading demands (Frost 1987; Tanck et al. 2006; van Oers et al. 2008). For the mouse vertebral bodies, normal mechanical function was defined as compressive load transfer. Paths critical to load transfer are expected to be retained and paths that are not critical to load transfer would be expected to be resorbed. Although phenotypic integration ensures that the vertebral body is mechanically functional for normal activity during growth, not all genotypes are expected to show the same capacity to maintain strength with aging (Christian et al. 1989; Kelly et al. 1993; Duan et al. 2005). The RI analysis in the current study indicated that genetic variants affecting skeletal size influence the load transfer characteristics of structures that are functional for daily loads. However, it is unclear how genetic variation

in osteoblast and osteoclast activity on existing bone surfaces during growth impacts adult whole-bone mechanical properties. The age-related changes in trabecular bone mass are associated with age-related changes in cortical bone morphology, suggesting that expansion of the cortical shell may compensate mechanically for the loss of trabecular bone mass (Glatt et al. 2007). However, the nature of this compensatory relationship between cortical and trabecular traits with aging is not fully understood (Waarsing et al. 2006). The network topology of the adult structure (quantified by percolation theory) has potential for determining the severity of changes in mechanical function due to loss with aging (Tommasini et al. 2008). This is important because bones may lose similar amounts of bone mass in different ways. Thus, understanding the biological control mechanisms coordinating the set of trabecular and cortical traits into functional networks during growth and with aging is important to improving analyses studying the genetic basis of skeletal fragility.

Specific nature of the relationship between cortical and trabecular traits

Because the relationships between RCA and Tt.TMD, and RCA and BV/TV were critical for the Path model of the mouse vertebral body (Figure 4.5), we tested the specific nature of the relationships between cortical and trabecular traits. We postulate that there exists a temporal and ordered relationship between cortical and trabecular traits such that during growth, the amount and composition of the cortical shell determine the amount, morphology, and composition of the trabecular bone in corticocancellous structures (Figure 4.1). Although the model with the trabecular traits determining the cortical traits was slightly preferred based on model selection criteria (Table 4.4), both models (Figure 4.9) fit the data well indicating that the functional relationships are tightly

coupled and it is not possible to clearly state which traits determine which. Further, the physical traits are the result of multiple causal effects, some of which may be influenced by unobserved factors. Thus, the true nature of the relationship between adult cortical and trabecular traits may not be determined without knowledge of how the traits develop over multiple time-points during growth (Price et al. 2005).

Phenotypic integration in inbred mouse vertebrae has relevance to the human skeleton

Inbred mouse models have proven to be an extremely valuable resource for understanding the genetic basis of complex traits (Rosen et al. 2001). Recombinant Inbred (RI) mouse strains are a powerful experimental model to quantify phenotypic integration among traits (Nadeau et al. 2003; Li et al. 2006). Random segregation of naturally occurring allelic variants during meiosis result in each RI strain having a random assortment of parental genomic regions. This randomization results in a wide range of phenotypes among the strains. The specific combination of adult traits for each RI strain is a reflection of how the particular genes for that strain work together to influence cellular activities involved in phenotypic integration.

Inbred mouse models also have proven to be reliable models for studying both growth (Price et al. 2005) and aging (Halloran et al. 2002; Glatt et al. 2007) of human bone. Although mouse bone is small and does not have an extensive osteonal microstructure compared to human bone, the biological concepts learned from the mouse diaphysis (Jepsen et al. 2003; Jepsen et al. 2007) have been successfully translated to the human skeleton (Tommasini et al. 2005; Tommasini et al. 2007; Tommasini et al. 2008). This suggests that phenotypic integration required to establish mechanical function is similar in mouse and human long bone. Although the mouse vertebral body has

proportionally fewer trabeculae compared to the human vertebral body, the age-related changes in mouse trabecular bone and the associated changes in the cortex are consistent with those observed in the human skeleton (Glatt et al. 2007). Further, the cortical shell of the mouse vertebral body comprises 20-26% of the total area fraction of the structure, consistent with the human vertebrae (Eswaran et al. 2006). Thus, the mouse vertebral body provides a relevant model to study phenotypic integration in the human skeleton.

Summary

The results of this study revealed that phenotypic integration among cortical, trabecular, and compositional traits contributes to the mechanical functionality of corticocancellous structures. Based on the RI analysis, smaller vertebrae relative to body size achieved stiffness sufficient for mechanical functionality by increasing TMD and the relative amounts of cortical and trabecular bone. A network analysis using measures provided by percolation theory indicated that this phenotypic integration among cortical and trabecular traits responds to genetic variants affecting skeletal size and mass in a manner that creates functional load transfer networks. Together, the data suggest that there is tremendous order in the way a functional bone is constructed. Bone is constructed not with a random set of traits, but with a highly integrated set of traits with the aim to transfer load as efficiently as possible (i.e., using limited available resources). Without phenotypic integration, smaller vertebrae relative to body size would be unable to support daily loads (i.e., not functional). This is consistent with previous work examining phenotypic integration in mouse and human long bones (Jepsen et al. 2007; Tommasini et al. 2008). The results of these studies and the current study have great clinical significance because they provide two new areas of focus in studying skeletal fragility: 1)

sets of traits arising from phenotypic integration that may be susceptible to fracture under challenging physiological conditions, 2) genetic or environmental variants that disrupt the biological processes involved in phenotypic integration and thus affect functionality. This study demonstrated that, together, the systems biology and network approaches offer the potential to identify sets of traits that are susceptible to fracture and biological mechanisms controlling phenotypic integration for corticocancellous structures. By understanding the genetic variation in the interaction among sets of traits and how this variation defines complex traits like BMD, strength, and fragility, our understanding of the genetic basis of skeletal functionality and fragility can be improved.

ACKNOWLEDGMENTS

The authors thank the National Institutes of Health (AR44927, RR12305) for their support of this research.

CHAPTER 5

GENERAL CONCLUSIONS AND FUTURE DIRECTIONS

General Conclusions

The goal of this dissertation was to better understand how phenotypic integration creates sets of bone traits that are functional for daily activities, but also may contribute to skeletal fragility. Previous studies found that mouse femora that were slender relative to body weight established whole-bone stiffness and strength through compensatory increases in cortical thickness and matrix mineralization. However, this phenotypic integration occurred at the expense of increased brittleness as the increased mineralization led to reduced tissue-ductility (Jepsen et al. 2007).

Our first objective was to test whether the biological concepts observed in the mouse femur can be translated to the human skeleton. We examined the morphology, tissue-level mechanical properties, and tissue-level quality of tibiae from young adult human males and females. The results of this study identified functional interactions among physical bone traits suggesting that bone possesses important biological processes that co-adapt morphological and compositional traits so the set of traits results in a structure sufficiently stiff for daily activities (Chapter 2). These results have important clinical implications as they also may explain why having a narrow (i.e., more slender) tibia relative to body mass has been shown to be a major predictor of stress fracture risk. Phenotypic integration among traits produced structures functional for daily activities, but the disadvantage to co-adapting matrix composition is that increases in mineralization resulted in a more brittle and damageable material that would be expected to perform poorly under extreme load conditions. Thus, for more slender bones, reduced tissue ductility and toughness associated with greater ash content may increase the risk of fracturing from low-cycle fatigue (e.g., military training) and overload (e.g., falling).

This study also suggested that bone functionality and bone biology may be better understood based on knowledge of sets of traits rather than a single complex trait such as bone mass. An analysis of young adults identified relationships among physical bone traits at the end of the growth phase and before appreciable bone loss begins. Females tended to have slightly larger mineralization, thicker cortices, and more slender bones compared to males. Marrow area proved to be a strong covariate for ash content in the Path analysis for females, but not males (Chapter 2). This is consistent with dimorphic growth patterns after puberty, in which the endosteum switches from expansion to infilling for females (Garn 1970). In males, the marrow space continues to expand in proportion to periosteal expansion. Prior work showed that females prone to stress fractures had more narrow tibiae and thinner cortices compared to females that did not develop stress fracture (Beck et al. 2000). Having slender bones plus thinner cortices may indicate that for these individuals there was a lack of infilling or lack of co-adaptation between periosteal and endosteal surface movements during growth. Variation in the ability of bone to co-adapt traits would be expected to lead to under- and over-designed structures. Therefore, rather than using complex traits or a series of unrelated traits, clinical assessment of fracture risk may benefit from knowledge of sets of traits and the functional interactions among the traits.

The relationship observed between bone morphology and tissue quality of young adult human cortical bone was consistent with past work that observed a coordinated relationship across a large range of bones from many species (Currey 1979) and for inbred mice (Jepsen et al. 2001; Price et al. 2005; Tommasini et al. 2005), bats (Swartz et al. 1992), gulls (Carrier et al. 1990), and polar bears (Brear et al. 1990). The results of

this study also validated the use of mouse models for studying fracture risk in the human skeleton. Despite differences between mouse and human bone, and differences in traits that were measured (i.e., remodeled tissue, porosity), the basic principles of phenotypic integration held in both skeletons. In both the mouse and human skeletons, genetic heterogeneity led to variability in adult long bone morphology and tissue-level mechanical properties. Therefore, the mouse models offer tremendous potential for studying the genetic basis of fracture risk in more complex corticocancellous structures.

In Chapter 3, we moved back to the mouse model, using genetically distinct inbred mouse strains to study functional relationships among trabecular, cortical, and compositional bone traits in the vertebral body. Previous studies examining details of trabecular bone architecture revealed that differences in mechanical properties could be explained by regional variation in trabecular architecture (Beamer et al. 1996; Ritzel et al. 1997; Tabor 2003). These studies failed to relate form and functionality because they did not consider the interactions of the trabecular and cortical components of the structure. Therefore, we developed a novel approach using percolation theory that presented a new way of associating the genetically determined architecture of corticocancellous structures, such as the proximal femur and vertebral body, with mechanical function (Chapter 3). Specifically, parameters derived from percolation theory showed that A and B6 mice transfer compressive load through trabecular pathways in the middle of the vertebral body in addition to the cortical shell. C3H mice transfer load primarily through the highly mineralized cortical shell. Thus, the measures provided by percolation theory provide a quantitative approach to study how genetic variation in the combination of cortical and trabecular traits leads to mechanically functional structures. The data further emphasize

the interdependent nature of these physical bone traits suggesting similar genetic variants may affect both trabecular and cortical bone.

The network-based approach developed here also introduces a shift in the perspective of bone as a highly organized, aligned, and adapted structure. Although previous studies were successful in identifying structure-function relationships, the biologically significant aspect of Wolff's law has not been presented (Cowin 2001). The network approach developed here was not meant to replace the methods used to understand the structure-function relationships, but to supplement them. The percolation parameters related the inter-relationships among trabecular, cortical, and compositional bone traits to mechanical load transfer and suggested the coordination of the biological activity of each cell population solves the global problem of mechanical functionality by creating and maintaining connected structures throughout life (Chapter 3). However, as seen in mouse and human long bones, not all trait sets are ideal under extreme loading. C3H vertebrae had thicker cortices and higher mineral leading to reduced tissue-ductility. Thus, the measures provided by percolation theory offer potential for studies of the biological basis of skeletal fragility and provide novel engineering approaches to studying the genetic basis of fracture risk.

Our final objective was to combine a systems biology approach using Path analysis with our newly developed network approach using percolation theory to study phenotypic integration among cortical, trabecular, and compositional traits in Recombinant inbred mouse vertebrae (Chapter 4). The results of this study indicated that this phenotypic integration among cortical and trabecular traits responded to genetic variants affecting skeletal size and mass in a manner that created functional load transfer

networks. Based on the RI analysis, smaller vertebrae relative to body size achieved stiffness sufficient for mechanical functionality by increasing tissue mineral density and the relative amounts of cortical and trabecular bone. Without phenotypic integration, smaller vertebrae relative to body size would have been unable to support daily loads (i.e., not functional). However, increases in mineral content may lead to fracture risk under extreme loading. This was consistent with the results in mouse and human long bones where genetic variants affecting skeletal size were compensated by increases in cortical thickness and mineralization while using minimum mass (Jepsen et al. 2007; Tommasini et al. 2008).

The data suggested that there is tremendous order in the way a functional bone is constructed (Chapter 4). Although we postulate that there is a temporal and ordered relationship between cortical and trabecular traits such that the amount and composition of the cortical shell determine the amount, morphology, and composition of trabecular bone during growth, this dissertation was not intended to establish the causality of these relationships. Multiple models for the mouse vertebrae were explored to better understand bone as a system. The statistical relationships among bone traits were perceived as being functional rather than causal. The observed significant correlations support the hypothesis that trabecular, cortical, and compositional bone traits are functionally related (Chapter 4) and share common biological controls affecting growth (Wright 1918). Future investigations characterizing these relationships during growth will confirm the causal nature of the trait interactions.

The results of this study also provided new insight into the genetic basis of fracture susceptibility for the lumbar vertebral body, which is a clinically relevant site.

This approach focused on the adaptive response of bone, not in terms of how bone responds to changes in loading environment, but how the system adjusts to genetic variants altering skeletal size and mass relative to body size. The analysis of the RI strains identified compensatory relationships that contributed to vertebral stiffness and strength (Chapter 4). Thus, all individuals inherit sets of traits, but certain individuals inherit sets that are more susceptible to fracturing ("at risk" sets of traits). Further, phenotypic integration is genetically controlled so bone is not constructed with a random set of traits, but with a highly integrated set of traits with the function to transfer loads as efficiently as possible (i.e., using limited available resources). A better understanding of the biological principles of how bone establishes functionality will lead to new ways to monitor bone health to reduce fracture risk.

Together, the results of this dissertation have great clinical significance because they provide two new areas of focus in studying skeletal fragility: 1) sets of traits arising from phenotypic integration that may be susceptible to fracture under challenging physiological conditions and 2) genetic or environmental variants that disrupt the biological processes involved in phenotypic integration and thus affect functionality. By successfully translating the biological concepts previously learned in mouse femora to the human skeleton, we have shown that inbred mouse models are reliable models to study phenotypic integration in the human skeleton. Further, the mouse models are a tremendous resource for understanding the genetic basis of complex traits associated with fracture risk. The systems biology and network approaches offer the potential to identify sets of traits that are susceptible to fracture and biological mechanisms controlling phenotypic integration for corticocancellous structures. By understanding the genetic

variation in the interaction among sets of traits and how this variation defines complex traits like BMD, strength, and fragility, our understanding of the genetic basis of skeletal functionality and fragility can be improved.

Future directions

The interactions among trabecular, cortical, and compositional bone traits were observed in the young adult skeleton. The next step in understanding how phenotypic integration contributes to skeletal functionality and fragility is to determine how these functional interactions arise during growth. The functional interactions among cortical and trabecular traits are thought to be dependent on the mechano-responsiveness of bone to normal physiological loads. Principal strains experienced during normal physiological loading direct the development of trabecular bone mass as well as trabecular alignment (Biewener et al. 1996). We hypothesize that load sharing is important for interactions among cortical and trabecular traits. Because trabecular bone is mechanically responsive (Guldberg et al. 1997), the amount of load passing to the trabeculae will determine the extent of remodeling. A stiffer cortical shell would thus result in stress shielding of trabeculae and a greater amount of resorption of primary cancellous bone.

Understanding the temporal sequence of trabecular and cortical bone development is critical for understanding how genetic variation in the timing and degree of trabecular remodeling leads to genotype- and sex-specific adult trabecular architecture. The RI mouse model used in this dissertation (Chapter 4) can be used to determine how phenotypic integration among cortical and trabecular traits changes with growth. Trabecular bone is thought to start as a generic, isotropic structure that remodels over

time into a highly adapted, anisotropic structure (Fazzalari et al. 1997; Tanck et al. 2001). To test whether functional interactions among adult traits can be explained based on load sharing mechanisms during ontogeny, the evolution of topological variation can be examined using percolation traits, and then the fraction of load borne by cortical and trabecular components can be estimated using finite element analysis. If trabecular traits are being remodeled to transfer load through a thicker cortical shell, then the percolation parameter %hub (Chapters 3,4) will show greater increases over time for that genotype. These results can then be combined with histological analyses to examine the amount and location of osteoblastic and osteoclastic activity responsible for variable trabecular traits. Further, a Path analysis can test for functional relationships among measures of bone formation and bone resorption during growth.

Age-related changes in bone also have a genetic basis and it is not expected that all geontypes will have same capacity for maintaining strength with aging. We hypothesize that age-related changes are an extension of the adaptive nature of bone that establishes functionality during growth. The net loss of bone mass and high amount of trabecular bone remodeling associated with aging appears adaptive in nature (Waarsing et al. 2006). Observed age-related changes in trabecular bone mass also relate to changes in cortical morphology, suggesting that expansion of the cortical shell may compensate mechanically for the loss of trabecular bone mass (Glatt et al. 2007). This is important because the amount of periosteal expansion affects overall bone strength (Szulc et al. 2006). Small increases in bone size offset deleterious effects associated with large losses of bone on endosteal surface and play an important role in maintaining long bone (Smith et al. 1964; Martin et al. 1977; Ahlborg et al. 2003; Szulc et al. 2006) and vertebral body

(Duan et al. 2005) strength. However, the compensatory nature of this association has not been tested in longitudinal studies and it is unclear how variable remodeling events during aging impact whole-bone strength. This has clinical importance because two bones may lose similar amount of bone mass, but in different ways. The amount and location of loss have critical impact on strength. Thus, to advance our understanding of the biological processes operating to maintain strength with aging, a better understanding of how phenotypic integration among traits changes with age is needed.

This dissertation also demonstrated that the results from future mouse studies could be translated to studies of the human skeleton (Chapter 2). Therefore, another area for future studies could be to use the tools presented here to quantify changes in architecture observed in clinically relevant corticocancellous sites such as proximal femur (Singh et al. 1970) and distal radius in the human skeleton. Although BMD is a key determinant of fracture risk, the biology of bone loss is not understood completely and traditional measures do not reveal how the changes in architecture relate to mechanical load. Before thorough analysis of more mechanically complex sites such as the human proximal femur can be done, the percolation algorithms must be further developed for three-dimensional application (Chapter 3). A network analysis will allow for quantitative examination of trabecular bone patterns in relation to the transmission of stresses, and thus may provide a powerful tool for studying age-related bone loss patterns in the human skeleton.

Network science further eliminates some of the shortcomings of traditional measures by revealing a way to quantify how bone cells establish and maintain a mechanically functional, connected structure throughout life. Fitness, or the probability

of a structure to survive, provides a way to test the hypothesis that skeletal architecture changes to meet mechanical demands (Ruimerman et al. 2005; Glatt et al. 2007). In bone, the idea of fitness could describe the architectural changes in cancellous bone observed during growth and with aging. This could help explain the biological basis behind the functional adaptation described by Wolff's Law. Specific load transfer pathways can have different fitness levels based on the size (length and diameter), shape (plate vs. rod), composition, and geometric location and orientation (relative to loading) of the trabecular struts that make up the pathway. To satisfy mechanical demands during growth, osteoblasts and osteoclasts are expected to arrange and maintain trabecular struts with the highest fitness relative to load transfer through the whole bone and remove struts that have low fitness or are unloaded. Paths with the highest fitness (i.e., critical to load transfer) would be hypothesized to be the pathways that are retained throughout growth. Thus, this analysis is in line with the idea that mechanical stresses (i.e., fluid flow) on osteocytes are critical for cells to remain viable and for individual bone components to adapt as part of the global structure (Wang et al. 2005). The combinations of high-fitness pathways involved in load transfer are expected to be genotype-specific. Therefore, by combining histological studies examining the amount and location of osteoblastic and osteoclastic activity with knowledge of morphology and composition of the most used load transfer paths will advance our understanding of the biological basis of fracture.

Future studies can also test whether the observed relationships hold for other perturbations to the complex bone system. For example, hormonal (Turner et al. 1992; Kim et al. 2003) and mechanical (van der Meulen et al. 1995; Moro et al. 1996; Gilsanz et al. 1997; Bradney et al. 1998; Bradney et al. 2000; Hogler et al. 2003) factors are

known to influence bone remodeling during growth (Sumner et al. 1996; van der Meulen et al. 1996; van der Meulen 1997; van der Meulen et al. 2000; Lee et al. 2003; Jessop et al. 2004; Bord et al. 2005). Functionally related traits are thought to result from a common biological control affecting growth (Wright 1918). Insulin-like growth factor-I (IGF-I) has been hypothesized to be involved in the functional adaptation of bone, but the mechanism by which this occurs is unclear (Turner 1992). IGF-I is produced primarily by the liver under growth hormone control and acts as a systemic hormone as well as an autocrine/paracrine growth factor that may mediate the response of bone to mechanical loading (Gross et al. 2002). IGF-I increases both osteoblast (Slootweg et al. 1990) and osteoclast (Mochizuki et al. 1992) differentiation, and appears to be a coupling agent for bone formation and resorption (Rubin et al. 2002; Clemens et al. 2003). Significant correlations between IGF-I levels and BMD (Langlois et al. 1998F) and fracture risk (Gamero et al. 2000) suggest that IGF-I plays an important role in bone strength as circulating IGF-I levels regulate the amount of bone relative to body weight (Rosen et al. 2000) (Mora et al. 1999). Because phenotypic integration depends on the precise coordination of osteoblasts and osteoclasts, individuals with altered phenotypic integration also would be expected to show altered levels of serum IGF-I and other growth factors. Therefore, to better understand how hormonal factors relate to corticocancellous growth patterns, the tools presented in this dissertation (i.e., mouse models and Path analysis) can be used to identify the traits and trait interactions that are regulated by serum IGF-I and other growth factors.

Mechanical forces are also critical stimuli for the development of bone size and shape. Bone is mechanically responsive during growth and QTLs having direct effects on

bone may represent genes that alter the responsiveness of bone to its external loading demands. Skeletal variation also may arise indirectly through genetic variants affecting muscle mass and activity levels, which are key determinants of the loads applied to bone (Sharkey et al. 2007). Thus, QTLs that affect bone indirectly may represent genes that do not alter the responsiveness of bone, but alter the stimulus imposed on the system during ontogeny. Therefore, variation in bone size can arise from multiple genetic pathways. A natural environment perturbation study can determine whether genetic factors that regulate phenotypic integration to meet loading demands during growth also alter the response to changes in loading environment. Mouse models exposed to increased levels of voluntary activity can be used to account for endocrine (Moraska et al. 2000; Girard et al. 2002; Ogawa et al. 2003), muscle (Allen et al. 2001), genetic (Lerman et al. 2002), age (Sahlman et al. 2001), and physiological (Davidson et al. 2006) effects on skeletal adaptation. This will move us closer to understanding the mechanisms in which physiological loads influence corticocancellous development leading to mechanically functional structures.

The results of this dissertation suggested that the biological mechanism that matches structure with function must be capable of precisely coordinating changes in architecture in order to match structure with normal physiological loads. Osteoblastic and osteoclastic activities vary with genetic background (Sheng et al. 1999; Richman et al. 2001), but there has been no study showing how genetic variation in the coordination of the relative activities of these cell populations affects function. In addition to hormone and mechanical perturbation studies, genetic perturbation studies can be used to map QTLs regulating bone traits and the phenotypic integration among bone traits. Mouse

models including RI and Chromosome Substitution Strains (CSS) can be used to identify genetic controls. Path models can be used to identify how relationship QTLs affect the variation in cortical and trabecular traits. Further, these proposed future analyses all can be extended to other clinically relevant sites including the metaphysis of long bones (e.g., distal radius), the epiphysis of long bones (e.g., knee joint), and other vertebrae (e.g., cervical, thoracic, and sacral vertebrae). Through the potential use of these resources we hope to advance our understanding of how skeletal fragility arises clinically, and to promote the development of diagnosis, prevention, and treatment methodologies aimed at controlling fragility and fracture risk.

BIBLIOGRAPHY

Aarden, E. M., Burger, E. H. and Nijweide, P. J. (1994). "Function of osteocytes in bone." J Cell Biochem **55**(3): 287-99.

Aaron, J. E., Makins, N. B. and Sagreiya, K. (1987). "The microanatomy of trabecular bone loss in normal aging men and women." Clin Orthop Relat Res(215): 260-71.

Ahlborg, H. G., Johnell, O., Turner, C. H., Rannevik, G. and Karlsson, M. K. (2003). "Bone loss and bone size after menopause." N Engl J Med **349**(4): 327-334.

Akaike, H. (1973). Information theory as an extension of the maximum likelihood principle. Budapest, Akademiai Kiado.

Akhter, M. P., Iwaniec, U. T., Covey, M. A., Cullen, D. M., Kimmel, D. B. and Recker, R. R. (2000). "Genetic variations in bone density, histomorphometry, and strength in mice." Calcif Tissue Int **67**(4): 337-44.

Albright, F., Smith, P. H. and Richardson, A. M. (1941). "Post-menopausal osteoporosis. Its clinical features." JAMA **116**: 2465-2474.

Allen, D. L., Harrison, B. C., Maass, A., Bell, M. L., Byrnes, W. C. and Leinwand, L. A. (2001). "Cardiac and skeletal muscle adaptations to voluntary wheel running in the mouse." J Appl Physiol **90**(5): 1900-8.

Ashizawa, N., Nonaka, K., Michikami, S., Mizuki, T., Amagai, H., Tokuyama, K. and Suzuki, M. (1999). "Tomographical description of tennis-loaded radius: reciprocal relation between bone size and volumetric BMD." J Appl Physiol **86**(4): 1347-51.

Aubin, J. E. (1998). "Advances in the osteoblast lineage." Biochem Cell Biol **76**(6): 899-910.

Bailey, D. W. (1986). "Genes that affect morphogenesis of the murine mandible. Recombinant-inbred strain analysis." J Hered **77**(1): 17-25.

Baldock, P. A. and Eisman, J. A. (2004). "Genetic determinants of bone mass." Curr Opin Rheumatol **16**(4): 450-6.

Balena, R., Shih, M. S. and Parfitt, A. M. (1992). "Bone resorption and formation on the periosteal envelope of the ilium: a histomorphometric study in healthy women." J Bone Miner Res **7**(12): 1475-82.

Barbasi, A.-L. (2002). Linked: The New Science of Networks. Cambridge, Perseus Publishing.

Bass, S. L., Saxon, L., Daly, R. M., Turner, C. H., Robling, A. G., Seeman, E. and Stuckey, S. (2002). "The effect of mechanical loading on the size and shape of bone in pre-, peri-, and postpubertal girls: a study in tennis players." J Bone Miner Res **17**(12): 2274-80.

Beamer, W. G., Donahue, L. R., Rosen, C. J. and Baylink, D. J. (1996). "Genetic variability in adult bone density among inbred strains of mice." Bone **18**(5): 397-403.

Beamer, W. G., Shultz, K. L., Churchill, G. A., Frankel, W. N., Baylink, D. J., Rosen, C. J. and Donahue, L. R. (1999). "Quantitative trait loci for bone density in C57BL/6J and CAST/EiJ inbred mice." Mamm Genome **10**(11): 1043-9.

Beck, J. A., Lloyd, S., Hafezparast, M., Lennon-Pierce, M., Eppig, J. T., Festing, M. F. and Fisher, E. M. (2000). "Genealogies of mouse inbred strains." Nat Genet **24**(1): 23-5.

Beck, T. J., Ruff, C. B., Mourtada, F. A., Shaffer, R. A., Maxwell-Williams, K., Kao, G. L., Sartoris, D. J. and Brodine, S. (1996). "Dual-energy X-ray absorptiometry derived structural geometry for stress fracture prediction in male U.S. Marine Corps recruits." J Bone Miner Res **11**(5): 645-53.

Beck, T. J., Ruff, C. B., Shaffer, R. A., Betsinger, K., Trone, D. W. and Brodine, S. K. (2000). "Stress fracture in military recruits: gender differences in muscle and bone susceptibility factors." Bone **27**(3): 437-44.

Belknap, J. K. (1998). "Effect of within-strain sample size on QTL detection and mapping using recombinant inbred mouse strains." Behav Genet **28**(1): 29-38.

Bennell, K., Matheson, G., Meeuwisse, W. and Brukner, P. (1999). "Risk factors for stress fractures." Sports Med **28**(2): 91-122.

Biewener, A. A., Fazzalari, N. L., Konieczynski, D. D. and Baudinette, R. V. (1996). "Adaptive changes in trabecular architecture in relation to functional strain patterns and disuse." Bone **19**(1): 1-8.

Bonadio, J., Jepsen, K. J., Mansoura, M. K., Jaenisch, R., Kuhn, J. L. and Goldstein, S. A. (1993). "A murine skeletal adaptation that significantly increases cortical bone mechanical properties. Implications for human skeletal fragility." J Clin Invest **92**(4): 1697-705.

Bord, S., Ireland, D. C., Moffatt, P., Thomas, G. P. and Compston, J. E. (2005). "Characterization of Osteocrin Expression in Human Bone." J Histochem Cytochem.

Boskey, A. L. and Posner, A. S. (1984). "Bone structure, composition, and mineralization." Orthop Clin North Am **15**(4): 597-612.

Bouxsein, M. L., Rosen, C. J., Turner, C. H., Ackert, C. L., Shultz, K. L., Donahue, L. R., Churchill, G., Adamo, M. L., Powell, D. R., Turner, R. T., Muller, R. and Beamer, W. G. (2002). "Generation of a new congenic mouse strain to test the relationships among serum insulin-like growth factor I, bone mineral density, and skeletal morphology in vivo." J Bone Miner Res **17**(4): 570-9.

Bower, A. L., Lang, D. H., Vogler, G. P., Vandenbergh, D. J., Blizard, D. A., Stout, J. T., McClearn, G. E. and Sharkey, N. A. (2006). "QTL analysis of trabecular bone in BXD F2 and RI mice." J Bone Miner Res **21**(8): 1267-75.

Boyce, T. M., Fyhrie, D. P., Glotkowski, M. C., Radin, E. L. and Schaffler, M. B. (1998). "Damage type and strain mode associations in human compact bone bending fatigue." J Orthop Res **16**(3): 322-9.

Bradney, M., Karlsson, M. K., Duan, Y., Stuckey, S., Bass, S. and Seeman, E. (2000). "Heterogeneity in the growth of the axial and appendicular skeleton in boys: implications for the pathogenesis of bone fragility in men." J Bone Miner Res **15**(10): 1871-8.

Bradney, M., Pearce, G., Naughton, G., Sullivan, C., Bass, S., Beck, T., Carlson, J. and Seeman, E. (1998). "Moderate exercise during growth in prepubertal boys: changes in bone mass, size, volumetric density, and bone strength: a controlled prospective study." J Bone Miner Res **13**(12): 1814-21.

Brear, K., Currey, J. D. and Pond, C. M. (1990). "Ontogenetic changes in the mechanical properties of the femur of the polar bear Ursus maritimus." J Zool, London **222**: 49-58.

Browne, M. and Cudeck, R. (1993). Alternative ways of assessing model fit. Thousand Oaks, CA, Sage Press.

Brudvig, T. J., Gudger, T. D. and Obermeyer, L. (1983). "Stress fractures in 295 trainees: a one-year study of incidence as related to age, sex, and race." Mil Med **148**(8): 666-7.

Burnham, K. and Anderson, D. (1998). Model selection and multimodel inference: A Practical information-theoretic approach. New York, Springer.

Burr, D. B., Forwood, M. R., Fyhrie, D. P., Martin, R. B., Schaffler, M. B. and Turner, C. H. (1997). "Bone microdamage and skeletal fragility in osteoporotic and stress fractures." J Bone Miner Res **12**(1): 6-15.

Burr, D. B., Martin, R. B., Schaffler, M. B. and Radin, E. L. (1985). "Bone remodeling in response to in vivo fatigue microdamage." J Biomech **18**(3): 189-200.

Burr, D. B., Milgrom, C., Fyhrie, D., Forwood, M., Nyska, M., Finestone, A., Hoshaw, S., Saiag, E. and Simkin, A. (1996). "In vivo measurement of human tibial strains during vigorous activity." Bone **18**(5): 405-10.

Burstein, A. H., Currey, J. D., Frankel, V. H. and Reilly, D. T. (1972). "The ultimate properties of bone tissue: the effects of yielding." J Biomech **5**(1): 35-44.

Burstein, A. H., Reilly, D. T. and Martens, M. (1976). "Aging of bone tissue: mechanical properties." J Bone Joint Surg Am **58**(1): 82-6.

Carrier, D. and Leon, L. R. (1990). "Skeletal growth and function in the California gull (Larus californicus)." J Zool, London **222**: 375-389.

Carrier, D. R. (1983). "Postnatal ontogeny of the musculo-skeletal system in the Black-tailed jack rabbit." J. Zool., Lond. **201**: 27-55.

Carter, D. R. and Beaupre, G. S. (2001). Skeletal Function and Form: Mechanobiology of Skeletal Development, Aging, and Regeneration. Cambridge, Cambridge University Press.

Chan, G. M., Hess, M., Hollis, J. and Book, L. S. (1984). "Bone mineral status in childhood accidental fractures." Am J Dis Child **138**(6): 569-70.

Chatterjee, S., Das, N. and Chatterjee, P. (1999). "The estimation of the heritability of anthropometric measurements." Appl Human Sci **18**(1): 1-7.

Cheverud, J. M. (1996). "Developmental integration and the evolution of pleiotropy." American Zoologist **36**: 44-50.

Cheverud, J. M., Ehrich, T. H., Vaughn, T. T., Koreishi, S. F., Linsey, R. B. and Pletscher, L. S. (2004). "Pleiotropic effects on mandibular morphology II: differential epistasis and genetic variation in morphological integration." J Exp Zoolog B Mol Dev Evol **302**(5): 424-35.

Christian, J. C., Yu, P. L., Slemenda, C. W. and Johnston, C. C., Jr. (1989). "Heritability of bone mass: a longitudinal study in aging male twins." Am J Hum Genet **44**(3): 429-33.

Churchill, G. A. and Doerge, R. W. (1994). "Empirical threshold values for quantitative trait mapping." Genetics **138**(3): 963-71.

Ciarelli, T. E., Fyhrie, D. P., Schaffler, M. B. and Goldstein, S. A. (2000). "Variations in three-dimensional cancellous bone architecture of the proximal femur in female hip fractures and in controls." J Bone Miner Res **15**(1): 32-40.

Clemens, T. L. and Rosen, C. J. (2003). The Insulin-Like Growth Factor System and Bone. New York, NY, Kluwer Academic / Plenum Publishers.

Cooper, C., Campion, G. and Melton, L. J., 3rd (1992). "Hip fractures in the elderly: a world-wide projection." Osteoporos Int **2**(6): 285-9.

Cowin, S. C. (1997). "Remarks on the paper entitled 'Fabric and elastic principal directions of cancellous bone are closely related'." J Biomech **30**(11-12): 1191-3.

Cowin, S. C. (2001). The false premise in Wolff's Law. Bone Mechanics Handbook. S. C. Cowin. Boca Raton, CRC Press**:** 30.1-15.

Cowin, S. C., Weinbaum, S. and Zeng, Y. (1995). "A case for bone canaliculi as the anatomical site of strain generated potentials." J Biomech **28**(11): 1281-97.

Crossley, K., Bennell, K. L., Wrigley, T. and Oakes, B. W. (1999). "Ground reaction forces, bone characteristics, and tibial stress fracture in male runners." Med Sci Sports Exerc **31**(8): 1088-93.

Cummings, S. R. and Melton, L. J. (2002). "Epidemiology and outcomes of osteoporotic fractures." Lancet **359**(9319): 1761-1767.

Currey, J. D. (1979). "Changes in the impact energy absorption of bone with age." J Biomech **12**(6): 459-69.

Currey, J. D. (1979). "Mechanical properties of bone tissues with greatly differing functions." J Biomech **12**(4): 313-9.

Currey, J. D. (1984). "Effects of differences in mineralization on the mechanical properties of bone." Philos Trans R Soc Lond B Biol Sci **304**(1121): 509-18.

Currey, J. D. (1988). "The effect of porosity and mineral content on the Young's modulus of elasticity of compact bone." J Biomech **21**(2): 131-9.

Currey, J. D. (2002). Bones: Structure and Mechanics. Princeton, Princeton University Press.

Currey, J. D. (2005). "Bone architecture and fracture." Curr Osteoporos Rep **3**(2): 52-6.

Currey, J. D. and Alexander, R. M. c. N. (1985). "The thickness of the walls of tubular bones." J Zool, London **206**: 453-68.

Currey, J. D. and Brear, K. (1992). "Fractal analysis of compact bone and antler fracture surfaces." Biomimetics **1**(2): 103-118.

Currey, J. D. and Butler, G. (1975). "The mechanical properties of bone tissue in children." J Bone Joint Surg Am **57**(6): 810-4.

Davidson, S. R., Burnett, M. and Hoffman-Goetz, L. (2006). "Training effects in mice after long-term voluntary exercise." Med Sci Sports Exerc **38**(2): 250-5.

Davy, D. T., Kotzar, G. M., Brown, R. H., Heiple, K. G., Goldberg, V. M., Heiple, K. G., Jr., Berilla, J. and Burstein, A. H. (1988). "Telemetric force measurements across the hip after total arthroplasty." J Bone Joint Surg Am **70**(1): 45-50.

Denis, D. and Legerski, J. (2006) "Causal modeling and the origins of Path Analysis." Theory and Science **Volume**, DOI:

Di Masso, R. J., Font, M. T., Capozza, R. F., Detarsio, G., Sosa, F. and Ferretti, J. L. (1997). "Long-bone biomechanics in mice selected for body conformation." Bone **20**(6): 539-45.

Doty, S. B. (2004). "Space flight and bone formation." Materwiss Werksttech **35**(12): 951-61.

Drake, T. A., Hannani, K., Kabo, J. M., Villa, V., Krass, K. and Lusis, A. J. (2001). "Genetic loci influencing natural variations in femoral bone morphometry in mice." J Orthop Res **19**(4): 511-7.

Drake, T. A., Schadt, E., Hannani, K., Kabo, J. M., Krass, K., Colinayo, V., Greaser, L. E., 3rd, Goldin, J. and Lusis, A. J. (2001). "Genetic loci determining bone density in mice with diet-induced atherosclerosis." Physiol Genomics **5**(4): 205-15.

Duan, Y., Beck, T. J., Wang, X. F. and Seeman, E. (2003). "Structural and biomechanical basis of sexual dimorphism in femoral neck fragility has its origins in growth and aging." J Bone Miner Res **18**(10): 1766-74.

Duan, Y., Parfitt, A. and Seeman, E. (1999). "Vertebral bone mass, size, and volumetric density in women with spinal fractures." J Bone Miner Res **14**(10): 1796-802.

Duan, Y., Seeman, E. and Turner, C. H. (2001). "The biomechanical basis of vertebral body fragility in men and women." J Bone Miner Res **16**(12): 2276-83.

Duan, Y., Turner, C. H., Kim, B. T. and Seeman, E. (2001). "Sexual dimorphism in vertebral fragility is more the result of gender differences in age-related bone gain than bone loss." J Bone Miner Res **16**(12): 2267-75.

Duan, Y., Wang, X. F., Evans, A. and Seeman, E. (2005). "Structural and biomechanical basis of racial and sex differences in vertebral fragility in Chinese and Caucasians." Bone **36**(6): 987-98.

Ducy, P. and Karsenty, G. (1998). "Genetic control of cell differentiation in the skeleton." Curr Opin Cell Biol **10**(5): 614-9.

Duncan, R. L. and Turner, C. H. (1995). "Mechanotransduction and the functional response of bone to mechanical strain." Calcif Tissue Int **57**(5): 344-58.

Edderkaoui, B., Baylink, D. J., Beamer, W. G., Shultz, K. L., Wergedal, J. E. and Mohan, S. (2007). "Genetic regulation of femoral bone mineral density: complexity of sex effect in chromosome 1 revealed by congenic sublines of mice." Bone **41**(3): 340-5.

Eisman, J. A. (1999). "Genetics of osteoporosis." Endocr Rev **20**(6): 788-804.

Enlow, D. H. (1963). Principles of bone remodeling; an account of post-natal growth and remodeling processes in long bones and the mandible, Thomas.

Eswaran, S. K., Gupta, A., Adams, M. F. and Keaveny, T. M. (2006). "Cortical and trabecular load sharing in the human vertebral body." J Bone Miner Res **21**(2): 307-14.

Evans, F. G. and Riolo, M. L. (1970). "Relations between the fatigue life and histology of adult human cortical bone." J Bone Joint Surg Am **52**(8): 1579-86.

Faulkner, R. A. and Bailey, D. A. (2007). "Osteoporosis: a pediatric concern?" Med Sport Sci **51**: 1-12.

Fazzalari, N. L., Moore, A. J., Byers, S. and Byard, R. W. (1997). "Quantitative analysis of trabecular morphogenesis in the human costochondral junction during the postnatal period in normal subjects." Anat Rec **248**(1): 1-12.

Ferretti, J. L., Capozza, R. F., Mondelo, N. and Zanchetta, J. R. (1993). "Interrelationships between densitometric, geometric, and mechanical properties of rat femora: inferences concerning mechanical regulation of bone modeling." J Bone Miner Res **8**(11): 1389-96.

Ferretti, J. L., Cointry, G. R., Capozza, R. F. and Frost, H. M. (2003). "Bone mass, bone strength, muscle-bone interactions, osteopenias and osteoporoses." Mech Ageing Dev **124**(3): 269-79.

Forwood, M. R., Bailey, D. A., Beck, T. J., Mirwald, R. L., Baxter-Jones, A. D. and Uusi-Rasi, K. (2004). "Sexual dimorphism of the femoral neck during the adolescent growth spurt: a structural analysis." Bone **35**(4): 973-81.

Friedl, K. E., Nuovo, J. A., Patience, T. H. and Dettori, J. R. (1992). "Factors associated with stress fracture in young army women: indications for further research." Mil Med **157**(7): 334-8.

Frost, H. M. (1983). "A determinant of bone architecture. The minimum effective strain." Clin Orthop(175): 286-92.

Frost, H. M. (1987). "Bone "mass" and the "mechanostat": a proposal." Anat Rec **219**(1): 1-9.

Frost, H. M. (1990). "Skeletal structural adaptations to mechanical usage (SATMU): 1. Redefining Wolff's law: the bone modeling problem." Anat Rec **226**(4): 403-13.

Frost, H. M. (1990). "Skeletal structural adaptations to mechanical usage (SATMU): 2. Redefining Wolff's law: the remodeling problem." Anat Rec **226**(4): 414-22.

Fyhrie, D. P. and Schaffler, M. B. (1994). "Failure mechanisms in human vertebral cancellous bone." Bone **15**(1): 105-9.

Gallagher, J. C., Melton, L. J., Riggs, B. L. and Bergstrath, E. (1980). "Epidemiology of fractures of the proximal femur in Rochester, Minnesota." Clin Orthop Relat Res(150): 163-71.

Gamero, P., Sornay-Rendu, E. and Delmas, P. D. (2000). "Low serum IGF-1 and occurrence of osteoporotic fractures in postmenopausal women." Lancet **355**(9207): 898-9.

Garn, S. (1970). The earlier gain and the later loss of cortical bone. Springfield, IL, Charles C Thomas.

Genant, H. K., Cooper, C., Poor, G., Reid, I., Ehrlich, G., Kanis, J., Nordin, B. E., Barrett-Connor, E., Black, D., Bonjour, J. P., Dawson-Hughes, B., Delmas, P. D., Dequeker, J., Ragi Eis, S., Gennari, C., Johnell, O., Johnston, C. C., Jr., Lau, E. M., Liberman, U. A., Lindsay, R., Martin, T. J., Masri, B., Mautalen, C. A., Meunier, P. J. and Khaltaev, N. (1999). "Interim report and recommendations of the World Health Organization Task-Force for Osteoporosis." Osteoporos Int **10**(4): 259-64.

Geusens, P., Cantatore, F., Nijs, J., Proesmans, W., Emma, F. and Dequeker, J. (1991). "Heterogeneity of growth of bone in children at the spine, radius and total skeleton." Growth Dev Aging **55**(4): 249-56.

Giguere, Y. and Rousseau, F. (2000). "The genetics of osteoporosis: 'complexities and difficulties'." Clin Genet **57**(3): 161-9.

Giladi, M., Milgrom, C., Simkin, A. and Danon, Y. (1991). "Stress fractures. Identifiable risk factors." Am J Sports Med **19**(6): 647-52.

Giladi, M., Milgrom, C., Simkin, A., Stein, M., Kashtan, H., Margulies, J., Rand, N., Chisin, R., Steinberg, R., Aharonson, Z., Kadem, R. and Frankel, V. H. (1987). "Stress fractures and tibial bone width. A risk factor." J Bone Joint Surg Br **69**(2): 326-9.

Gilsanz, V., Kovanlikaya, A., Costin, G., Roe, T. F., Sayre, J. and Kaufman, F. (1997). "Differential effect of gender on the sizes of the bones in the axial and appendicular skeletons." J Clin Endocrinol Metab **82**(5): 1603-7.

Gilsanz, V., Loro, M. L., Roe, T. F., Sayre, J., Gilsanz, R. and Schulz, E. E. (1995). "Vertebral size in elderly women with osteoporosis. Mechanical implications and relationship to fractures." J Clin Invest **95**(5): 2332-7.

Girard, I. and Garland, T., Jr. (2002). "Plasma corticosterone response to acute and chronic voluntary exercise in female house mice." J Appl Physiol **92**(4): 1553-61.

Glatt, V., Canalis, E., Stadmeyer, L. and Bouxsein, M. L. (2007). "Age-related changes in trabecular architecture differ in female and male C57BL/6J mice." J Bone Miner Res **22**(8): 1197-207.

Gordon, K. R., Levy, C., Perl, M. and Weeks, O. I. (1994). "Experimental perturbation of the development of sexual size dimorphism in the mouse skeleton." Growth Dev Aging **58**(2): 95-104.

Gorski, J. P. (1998). "Is all bone the same? Distinctive distributions and properties of non-collagenous matrix proteins in lamellar vs. woven bone imply the existence of different underlying osteogenic mechanisms." Crit Rev Oral Biol Med **9**(2): 201-23.

Grace, J. B. (2006). Structural Equation Modeling and Natural Systems. Cambridge, Cambridge University Press.

Gross, T. S., Srinivasan, S., Liu, C. C., Clemens, T. L. and Bain, S. D. (2002). "Noninvasive loading of the murine tibia: an in vivo model for the study of mechanotransduction." J Bone Miner Res **17**(3): 493-501.

Guldberg, R. E., Caldwell, N. J., Guo, X. E., Goulet, R. W., Hollister, S. J. and Goldstein, S. A. (1997). "Mechanical stimulation of tissue repair in the hydraulic bone chamber." J Bone Miner Res **12**(8): 1295-302.

Guo, X. E. and Kim, C. H. (2002). "Mechanical consequence of trabecular bone loss and its treatment: a three-dimensional model simulation." Bone **30**(2): 404-11.

Gustafson, M. B., Martin, R. B., Gibson, V., Storms, D. H., Stover, S. M., Gibeling, J. and Griffin, L. (1996). "Calcium buffering is required to maintain bone stiffness in saline solution." J Biomech **29**(9): 1191-4.

Halloran, B. P., Ferguson, V. L., Simske, S. J., Burghardt, A., Venton, L. L. and Majumdar, S. (2002). "Changes in bone structure and mass with advancing age in the male C57BL/6J mouse." J Bone Miner Res **17**(6): 1044-50.

Heinrich, R. E. (1999). "Ontogenetic changes in mineralization and bone geometry in the femur of muskoxen (Ovibos moschatus)." J Zool, London **247**: 215-223.

Hogler, W., Blimkie, C. J., Cowell, C. T., Kemp, A. F., Briody, J., Wiebe, P., Farpour-Lambert, N., Duncan, C. S. and Woodhead, H. J. (2003). "A comparison of bone geometry and cortical density at the mid-femur between prepuberty and young adulthood using magnetic resonance imaging." Bone **33**(5): 771-8.

Horber, F. F., Gruber, B., Thomi, F., Jensen, E. X. and Jaeger, P. (1997). "Effect of sex and age on bone mass, body composition, and fuel metabolism in humans." Nutrition **13**(6): 524-34.

Huiskes, R. (2000). "If bone is the answer, then what is the question?" J Anat **197 (Pt 2)**: 145-56.

Iscan, M. Y. and Miller-Shaivitz, P. (1984). "Discriminant function sexing of the tibia." J Forensic Sci **29**(4): 1087-93.

Jee, W. S. (2001). Integrated bone tissue physiology: Anatomy and physiology. Bone Mechanics Handbook. S. C. Cowin. Boca Raton, CRC Press**:** 1-68.

Jepsen, K. J., Akkus, O. J., Majeska, R. J. and Nadeau, J. H. (2003). "Hierarchical relationship between bone traits and mechanical properties in inbred mice." Mamm Genome **14**(2): 97-104.

Jepsen, K. J. and Davy, D. T. (1997). "Comparison of damage accumulation measures in human cortical bone." J Biomech **30**(9): 891-4.

Jepsen, K. J., Davy, D. T. and Krzypow, D. J. (1999). "The role of the lamellar interface during torsional yielding of human cortical bone." J Biomech **32**(3): 303-10.

Jepsen, K. J., Hu, B., Tommasini, S. M., Courtland, H. W., Price, C., Terranova, C. J. and Nadeau, J. H. (2007). "Genetic randomization reveals functional relationships among morphologic and tissue-quality traits that contribute to bone strength and fragility." Mamm Genome **18**(6-7): 492-507.

Jepsen, K. J., Pennington, D. E., Lee, Y. L., Warman, M. and Nadeau, J. (2001). "Bone brittleness varies with genetic background in A/J and C57BL/6J inbred mice." J Bone Miner Res **16**(10): 1854-62.

Jessop, H. L., Suswillo, R. F., Rawlinson, S. C., Zaman, G., Lee, K., Das-Gupta, V., Pitsillides, A. A. and Lanyon, L. E. (2004). "Osteoblast-like cells from estrogen receptor alpha knockout mice have deficient responses to mechanical strain." J Bone Miner Res **19**(6): 938-46.

Jones, B. H., Bovee, M. W., Harris, J. M., 3rd and Cowan, D. N. (1993). "Intrinsic risk factors for exercise-related injuries among male and female army trainees." Am J Sports Med **21**(5): 705-10.

Jones, B. H., Thacker, S. B., Gilchrist, J., Kimsey, C. D., Jr. and Sosin, D. M. (2002). "Prevention of lower extremity stress fractures in athletes and soldiers: a systematic review." Epidemiol Rev **24**(2): 228-47.

Jones, H. H., Priest, J. D., Hayes, W. C., Tichenor, C. C. and Nagel, D. A. (1977). "Humeral hypertrophy in response to exercise." J Bone Joint Surg Am **59**(2): 204-8.

Kannus, P., Haapasalo, H., Sankelo, M., Sievanen, H., Pasanen, M., Heinonen, A., Oja, P. and Vuori, I. (1995). "Effect of starting age of physical activity on bone mass in the dominant arm of tennis and squash players." Ann Intern Med **123**(1): 27-31.

Karsenty, G. (1998). "Genetics of skeletogenesis." Dev Genet **22**(4): 301-13.

Keaveny, T. M. and Yeh, O. C. (2002). "Architecture and trabecular bone - toward an improved understanding of the biomechanical effects of age, sex and osteoporosis." J Musculoskelet Neuronal Interact **2**(3): 205-8.

Kelly, P. J., Nguyen, T., Hopper, J., Pocock, N., Sambrook, P. and Eisman, J. (1993). "Changes in axial bone density with age: a twin study." J Bone Miner Res **8**(1): 11-7.

Kenney-Hunt, J. P., Vaughn, T. T., Pletscher, L. S., Peripato, A., Routman, E., Cothran, K., Durand, D., Norgard, E., Perel, C. and Cheverud, J. M. (2006). "Quantitative trait loci for body size components in mice." Mamm Genome **17**(6): 526-37.

Khosla, S., Riggs, B. L., Atkinson, E. J., Oberg, A. L., McDaniel, L. J., Holets, M., Peterson, J. M. and Melton, L. J., 3rd (2006). "Effects of sex and age on bone microstructure at the ultradistal radius: a population-based noninvasive in vivo assessment." J Bone Miner Res **21**(1): 124-31.

Kiel, D. P., Hannan, M. T., Broe, K. E., Felson, D. T. and Cupples, L. A. (2001). "Can metacarpal cortical area predict the occurrence of hip fracture in women and men

over 3 decades of follow-up? Results from the Framingham Osteoporosis Study." J Bone Miner Res **16**(12): 2260-6.

Kim, B. T., Mosekilde, L., Duan, Y., Zhang, X. Z., Tornvig, L., Thomsen, J. S. and Seeman, E. (2003). "The structural and hormonal basis of sex differences in peak appendicular bone strength in rats." J Bone Miner Res **18**(1): 150-5.

Klein, R. F., Allard, J., Avnur, Z., Nikolcheva, T., Rotstein, D., Carlos, A. S., Shea, M., Waters, R. V., Belknap, J. K., Peltz, G. and Orwoll, E. S. (2004). "Regulation of bone mass in mice by the lipoxygenase gene Alox15." Science **303**(5655): 229-32.

Klein, R. F., Mitchell, S. R., Phillips, T. J., Belknap, J. K. and Orwoll, E. S. (1998). "Quantitative trait loci affecting peak bone mineral density in mice." J Bone Miner Res **13**(11): 1648-56.

Klein, R. F., Shea, M., Gunness, M. E., Pelz, G. B., Belknap, J. K. and Orwoll, E. S. (2001). "Phenotypic characterization of mice bred for high and low peak bone mass." J Bone Miner Res **16**(1): 63-71.

Klein, R. F., Turner, R. J., Skinner, L. D., Vartanian, K. A., Serang, M., Carlos, A. S., Shea, M., Belknap, J. K. and Orwoll, E. S. (2002). "Mapping quantitative trait loci that influence femoral cross-sectional area in mice." J Bone Miner Res **17**(10): 1752-60.

Knothe Tate, M. L., Adamson, J. R., Tami, A. E. and Bauer, T. W. (2004). "The osteocyte." Int J Biochem Cell Biol **36**(1): 1-8.

Koller, D. L., Schriefer, J., Sun, Q., Shultz, K. L., Donahue, L. R., Rosen, C. J., Foroud, T., Beamer, W. G. and Turner, C. H. (2003). "Genetic effects for femoral biomechanics, structure, and density in C57BL/6J and C3H/HeJ inbred mouse strains." J Bone Miner Res **18**(10): 1758-65.

Landin, L. and Nilsson, B. E. (1983). "Bone mineral content in children with fractures." Clin Orthop Relat Res(178): 292-6.

Lang, D. H., Sharkey, N. A., Mack, H. A., Vogler, G. P., Vandenbergh, D. J., Blizard, D. A., Stout, J. T. and McClearn, G. E. (2005). "Quantitative trait loci analysis of structural and material skeletal phenotypes in C57BL/6J and DBA/2 second-generation and recombinant inbred mice." J Bone Miner Res **20**(1): 88-99.

Langlois, J. A., Rosen, C. J., Visser, M., Hannan, M. T., Harris, T., Wilson, P. W. and Kiel, D. P. (1998). "Association between insulin-like growth factor I and bone mineral density in older women and men: the Framingham Heart Study." J Clin Endocrinol Metab **83**(12): 4257-62.

Lanyon, L. E., Hampson, W. G., Goodship, A. E. and Shah, J. S. (1975). "Bone deformation recorded in vivo from strain gauges attached to the human tibial shaft." Acta Orthop Scand **46**(2): 256-68.

Lappe, J. M., Stegman, M. R. and Recker, R. R. (2001). "The impact of lifestyle factors on stress fractures in female Army recruits." Osteoporos Int **12**(1): 35-42.

Leamy, L. J., Pomp, D., Eisen, E. J. and Cheverud, J. M. (2002). "Pleiotropy of quantitative trait loci for organ weights and limb bone lengths in mice." Physiol Genomics **10**(1): 21-9.

Lee, K., Jessop, H., Suswillo, R., Zaman, G. and Lanyon, L. (2003). "Endocrinology: bone adaptation requires oestrogen receptor-alpha." Nature **424**(6947): 389.

Lemaãitre, J. (1992). A course on damage mechanics. Berlin; New York, Springer-Verlag.

Lerman, I., Harrison, B. C., Freeman, K., Hewett, T. E., Allen, D. L., Robbins, J. and Leinwand, L. A. (2002). "Genetic variability in forced and voluntary endurance exercise performance in seven inbred mouse strains." J Appl Physiol **92**(6): 2245-55.

Li, R., Tsaih, S. W., Shockley, K., Stylianou, I. M., Wergedal, J., Paigen, B. and Churchill, G. A. (2006). "Structural model analysis of multiple quantitative traits." PLoS Genet **2**(7): e114.

Li, X., Masinde, G., Gu, W., Wergedal, J., Hamilton-Ulland, M., Xu, S., Mohan, S. and Baylink, D. J. (2002). "Chromosomal regions harboring genes for the work to femur failure in mice." Funct Integr Genomics **1**(6): 367-74.

Li, X., Wang, H., Touma, E., Rousseau, E., Quigg, R. J. and Ryaby, J. T. (2007). "Genetic network and pathway analysis of differentially expressed proteins during critical cellular events in fracture repair." J Cell Biochem **100**(2): 527-43.

Liebschner, M. A., Muller, R., Wimalawansa, S. J., Rajapakse, C. S. and Gunaratne, G. H. (2005). "Testing two predictions for fracture load using computer models of trabecular bone." Biophys J **89**(2): 759-67.

Little, R. D., Carulli, J. P., Del Mastro, R. G., Dupuis, J., Osborne, M., Folz, C., Manning, S. P., Swain, P. M., Zhao, S. C., Eustace, B., Lappe, M. M., Spitzer, L., Zweier, S., Braunschweiger, K., Benchekroun, Y., Hu, X., Adair, R., Chee, L., FitzGerald, M. G., Tulig, C., Caruso, A., Tzellas, N., Bawa, A., Franklin, B., McGuire, S., Nogues, X., Gong, G., Allen, K. M., Anisowicz, A., Morales, A. J., Lomedico, P. T., Recker, S. M., Van Eerdewegh, P., Recker, R. R. and Johnson, M. L. (2002). "A mutation in the LDL receptor-related protein 5 gene results in the autosomal dominant high-bone-mass trait." Am J Hum Genet **70**(1): 11-9.

Looker, A. C., Beck, T. J. and Orwoll, E. S. (2001). "Does body size account for gender differences in femur bone density and geometry?" J Bone Miner Res **16**(7): 1291-9.

MacCallum, R. C. and Hong, S. (1997). "Power analysis in covariance structural modeling using GFI and AGFI." Multivariate Behavioral Research **32**(2): 193-210.

Martin, R. B. and Atkinson, P. J. (1977). "Age and sex-related changes in the structure and strength of the human femoral shaft." J Biomech **10**(4): 223-31.

Martin, R. B. and Boardman, D. L. (1993). "The effects of collagen fiber orientation, porosity, density, and mineralization on bovine cortical bone bending properties." J Biomech **26**(9): 1047-54.

Martin, R. B. and Ishida, J. (1989). "The relative effects of collagen fiber orientation, porosity, density, and mineralization on bone strength." J Biomech **22**(5): 419-26.

McCalden, R. W., McGeough, J. A., Barker, M. B. and Court-Brown, C. M. (1993). "Age-related changes in the tensile properties of cortical bone. The relative importance of changes in porosity, mineralization, and microstructure." J Bone Joint Surg Am **75**(8): 1193-205.

Melick, R. A. and Miller, D. R. (1966). "Variations of tensile strength of human cortical bone with age." Clin Sci **30**(2): 243-8.

Milgrom, C., Finestone, A., Sharkey, N., Hamel, A., Mandes, V., Burr, D., Arndt, A. and Ekenman, I. (2002). "Metatarsal strains are sufficient to cause fatigue fracture during cyclic overloading." Foot Ankle Int **23**(3): 230-5.

Milgrom, C., Giladi, M., Simkin, A., Rand, N., Kedem, R., Kashtan, H., Stein, M. and Gomori, M. (1989). "The area moment of inertia of the tibia: a risk factor for stress fractures." J Biomech **22**(11-12): 1243-8.

Milgrom, C., Giladi, M., Stein, M., Kashtan, H., Margulies, J. Y., Chisin, R., Steinberg, R. and Aharonson, Z. (1985). "Stress fractures in military recruits. A prospective study showing an unusually high incidence." J Bone Joint Surg Br **67**(5): 732-5.

Miller, P. D., Zapalowski, C., Kulak, C. A. and Bilezikian, J. P. (1999). "Bone densitometry: the best way to detect osteoporosis and to monitor therapy." J Clin Endocrinol Metab **84**(6): 1867-71.

Mochizuki, H., Hakeda, Y., Wakatsuki, N., Usui, N., Akashi, S., Sato, T., Tanaka, K. and Kumegawa, M. (1992). "Insulin-like growth factor-I supports formation and activation of osteoclasts." Endocrinology **131**(3): 1075-80.

Mohan, S., Masinde, G., Li, X. and Baylink, D. J. (2003). "Mapping quantitative trait loci that influence serum insulin-like growth factor binding protein-5 levels in F2 mice (MRL/MpJ X SJL/J)." Endocrinology **144**(8): 3491-6.

Mora, S., Pitukcheewanont, P., Nelson, J. C. and Gilsanz, V. (1999). "Serum levels of insulin-like growth factor I and the density, volume, and cross-sectional area of cortical bone in children." J Clin Endocrinol Metab **84**(8): 2780-3.

Moraska, A., Deak, T., Spencer, R. L., Roth, D. and Fleshner, M. (2000). "Treadmill running produces both positive and negative physiological adaptations in Sprague-Dawley rats." Am J Physiol Regul Integr Comp Physiol **279**(4): R1321-9.

Mori, S. and Burr, D. B. (1993). "Increased intracortical remodeling following fatigue damage." Bone **14**(2): 103-9.

Moro, M., van der Meulen, M. C., Kiratli, B. J., Marcus, R., Bachrach, L. K. and Carter, D. R. (1996). "Body mass is the primary determinant of midfemoral bone acquisition during adolescent growth." Bone **19**(5): 519-26.

Mosekilde, L., Ebbesen, E. N., Tornvig, L. and Thomsen, J. S. (2000). "Trabecular bone structure and strength - remodelling and repair." J Musculoskelet Neuronal Interact **1**(1): 25-30.

Nádai, A. (1950). Theory of flow and fracture of solids. New York, McGraw-Hill.

Nadeau, J. H., Arbuckle, L. D. and Skamene, E. (1995). "Genetic dissection of inflammatory responses." J Inflamm **45**(1): 27-48.

Nadeau, J. H., Burrage, L. C., Restivo, J., Pao, Y. H., Churchill, G. and Hoit, B. D. (2003). "Pleiotropy, homeostasis, and functional networks based on assays of cardiovascular traits in genetically randomized populations." Genome Res **13**(9): 2082-91.

Nadeau, J. H. and Dunn, P. J. (1998). "Genomic strategies for defining and dissecting developmental and physiological pathways." Curr Opin Genet Dev **8**(3): 311-5.

Nelson, D. A., Barondess, D. A., Hendrix, S. L. and Beck, T. J. (2000). "Cross-sectional geometry, bone strength, and bone mass in the proximal femur in black and white postmenopausal women." J Bone Miner Res **15**(10): 1992-7.

Ng, A. H., Wang, S. X., Turner, C. H., Beamer, W. G. and Grynpas, M. D. (2007). "Bone quality and bone strength in BXH recombinant inbred mice." Calcif Tissue Int **81**(3): 215-23.

Nieves, J. W., Formica, C., Ruffing, J., Zion, M., Garrett, P., Lindsay, R. and Cosman, F. (2005). "Males have larger skeletal size and bone mass than females, despite comparable body size." J Bone Miner Res **20**(3): 529-35.

NIH (2001). "Osteoporosis prevention, diagnosis, and therapy." Jama **285**(6): 785-95.

Noble, B. (2003). "Bone microdamage and cell apoptosis." Eur Cell Mater **6**: 46-55; discusssion 55.

Noble, B. (2005). "Microdamage and apoptosis." Eur J Morphol **42**(1-2): 91-8.

NOF National Osteoporosis Foundation Fast Facts on Osteoporosis.

Odgaard, A., Kabel, J., van Rietbergen, B., Dalstra, M. and Huiskes, R. (1997). "Fabric and elastic principal directions of cancellous bone are closely related." J Biomech **30**(5): 487-95.

Ogawa, S., Chan, J., Gustafsson, J. A., Korach, K. S. and Pfaff, D. W. (2003). "Estrogen increases locomotor activity in mice through estrogen receptor alpha: specificity for the type of activity." Endocrinology **144**(1): 230-9.

Olson, E. C. and Miller, R. L. (1958). Morphological Integration. Chicago, The University of Chicago Press, Ltd.

Orwoll, E. S., Belknap, J. K. and Klein, R. F. (2001). "Gender specificity in the genetic determinants of peak bone mass." J Bone Miner Res **16**(11): 1962-71.

Papadimitriou, H. M., Swartz, S. M. and Kunz, T. H. (1996). "Ontogenetic and anatomic variation in mineralization of the wing skeleton of the Mexican free-tailed bat, Tadarida brasiliensis." J Zool, London **240**: 411-426.

Parfitt, A. M. (1984). "Age-related structural changes in trabecular and cortical bone: cellular mechanisms and biomechanical consequences." Calcified Tissue International **36**(Suppl 1): S123-8.

Parfitt, A. M., Mathews, C. H., Villanueva, A. R., Kleerekoper, M., Frame, B. and Rao, D. S. (1983). "Relationships between surface, volume, and thickness of iliac trabecular bone in aging and in osteoporosis. Implications for the microanatomic and cellular mechanisms of bone loss." J Clin Invest **72**(4): 1396-409.

Pearson, O. M. and Lieberman, D. E. (2004). "The aging of Wolff's "law": Ontogeny and responses to mechanical loading in cortical bone." Am J Phys Anthropol **Suppl 39**: 63-99.

Petit, M. A., Beck, T. J., Shults, J., Zemel, B. S., Foster, B. J. and Leonard, M. B. (2005). "Proximal femur bone geometry is appropriately adapted to lean mass in overweight children and adolescents." Bone **36**(3): 568-76.

Pigliucci, M. and Preston, K. (2004). Phenotypic Integration. Studying the Ecology and Evolution of Complex Phenotypes. New York, Oxford University Press.

Plotkin, L. I., Weinstein, R. S., Parfitt, A. M., Roberson, P. K., Manolagas, S. C. and Bellido, T. (1999). "Prevention of osteocyte and osteoblast apoptosis by bisphosphonates and calcitonin." J Clin Invest **104**(10): 1363-74.

Portigliatti Barbos, M., Bianco, P., Ascenzi, A. and Boyde, A. (1984). "Collagen orientation in compact bone: II. Distribution of lamellae in the whole of the human femoral shaft with reference to its mechanical properties." Metab Bone Dis Relat Res **5**(6): 309-15.

Pothuaud, L., Van Rietbergen, B., Mosekilde, L., Beuf, O., Levitz, P., Benhamou, C. L. and Majumdar, S. (2002). "Combination of topological parameters and bone volume fraction better predicts the mechanical properties of trabecular bone." J Biomech **35**(8): 1091-9.

Price, C., Herman, B. C., Lufkin, T., Goldman, H. M. and Jepsen, K. J. (2005). "Genetic variation in bone growth patterns defines adult mouse bone fragility." J Bone Miner Res **20**(11): 1983-91.

Rauch, F. and Schoenau, E. (2001). "The developing bone: slave or master of its cells and molecules?" Pediatr Res **50**(3): 309-14.

Reid, S. A. and Boyde, A. (1987). "Changes in the mineral density distribution in human bone with age: image analysis using backscattered electrons in the SEM." J Bone Miner Res **2**(1): 13-22.

Reilly, G. C. (2000). "Observations of microdamage around osteocyte lacunae in bone." J Biomech **33**(9): 1131-4.

Richman, C., Kutilek, S., Miyakoshi, N., Srivastava, A. K., Beamer, W. G., Donahue, L. R., Rosen, C. J., Wergedal, J. E., Baylink, D. J. and Mohan, S. (2001). "Postnatal and pubertal skeletal changes contribute predominantly to the differences in peak bone density between C3H/HeJ and C57BL/6J mice." J Bone Miner Res **16**(2): 386-97.

Riggs, B. L., Melton III, L. J., Robb, R. A., Camp, J. J., Atkinson, E. J., Peterson, J. M., Rouleau, P. A., McCollough, C. H., Bouxsein, M. L. and Khosla, S. (2004). "Population-based study of age and sex differences in bone volumetric density, size, geometry, and structure at different skeletal sites." J Bone Miner Res **19**(12): 1945-54.

Riggs, C. M., Vaughan, L. C., Evans, G. P., Lanyon, L. E. and Boyde, A. (1993). "Mechanical implications of collagen fibre orientation in cortical bone of the equine radius." Anat Embryol (Berl) **187**(3): 239-48.

Ritzel, H., Amling, M., Posl, M., Hahn, M. and Delling, G. (1997). "The thickness of human vertebral cortical bone and its changes in aging and osteoporosis: a histomorphometric analysis of the complete spinal column from thirty-seven autopsy specimens." J Bone Miner Res **12**(1): 89-95.

Robling, A. G., Li, J., Shultz, K. L., Beamer, W. G. and Turner, C. H. (2003). "Evidence for a skeletal mechanosensitivity gene on mouse chromosome 4." Faseb J **17**(2): 324-6.

Roodman, G. D. (1999). "Cell biology of the osteoclast." Exp Hematol **27**(8): 1229-41.

Rosen, C. J., Beamer, W. G. and Donahue, L. R. (2001). "Defining the genetics of osteoporosis: using the mouse to understand man." Osteoporos Int **12**(10): 803-10.

Rosen, C. J., Churchill, G. A., Donahue, L. R., Shultz, K. L., Burgess, J. K., Powell, D. R., Ackert, C. and Beamer, W. G. (2000). "Mapping quantitative trait loci for serum insulin-like growth factor-1 levels in mice." Bone **27**(4): 521-8.

Roux, W. (1881). Der Kampf der Teile im Organismus. Leipzig, Engelmann.

Rubin, C. D. (2005). "Emerging concepts in osteoporosis and bone strength." Curr Med Res Opin **21**(7): 1049-56.

Rubin, C. T. and Lanyon, L. E. (1984). "Dynamic strain similarity in vertebrates; an alternative to allometric limb bone scaling." J Theor Biol **107**(2): 321-7.

Rubin, J., Ackert-Bicknell, C. L., Zhu, L., Fan, X., Murphy, T. C., Nanes, M. S., Marcus, R., Holloway, L., Beamer, W. G. and Rosen, C. J. (2002). "IGF-I regulates osteoprotegerin (OPG) and receptor activator of nuclear factor-kappaB ligand in vitro and OPG in vivo." J Clin Endocrinol Metab **87**(9): 4273-9.

Ruff, C. (2003). "Growth in bone strength, body size, and muscle size in a juvenile longitudinal sample." Bone **33**(3): 317-29.

Ruff, C. (2003). "Ontogenetic adaptation to bipedalism: age changes in femoral to humeral length and strength proportions in humans, with a comparison to baboons." J Hum Evol **45**(4): 317-49.

Ruff, C., Holt, B. and Trinkaus, E. (2006). "Who's afraid of the big bad Wolff? "Wolff's law" and bone functional adaptation." Am J Phys Anthropol **129**(4): 484-98.

Ruff, C. B. (1984). "Allometry between length and cross-sectional dimensions of the femur and tibia in Homo sapiens sapiens." Am J Phys Anthropol **65**(4): 347-58.

Ruff, C. B. (2000). "Body size, body shape, and long bone strength in modern humans." J Hum Evol **38**(2): 269-90.

Ruimerman, R., Hilbers, P., van Rietbergen, B. and Huiskes, R. (2005). "A theoretical framework for strain-related trabecular bone maintenance and adaptation." J Biomech **38**(4): 931-41.

Sahlman, J., Inkinen, R., Hirvonen, T., Lammi, M. J., Lammi, P. E., Nieminen, J., Lapvetelainen, T., Prockop, D. J., Arita, M., Li, S. W., Hyttinen, M. M., Helminen, H. J. and Puustjarvi, K. (2001). "Premature vertebral endplate ossification and mild disc degeneration in mice after inactivation of one allele belonging to the Col2a1 gene for Type II collagen." Spine **26**(23): 2558-65.

Seeman, E. (1999). "The structural basis of bone fragility in men." Bone **25**(1): 143-7.

Seeman, E. (2001). "Unresolved issues in osteoporosis in men." Rev Endocr Metab Disord **2**(1): 45-64.

Seeman, E. and Delmas, P. D. (2006). "Bone quality--the material and structural basis of bone strength and fragility." N Engl J Med **354**(21): 2250-61.

Seeman, E., Hopper, J. L., Young, N. R., Formica, C., Goss, P. and Tsalamandris, C. (1996). "Do genetic factors explain associations between muscle strength, lean mass, and bone density? A twin study." Am J Physiol **270**(2 Pt 1): E320-7.

Selker, F. and Carter, D. R. (1989). "Scaling of long bone fracture strength with animal mass." J Biomech **22**(11-12): 1175-83.

Shaffer, R. A., Brodine, S. K., Almeida, S. A., Williams, K. M. and Ronaghy, S. (1999). "Use of simple measures of physical activity to predict stress fractures in young men undergoing a rigorous physical training program." Am J Epidemiol **149**(3): 236-42.

Sharkey, N. A. and Lang, D. H. (2007). "Genes in context: probing the genetics of fracture resistance." Exerc Sport Sci Rev **35**(3): 86-96.

Sheng, M. H., Baylink, D. J., Beamer, W. G., Donahue, L. R., Rosen, C. J., Lau, K. H. and Wergedal, J. E. (1999). "Histomorphometric studies show that bone formation and bone mineral apposition rates are greater in C3H/HeJ (high-density) than C57BL/6J (low-density) mice during growth." Bone **25**(4): 421-9.

Shimizu, M., Higuchi, K., Bennett, B., Xia, C., Tsuboyama, T., Kasai, S., Chiba, T., Fujisawa, H., Kogishi, K., Kitado, H., Kimoto, M., Takeda, N., Matsushita, M.,

Okumura, H., Serikawa, T., Nakamura, T., Johnson, T. E. and Hosokawa, M. (1999). "Identification of peak bone mass QTL in a spontaneously osteoporotic mouse strain." Mamm Genome **10**(2): 81-7.

Sieberts, S. K. and Schadt, E. E. (2007). "Moving toward a system genetics view of disease." Mamm Genome **18**(6-7): 389-401.

Silva, M. J. and Gibson, L. J. (1997). "Modeling the mechanical behavior of vertebral trabecular bone: effects of age-related changes in microstructure." Bone **21**(2): 191-9.

Silva, M. J., Keaveny, T. M. and Hayes, W. C. (1997). "Load sharing between the shell and centrum in the lumbar vertebral body." Spine **22**(2): 140-50.

Silver, L. M. (1995). Mouse Genetics. Concepts and Applications. New York, Oxford University Press.

Sinervo, B. and Svensson, E. (2002). "Correlational selection and the evolution of genomic architecture." Heredity **89**(5): 329-38.

Singh, M., Nagrath, A. R. and Maini, P. S. (1970). "Changes in trabecular pattern of the upper end of the femur as an index of osteoporosis." J Bone Joint Surg Am **52**(3): 457-67.

Skaggs, D. L., Loro, M. L., Pitukcheewanont, P., Tolo, V. and Gilsanz, V. (2001). "Increased body weight and decreased radial cross-sectional dimensions in girls with forearm fractures." J Bone Miner Res **16**(7): 1337-42.

Skedros, J. G., Dayton, M. R., Sybrowsky, C. L., Bloebaum, R. D. and Bachus, K. N. (2003). "Are uniform regional safety factors an objective of adaptive modeling/remodeling in cortical bone?" J Exp Biol **206**(Pt 14): 2431-9.

Skedros, J. G. and Hunt, K. J. (2004). "Does the degree of laminarity correlate with site-specific differences in collagen fibre orientation in primary bone? An evaluation in the turkey ulna diaphysis." J Anat **205**(2): 121-34.

Skedros, J. G., Sybrowsky, C. L., Parry, T. R. and Bloebaum, R. D. (2003). "Regional differences in cortical bone organization and microdamage prevalence in Rocky Mountain mule deer." Anat Rec **274A**(1): 837-50.

Slootweg, M. C., Hoogerbrugge, C. M., de Poorter, T. L., Duursma, S. A. and van Buul-Offers, S. C. (1990). "The presence of classical insulin-like growth factor (IGF) type-I and -II receptors on mouse osteoblasts: autocrine/paracrine growth effect of IGFs?" J Endocrinol **125**(2): 271-7.

Smith, R. W. and Walker, R. R. (1964). "Femoral expansion in aging women: Implications for osteoporosis and fractures." Science **145**: 156-157.

Sornay-Rendu, E., Boutroy, S., Munoz, F. and Delmas, P. D. (2007). "Alterations of cortical and trabecular architecture are associated with fractures in postmenopausal women, partially independent of decreased BMD measured by DXA: the OFELY study." J Bone Miner Res **22**(3): 425-33.

Stauffer, D. and Aharony, A. (1994). Introduction to Percolation Theory. London, Taylor & Francis Ltd.

Stieger, J. H. and Lind, J. M. (1980). Statistically based tests for the number of common factors. Annual Meeting of the Psychometric Society May 1980, Iowa City.

Stock, J. and Pfeiffer, S. (2001). "Linking structural variability in long bone diaphyses to habitual behaviors: foragers from the southern African Later Stone Age and the Andaman Islands." Am J Phys Anthropol **115**(4): 337-48.

Sumner, D. R. and Andriacchi, T. P. (1996). "Adaptation to differential loading: comparison of growth-related changes in cross-sectional properties of the human femur and humerus." Bone **19**(2): 121-6.

Swartz, S. M., Bennett, M. B. and Carrier, D. R. (1992). "Wing bone stresses in free flying bats and the evolution of skeletal design for flight." Nature **359**(6397): 726-9.

Szulc, P., Munoz, F., Duboeuf, F., Marchand, F. and Delmas, P. D. (2006). "Low width of tubular bones is associated with increased risk of fragility fracture in elderly men--the MINOS study." Bone **38**(4): 595-602.

Szulc, P., Seeman, E., Duboeuf, F., Sornay-Rendu, E. and Delmas, P. D. (2006). "Bone fragility: failure of periosteal apposition to compensate for increased endocortical resorption in postmenopausal women." J Bone Miner Res **21**(12): 1856-63.

Taaffe, D. R., Snow-Harter, C., Connolly, D. A., Robinson, T. L., Brown, M. D. and Marcus, R. (1995). "Differential effects of swimming versus weight-bearing activity on bone mineral status of eumenorrheic athletes." J Bone Miner Res **10**(4): 586-93.

Tabor, Z. (2003). "Simulated aging--a novel method for estimating the risk of fracture of trabecular bone." Bone **33**(2): 229-36.

Tanck, E., Hannink, G., Ruimerman, R., Buma, P., Burger, E. H. and Huiskes, R. (2006). "Cortical bone development under the growth plate is regulated by mechanical load transfer." J Anat **208**(1): 73-9.

Tanck, E., Homminga, J., van Lenthe, G. H. and Huiskes, R. (2001). "Increase in bone volume fraction precedes architectural adaptation in growing bone." Bone **28**(6): 650-4.

Thompson, D. (1961). On Growth and Form. Cambridge, Cambridge University Press.

Tomkinson, A., Reeve, J., Shaw, R. W. and Noble, B. S. (1997). "The death of osteocytes via apoptosis accompanies estrogen withdrawal in human bone." J Clin Endocrinol Metab **82**(9): 3128-35.

Tommasini, S. M., Morgan, T. G., van der Meulen, M. and Jepsen, K. J. (2005). "Genetic variation in structure-function relationships for the inbred mouse lumbar vertebral body." J Bone Miner Res **20**(5): 817-27.

Tommasini, S. M., Nasser, P., Hu, B. and Jepsen, K. J. (2008). "Biological co-adaptation of morphological and composition traits contributes to mechanical functionality and skeletal fragility." J Bone Miner Res **23**(2): 236-46.

Tommasini, S. M., Nasser, P. and Jepsen, K. J. (2007). "Sexual dimorphism affects tibia size and shape but not tissue-level mechanical properties." Bone **40**(2): 498-505.

Tommasini, S. M., Nasser, P., Schaffler, M. B. and Jepsen, K. J. (2005). "The relationship between bone morphology and bone quality in male tibiae: Implications for stress fracture risk." J Bone Miner Res **20**(8): 1372-80.

Tommasini, S. M., Wearne, S. L., Hof, P. R. and Jepsen, K. J. (2008). "Percolation theory relates corticocancellous architecture to mechanical function in vertebrae of inbred mouse strains." Bone **42**(4): 743-50.

Tudor-Locke, C. and Bassett, D. R., Jr. (2004). "How many steps/day are enough? Preliminary pedometer indices for public health." Sports Med **34**(1): 1-8.

Turner, C. H. (1992). "Functional determinants of bone structure: beyond Wolff's law of bone transformation." Bone **13**(6): 403-9.

Turner, C. H. (2006). "Bone strength: current concepts." Ann N Y Acad Sci **1068**: 429-46.

Turner, C. H. and Forwood, M. R. (1995). "What role does the osteocyte network play in bone adaptation?" Bone **16**(3): 283-5.

Turner, C. H., Hsieh, Y. F., Muller, R., Bouxsein, M. L., Baylink, D. J., Rosen, C. J., Grynpas, M. D., Donahue, L. R. and Beamer, W. G. (2000). "Genetic regulation of cortical and trabecular bone strength and microstructure in inbred strains of mice." J Bone Miner Res **15**(6): 1126-31.

Turner, C. H., Hsieh, Y. F., Muller, R., Bouxsein, M. L., Rosen, C. J., McCrann, M. E., Donahue, L. R. and Beamer, W. G. (2001). "Variation in bone biomechanical properties, microstructure, and density in BXH recombinant inbred mice." J Bone Miner Res **16**(2): 206-13.

Turner, C. H. and Pavalko, F. M. (1998). "Mechanotransduction and functional response of the skeleton to physical stress: the mechanisms and mechanics of bone adaptation." J Orthop Sci **3**(6): 346-55.

Turner, C. H., Robling, A. G., Duncan, R. L. and Burr, D. B. (2002). "Do bone cells behave like a neuronal network?" Calcif Tissue Int **70**(6): 435-42.

Turner, C. H., Sun, Q., Schriefer, J., Pitner, N., Price, R., Bouxsein, M. L., Rosen, C. J., Donahue, L. R., Shultz, K. L. and Beamer, W. G. (2003). "Congenic mice reveal sex-specific genetic regulation of femoral structure and strength." Calcif Tissue Int **73**(3): 297-303.

Turner, R. T., Backup, P., Sherman, P. J., Hill, E., Evans, G. L. and Spelsberg, T. C. (1992). "Mechanism of action of estrogen on intramembranous bone formation: regulation of osteoblast differentiation and activity." Endocrinology **131**(2): 883-9.

Turner, R. T., Wakley, G. K. and Hannon, K. S. (1990). "Differential effects of androgens on cortical bone histomorphometry in gonadectomized male and female rats." J Orthop Res **8**(4): 612-7.

Ural, A. and Vashishth, D. (2006). "Interactions between microstructural and geometrical adaptation in human cortical bone." J Orthop Res **24**(7): 1489-98.

van der Meulen, M. C. (1997). "Diaphyseal bone growth and adaptation: models and data." Stud Health Technol Inform **40**: 17-23.

van der Meulen, M. C., Ashford, M. W., Jr., Kiratli, B. J., Bachrach, L. K. and Carter, D. R. (1996). "Determinants of femoral geometry and structure during adolescent growth." J Orthop Res **14**(1): 22-9.

van der Meulen, M. C., Jepsen, K. J. and Mikic, B. (2001). "Understanding bone strength: size isn't everything." Bone **29**(2): 101-4.

van der Meulen, M. C., Morey-Holton, E. R. and Carter, D. R. (1995). "Hindlimb suspension diminishes femoral cross-sectional growth in the rat." J Orthop Res **13**(5): 700-7.

van der Meulen, M. C., Moro, M., Kiratli, B. J., Marcus, R. and Bachrach, L. K. (2000). "Mechanobiology of femoral neck structure during adolescence." J Rehabil Res Dev **37**(2): 201-8.

van Oers, R. F., Ruimerman, R., Tanck, E., Hilbers, P. A. and Huiskes, R. (2008). "A unified theory for osteonal and hemi-osteonal remodeling." Bone **42**(2): 250-9.

Vega, E., Ghiringhelli, G., Mautalen, C., Rey Valzacchi, G., Scaglia, H. and Zylberstein, C. (1998). "Bone mineral density and bone size in men with primary osteoporosis and vertebral fractures." Calcif Tissue Int **62**(5): 465-9.

Viguet-Carrin, S., Roux, J. P., Arlot, M. E., Merabet, Z., Leeming, D. J., Byrjalsen, I., Delmas, P. D. and Bouxsein, M. L. (2006). "Contribution of the advanced glycation end product pentosidine and of maturation of type I collagen to compressive biomechanical properties of human lumbar vertebrae." Bone **39**(5): 1073-9.

Volkman, S. K., Galecki, A. T., Burke, D. T., Paczas, M. R., Moalli, M. R., Miller, R. A. and Goldstein, S. A. (2003). "Quantitative trait loci for femoral size and shape in a genetically heterogeneous mouse population." J Bone Miner Res **18**(8): 1497-505.

Waarsing, J. H., Day, J. S., van der Linden, J. C., Ederveen, A. G., Spanjers, C., De Clerck, N., Sasov, A., Verhaar, J. A. and Weinans, H. (2004). "Detecting and tracking local changes in the tibiae of individual rats: a novel method to analyse longitudinal in vivo micro-CT data." Bone **34**(1): 163-9.

Waarsing, J. H., Day, J. S., Verhaar, J. A., Ederveen, A. G. and Weinans, H. (2006). "Bone loss dynamics result in trabecular alignment in aging and ovariectomized rats." J Orthop Res **24**(5): 926-35.

Wang, L., Wang, Y., Han, Y., Henderson, S. C., Majeska, R. J., Weinbaum, S. and Schaffler, M. B. (2005). "In situ measurement of solute transport in the bone lacunar-canalicular system." Proc Natl Acad Sci U S A **102**(33): 11911-6.

Wang, X., Li, X., Shen, X. and Agrawal, C. M. (2003). "Age-related changes of noncalcified collagen in human cortical bone." Ann Biomed Eng **31**(11): 1365-71.

Wang, X., Shen, X., Li, X. and Agrawal, C. M. (2002). "Age-related changes in the collagen network and toughness of bone." Bone **31**(1): 1-7.

Wang, X. F., Duan, Y., Beck, T. J. and Seeman, E. (2005). "Varying contributions of growth and ageing to racial and sex differences in femoral neck structure and strength in old age." Bone **36**(6): 978-86.

Watts, D. J. (2003). Six Degrees: The Science of a Connected Age. New York, W.W. Norton & Company.

Wearne, S. L., Rodriguez, A., Ehlenberger, D. B., Rocher, A. B., Henderson, S. C. and Hof, P. R. (2005). "New techniques for imaging, digitization, and analysis of

three-dimensional neuronal morphology on multiple scales." Neuroscience **136**(3): 661-80.

Weinbaum, S., Cowin, S. C. and Zeng, Y. (1994). "A model for the excitation of osteocytes by mechanical loading-induced bone fluid shear stresses." J Biomech **27**(3): 339-60.

Winner, S. J., Morgan, C. A. and Evans, J. G. (1989). "Perimenopausal risk of falling and incidence of distal forearm fracture." Bmj **298**(6686): 1486-8.

Wiren, K. M., Zhang, X. W., Toombs, A. R., Kasparcova, V., Gentile, M. A., Harada, S. and Jepsen, K. J. (2004). "Targeted overexpression of androgen receptor in osteoblasts: unexpected complex bone phenotype in growing animals." Endocrinology **145**(7): 3507-22.

Wright, S. (1918). "On the nature of size factors." Genetics **3**: 367-374.

Wright, S. (1921). "Correlation and causation." Journal of Agricultural Research **20**: 557-585.

Wronski, T. J., Morey-Holton, E. R., Doty, S. B., Maese, A. C. and Walsh, C. C. (1987). "Histomorphometric analysis of rat skeleton following spaceflight." Am J Physiol **252**(2 Pt 2): R252-5.

Yamauchi, M., Sugimoto, T. and Chihara, K. (2004). "Determinants of vertebral fragility: the participation of cortical bone factors." J Bone Miner Metab **22**(2): 79-85.

Yershov, Y., Baldini, T. H., Villagomez, S., Young, T., Martin, M. L., Bockman, R. S., Peterson, M. G. and Blank, R. D. (2001). "Bone strength and related traits in HcB/Dem recombinant congenic mice." J Bone Miner Res **16**(6): 992-1003.

Yu, H., Mohan, S., Edderkaoui, B., Masinde, G. L., Davidson, H. M., Wergedal, J. E., Beamer, W. G. and Baylink, D. J. (2007). "Detecting novel bone density and bone size quantitative trait loci using a cross of MRL/MpJ and CAST/EiJ inbred mice." Calcif Tissue Int **80**(2): 103-10.